

ABSTRACT

Tara Ann Cartwright. THE BIOCHEMICAL CHARACTERIZATION OF NEURONAL K^+ CHANNEL N-GLYCANS AND THEIR ROLE IN REGULATING K^+ CHANNEL FUNCTION. (Under the direction of Dr. Ruth A. Schwalbe) Department of Biochemistry and Molecular Biology, June 2009.

The Kv3 and Kv1 subfamilies of voltage-gated K^+ channels are critical components which contribute to action potential repolarization throughout the central nervous system. Here, it was shown that both absolutely conserved N-glycosylation sites of the Kv3.1, Kv3.3 and Kv3.4 proteins were occupied in the central nervous system of the adult rat by complex oligosaccharides. Additionally, it was demonstrated that the expression patterns of the Kv3 glycoproteins were different from one another throughout the central nervous system. Electrophoretic migration patterns of the Kv3 glycoproteins from different membranes of the central nervous system digested with glycosidases were utilized to identify the attachment of unique sialylated N-glycan structures. An examination of these sialylated N-glycan structures revealed that the Kv3 glycoproteins, along with the Kv1.1, Kv1.2, and Kv1.4 glycoproteins, were terminated with atypical disialyl units. Moreover, at least one of the carbohydrate chains of the Kv3.1, Kv3.3 and Kv3.4 glycoproteins, like Kv3.1 heterologously expressed in B35 cells, was capped with an oligo/polysialic acid unit. Notably, this is the first time that di/oligo/polysialyl units have been shown to be associated with K^+ channels. Sialyl residues linked to internal carbohydrate residues were shown to be components of the N-glycans of the Kv1 glycoproteins, as well as the Kv3 glycoproteins and N-CAM. To date, this unusual glycosidic bond for sialyl residues has not been identified on N-glycans. Whole cell

current measurements of glycosylated (wild type), unglycosylated mutant (N220Q/N229Q) and partially glycosylated mutant (N220Q and N229Q) Kv3.1 channels heterologously expressed in B35 cells revealed that the glycosylated Kv3.1 protein could favor a subpopulation of channels with fast activation and inactivation rates for inactivating currents. However, this subpopulation was undetectable for the inactivating currents of the unglycosylated and partially glycosylated Kv3.1 channels. Additionally, the noninactivating current type of the glycosylated and partially glycosylated Kv3.1 channels revealed a subpopulation of Kv3.1 channels with fast activation and inactivation rates, as well as with fast activation and slow inactivation. We conclude that the presence of atypical sialylated N-glycans of Kv3 glycoproteins, and perhaps Kv1 glycoproteins, in mammalian brain is critical in modulating the expression of K^+ currents at the surface of neurons.

©2009

Tara Ann Cartwright

THE BIOCHEMICAL CHARACTERIZATION OF NEURONAL K⁺ CHANNEL
N-GLYCANS AND THEIR ROLE IN REGULATING K⁺ CHANNEL FUNCTION

A Dissertation

Presented to

The Faculty of the Department of Biochemistry and Molecular Biology

Brody School of Medicine at East Carolina University

In Partial Fulfillment

of the Requirements for the Degree

Doctor of Philosophy in Biochemistry and Molecular Biology

by

Tara Ann Cartwright

June 2009

THE BIOCHEMICAL CHARACTERIZATION OF NEURONAL K⁺ CHANNEL
N-GLYCANS AND THEIR ROLE IN REGULATING K⁺ CHANNEL FUNCTION

by
Tara Ann Cartwright

APPROVED BY:

DIRECTOR OF DISSERTATION

Ruth A. Schwalbe, PhD.

COMMITTEE MEMBER

Yan-Hua Chen, PhD.

COMMITTEE MEMBER

Joseph G. Cory, PhD.

COMMITTEE MEMBER

Cindy Putnam-Evans, PhD.

COMMITTEE MEMBER

Brett D. Keiper, PhD.

INTERIM CHAIR OF THE
DEPARTMENT OF BIOCHEMISTRY
AND MOLECULAR BIOLOGY

Phillip H. Pekala, PhD.

DEAN OF THE GRADUATE SCHOOL

Paul Gemperline, PhD.

DEDICATION

I would like to dedicate this Doctoral dissertation to my mother, Beverly D. DeWitt, who emphasized the importance of education, and who instilled in me the inspiration to set high goals and the confidence to achieve them. There is no doubt in my mind, that without her continued love, support and counsel, I could not have completed my graduate studies.

ACKNOWLEDGEMENTS

I would like to express my deepest gratitude to my doctoral advisor, Dr. Ruth A. Schwalbe, for her excellent guidance and patience, as well as, providing me with the opportunity to learn the patch clamp technique. I shall never forget her willingness to take a chance on me. Her kind words of encouragement and careful reading of my writings will never be overlooked. She is one of the rare doctoral advisors that students dream they will be mentored by, during their graduate studies. More importantly, she was more than a doctoral advisor; she was a monumental source of support.

To the members of my dissertation committee, Dr. Yan-Hua Chen, Dr. Joseph G. Cory, Dr. Cindy Putnam-Evans, and Dr. Brett D. Keiper, each of whom gave their time and expertise, which enabled me to enhance the writing of my research, I thank them. Their encouraging words, constructive criticism and support was inspirational in my successfully completing my graduate studies.

I am grateful to Dr. George J. Kaspersek, who assisted, advised, and supported my graduate career, during the course of my studies. But most of all, he believed in me when no else did.

I would also like to thank my mom, Beverly D. DeWitt, for always supporting me and being my emotional anchor, not only through the vagaries of graduate school but, my entire life. In addition, I would like to acknowledge my dad, Paul E. Cartwright, for

continuously encouraging and counseling me through the most challenging times.

Finally, I would like to thank my fiancé, Brian Y. Porter, for his encouragement.

TABLE OF CONTENTS

LIST OF PAPERS.....	x
LIST OF TABLES.....	xi
LIST OF FIGURES.....	xii
LIST OF ABBREVIATIONS.....	xv
CHAPTER 1 – INTRODUCTION.....	1
Brief overview of K ⁺ channels.....	1
Voltage-dependent K ⁺ (Kv) channels.....	1
Biophysical properties of the Kv3 channel subfamily.....	2
The structure of Kv3 channels.....	3
Expression of Kv3 mRNA in rat brain.....	4
Brain and spinal cord distribution of Kv3 proteins.....	5
Ablation of Kv3.1 and Kv3.3 channels.....	5
The Kv1 channel subfamily.....	6
Biological roles of oligosaccharides.....	7
The N-glycosylation pathway.....	7
N-Linked oligosaccharide structures.....	11
Diseases and disorders associated with N-linked glycosylation.....	14
The Mgat-I null mouse embryo.....	15
N-Glycosylation modifies Kv channel function and trafficking.....	15
Sialylated brain N-glycans.....	16
Specific Aims of this Investigation.....	18

TABLE OF CONTENTS (continued)

CHAPTER 2 - THE PATCH CLAMP TECHNIQUE.....	21
Mastering the patch clamp technique.....	21
CHAPTER 3 - MATERIALS AND METHODS.....	23
Brain, spinal cord and heart membrane extracts.....	23
Endoglycosidase N reactions.....	24
Peptide N-glycosidase F (PNGase F) reactions.....	24
Sialidase A, C, S, and neuraminidase reactions.....	25
Sialidase C and endoglycosidase N double digestion reactions.....	26
Double digestion reactions with PNGase F and either sialidase A or neuraminidase.....	26
Endoglycosidase H (Endo H) digestions.....	27
Construction of recombinant expression vectors.....	27
B35 neuroblastoma cell culture.....	28
Transient and stable transfection assay.....	29
Metabolic radiolabeling of sialylated N-glycans in B35 cells.....	30
M2 immunoaffinity purified Kv3.1 protein and glycosidase digestion reactions.....	31
B35 cell membrane isolation.....	32
Western blotting.....	33
Western blot analysis.....	34
Whole cell recordings.....	35
Current analysis	37

TABLE OF CONTENTS (continued)

CHAPTER 4 - COMPLEX OLIGOSACCHARIDES ARE N-LINKED TO KV3 VOLTAGE-GATED K ⁺ CHANNELS IN RAT BRAIN.....	39
Abstract.....	40
Introduction.....	41
Results.....	47
N-Glycosylation of Kv3 channels.....	47
Occupancy of both conserved N-glycosylation sites.....	51
N-Linked oligosaccharide are of complex type.....	54
Discussion.....	57
CHAPTER 5 - NOVEL KV3 GLYCOFORMS DIFFERENTIALLY EXPRESSED IN ADULT MAMMALIAN BRAIN CONTAIN SIALYLATED N-GLYCANS.....	59
Abstract.....	60
Introduction.....	61
Results.....	65
N-Glycans of neuronal Kv3 channels contain sialic acid residues.....	65
Protein levels of Kv3.1, Kv3.3 and Kv3.4 throughout the central nervous system.....	69
Different Kv3.1, Kv3.3 and Kv3.4 glycoforms identified throughout the central nervous system.....	72
Differentially expressed Kv3 glycoforms contain sialylated N-glycans.....	79
Discussion.....	82

TABLE OF CONTENTS (continued)

CHAPTER 6 - ATYPICAL SIALYLATED N-GLYCAN STRUCTURES ARE ATTACHED TO NEURONAL VOLTAGE-GATED POTASSIUM CHANNELS.....	86
Abstract.....	87
Introduction.....	88
Results.....	92
Neuronal Kv3 proteins are associated with α 2,3-, α 2,8-linked sialylated N-glycan structures.....	92
N-Glycan of Kv3.1 protein is heavily sialylated in neuroblastoma cells.....	100
Oligo/polysialyl moieties are attached to neuronal Kv3 proteins.....	103
Detection of branched sialyl residues attached to Kv3 glycoproteins.....	107
N-Glycans of Kv1.1, 1.2, and 1.4 proteins contain α 2,8-linked and branched sialyl residues.....	110
Discussion.....	117
CHAPTER 7 – NEURONAL N-GLYCOSYLATION PROCESSING REGULATES VOLTAGE-GATED POTASSIUM CHANNEL ACTIVITY.....	121
Abstract.....	122
Introduction.....	123
Results.....	126
Both N-glycans of the Kv3.1 protein are sialylated in B35 neuroblastoma cells.....	126

TABLE OF CONTENTS (continued)

Glycosylated Kv3.1 channels have faster inactivation kinetics than their unglycosylated counterparts.....	130
Neuronal N-glycosylation processing regulates the voltage dependence of channel activation and inactivation.....	141
Noninactivating current behavior was more common for the glycosylated Kv3.1 channel	146
N-Glycosylation of the Kv3.1 channel increased current density.....	149
Glycosylated Kv3.1 channels have faster activation rates than their unglycosylated counterpart.....	152
N-Glycosylation of the Kv3.1 channel increases the deactivation rate.....	155
Analysis of the partially glycosylated Kv3.1 channels.....	158
Discussion.....	163
CHAPTER 8 - SUMMARY.....	175
Conclusion.....	182
REFERENCES.....	185
APPENDICES.....	192
APPENDIX A: COPYRIGHT PERMISSION.....	192
APPENDIX B: COPYRIGHT PERMISSION.....	193
APPENDIX C: COPYRIGHT PERMISSION.....	194

LIST OF PAPERS

1. Cartwright, T. A., Corey, M. J., and Schwalbe, R. A. (2007) *Biochim Biophys Acta* **1770**(4), 666-671.
2. Schwalbe, R. A., Corey, M. J., and Cartwright, T. A. (2008) *Biochem Cell Biol* **86**(1), 21-30.
3. Cartwright, T. A., and Schwalbe, R. A. (2008) *Biosci Rep*. In press.
4. Cartwright, T.A. and Schwalbe, R.A. (2009) *Cell Biochem Biophys*. In review.

LIST OF TABLES**CHAPTER 7**

Table 1.	Electrophysiological parameters of glycosylated, unglycosylated and partially glycosylated forms of the Kv3.1 channel in B35 cells.....	136
Table 2.	Comparison of the biophysical parameters for the fast and slow forms of the wild type Kv3.1 channel.....	138

LIST OF FIGURES

CHAPTER 1

Figure 1.	The N-linked glycosylation pathway.....	10
Figure 2.	Schematic structures of different N-glycans.....	13

CHAPTER 4

Figure 3.	Topological model of Kv3 channels.....	43
Figure 4.	Amino acid sequence alignments of the S1–S2 linker of Kv3 channels.....	45
Figure 5.	Kv3 proteins are N-glycosylated in rat brain tissue.....	49
Figure 6.	Utilization of both N-glycosylation sites for Kv3 proteins.....	53
Figure 7.	N-Linked oligosaccharides of Kv3 proteins are of complex type.....	56

CHAPTER 5

Figure 8.	Topological model of a Kv3 monomeric unit with sialylated N- glycans.....	63
Figure 9.	N-Linked oligosaccharides of Kv3.1, Kv3.3, and Kv3.4 proteins are composed of sialic acid residues.....	67
Figure 10.	Differences in the Kv3.1, Kv3.3, and Kv3.4 protein expression levels in the various regions of the central nervous system.....	71
Figure 11.	The M_r values for Kv3 proteins are different in the various brain regions and spinal cord.....	75
Figure 12.	Differences in M_r values for the Kv3 proteins are due to N-glycosylation.....	77
Figure 13.	Sialylated N-glycans of Kv3.1, Kv3.3, and Kv3.4 channels were detected in the spinal cord and different brain regions.....	81

LIST OF FIGURES (continued)

CHAPTER 6

Figure 14.	Biochemically-derived sialic acid linkages of the N-glycans attached to Kv channels.....	90
Figure 15.	Removal of sialic acid residues from Kv3 glycoproteins.....	94
Figure 16.	Sialyl residues with α 2,8 linkages are present on neuronal Kv3 glycoproteins.....	99
Figure 17.	The N-glycans of Kv3.1 protein expressed in neuroblastoma cells are composed of oligo/polysialyl units.....	102
Figure 18.	Brain Kv3 glycoproteins are composed of oligo/polysialyl units.....	106
Figure 19.	Detection of branched sialyl residues attached to the N-glycans of Kv3 proteins.....	109
Figure 20.	Kv1.1, Kv1.2 and Kv1.4 glycoproteins in brain contain branched and α 2,8-linked sialyl residues.....	112
Figure 21.	Branched and α 2,8-linked sialic acid residues are attached to the N-linked oligosaccharides of Kv1.1, Kv1.2 and Kv1.4 proteins.....	115

CHAPTER 7

Figure 22.	Topological model of the Kv3.1 glycoprotein and immunoblot analysis of wild type and N-glycosylation mutants of Kv3.1 protein heterologously expressed in B35 cells	128
Figure 23.	Whole cell current recordings of wild type Kv3.1 and N220/N229Q channels display variations in the rate of inactivation	132
Figure 24.	Prolong depolarization steps enhance the differences in the inactivation rates of wild type Kv3.1 and N220Q/N229Q channels.....	140
Figure 25.	Activation (G-V) curves of wild type Kv3.1 and N220Q/ N229Q channels.....	143

LIST OF FIGURES (continued)

Figure 26.	Comparison of the noninactivating current patterns from wild type Kv3.1 and N220Q/N229Q channels.....	148
Figure 27.	Differences in the current density are expressed by the various whole cell current types of the wild type Kv3.1 and N220Q/N229Q channels.....	151
Figure 28.	Variations in the activation rates of the various whole cell current types for wild type Kv3.1 and N220Q/N229Q channels.....	154
Figure 29.	Deactivation rates of wild type Kv3.1 and N220Q/N229Q channels.....	157
Figure 30.	Functional characterization of B35 cells expressing the single N-glycosylation mutants, N220Q and N229Q.....	160

LIST OF ABBREVIATIONS

K ⁺	Potassium
K _v	Voltage-gated K ⁺ channel
HEK	Human Embryonic Kidney
CHO	Chinese Hamster Ovarian
Sf9	<i>Spodoptera frugiperda</i>
FS	Fast Spiking neurons
ER	Endoplasmic reticulum
OST	Oligosaccharyl transferase
Golgi	Golgi apparatus
CDG	Congenital Disorders of Glycosylation
V _{1/2}	voltage at which 50% of activation is reached based on conductance-voltage curve
SDS-PAGE	Sodium Dodecyl Sulfate Polyacrylamide Gel Electrophoresis
Endo N	Endoglycosidase N
PNGase F	Peptide N Glycosidase F
DTT	dithiothreitol
Endo H	Endoglycosidase H
dH ₂ O	distilled water
DATD	<i>N,N'</i> diallyltartardiamide
M _r	Relative molecular mass
Δ Rf	differences in the relative electrophoretic mobility
K _v AP	K _v channel from <i>Aeropyrum pernix</i>

LIST OF ABBREVIATIONS (continued)

N-CAM	Neuronal Cell Adhesion Molecule
g	conductance
g_{\max}	maximal conductance
g/g_{\max}	conductance divided by maximal conductance
dV	slope factor based on conductance-voltage curve
$V_{1/2 (\text{peak})}$	slope factor based on conductance-voltage curve determined from the current amplitude of the peak current
$V_{1/2 (\text{ss}')} $	slope factor based on conductance-voltage curve determined from the last 10 ms of the sweep
$dV_{(\text{peak})}$	slope factor based on conductance-voltage curve determined from the current amplitude of the peak current
$dV_{(\text{ss}')} $	slope factor based on conductance-voltage curve determined from the last 10 ms of the sweep
I_{\max}/cap	maximum current amplitude divided by the cell capacitance
τ_{deac}	deactivation time constant of deactivation
Asn	Asparagine
G-V curves	Conductance-Voltage curves

CHAPTER 1 - INTRODUCTION

Brief overview of K⁺ channels

Potassium channels are the largest and most diverse group of ion channels (1) which are present in a wide range of organisms from viruses and bacteria to plants and mammals (2). These channels are integral membrane proteins which mediate the flux of K⁺ ions across the phospholipid bilayer through a highly selective pore (3). The stimuli which gate K⁺ channels are quite diverse. Some K⁺ channels are opened by ligands or G proteins (4). Others are opened by changes in transmembrane voltage and yet others by a combination of mechanisms (4).

Voltage-dependent K⁺ (Kv) channels

Voltage-gated potassium channels (Kv channels), which open and close in response to changes in membrane potential, are expressed in both excitable and nonexcitable cells (5). In neurons, these channels are major determinants involved in the modulation and fine tuning of excitable properties (6,7). Their functional roles are to: regulate the resting membrane potentials, repolarization of the action potential, the shape and duration of the action potential, and firing frequencies (5,7). This wide range of functional diversity is reflected by the large variety of Kv channel polypeptides expressed in the central nervous system (8-11). In nonexcitable cells, Kv channels are critical contributors in cell proliferation, cell volume regulation, lymphocyte differentiation and hormone secretion (12).

Biophysical properties of the Kv3 channel subfamily

Kv channels comprise a large family of proteins with diverse structural and functional properties. There are twelve known subfamilies of Kv channels (Kv1-12) which have been described (13). Within the Kv3 subfamily, there are four α subunit genes which give rise to the Kv3.1, Kv3.2, Kv3.3, and Kv3.4 proteins. The Kv3 channels are thought to play an important role in facilitating sustained or repetitive high frequency firing in neurons (14). These channels have several unique functional properties which distinguish them from other voltage-gated K^+ channels (15). These functional properties include rapid activation at voltages more positive to -10 mV and very fast deactivation kinetics (15,16). These unusual electrophysiological properties support that Kv3 channels are activated at the peak of the action potential and rapidly deactivate after the spike, and therefore, modulate action potential duration and firing frequency (14). In heterologous expression systems Kv3.1 and Kv3.2 channels generate delayed rectifier type currents, which activate relatively fast and inactivate slowly with long durations (14,15). Kv3.3 and Kv3.4 channels on the other hand, produce A-type or transient currents which activate and inactivate very quickly (14,15).

Of interest to our laboratory and the primary focus of this dissertation are the functional properties of the Kv3.1 channel. The Kv3.1 channel is defined as a “delayed rectifier” since the channel changes the membrane conductance with a delay after a voltage step relative to Na^+ current (17). The Kv3.1 channel has been shown to produce delayed rectifier type currents when expressed in *Xenopus* oocytes (18-23). The Kv3.1 channel has also been expressed in several other heterologous expression systems

including: Human Embryonic Kidney (HEK 293) cells (24), L929 cells (25), NIH 3T3 fibroblasts (26) and Chinese Hamster Ovarian (CHO) cells (27,28). When expressed in mammalian cell lines, such as HEK 293, and NIH 3T3 fibroblasts, Kv3.1 channels produced noninactivating currents with transient peaks which lacked saturation at more positive potentials (24,26,29), as well as noninactivating currents without transient peaks (26,29).

The structure of Kv3 channels

The Kv3 subfamily members, Kv3.1-Kv3.4, have been found to localize specifically in the axonal and somatodendritic compartments of neurons (16,30). Each of the four Kv3 α subunit genes generates multiple protein isoforms via alternative splicing, which differ in the amino acid sequence of the cytoplasmic tail (15,18,31-33). Based on hydropathy plots, it is predicted that each of the Kv3 subfamily members are tetrameric assemblies of α subunits each containing six transmembrane segments, termed S1 through S6, with cytoplasmic amino- and carboxyl-termini (34). The fourth transmembrane segment (S4) is positively charged and functions as the voltage sensor, moving in response to changes in transmembrane potential (34). All of the Kv3 subfamily members and their multiple protein isoforms have two absolutely conserved sites for N-glycosylation which lay within the S1-S2 extracytoplasmic linker. Previous studies conducted in our laboratory showed that both sites of the Kv3.1 channel are occupied by simple type N-glycans when heterologously expressed in *Spodoptera frugiperdae* (Sf9) insect cells (35). More recently, our studies demonstrated that both absolutely conserved

N-glycosylation sites of the Kv3.1 channel protein are fully occupied when heterologously expressed in B35 neuroblastoma cells, as well as in native neuronal tissue, along with the Kv3.3 and Kv3.4 channel proteins. Data from these studies will be presented in greater detail in Specific Aims 4 and 1 of this dissertation respectively.

Expression of Kv3 mRNA in rat brain

Northern blot analysis and *in situ* hybridization has been utilized to analyze the distribution of Kv3.1, Kv3.3, and Kv3.4 mRNAs in the central nervous system of the adult rat (22,32). These studies provided evidentiary support that Kv3.1 and Kv3.3 transcripts were the highest, followed by Kv3.2, and lastly by Kv3.4, which was the lowest (22,32). Three of four Kv3 transcripts (Kv3.1, Kv3.2, and Kv3.3), were found to be predominantly expressed in the central nervous system (22). In contrast, Kv3.4 transcript levels were abundantly detected in skeletal muscle (22) and weakly detected in brain (15). Kv3.1 transcript levels were also observed at low but detectable levels in skeletal muscle (22), while low levels of Kv3.3 transcripts were found in both the kidney and lung (15).

These Kv3 channel mRNA studies also demonstrated that Kv3.1 transcript levels were abundant in both the cerebral cortex and spinal cord (22,32,36). In contrast, Kv3.2 transcript levels were prominent in the thalamus and minimal in the cerebral cortex (32). The expression of Kv3.1 and Kv3.2 transcripts has been known to overlap in some neuronal populations, particularly in the anterior part of the brain, including the cortex, hippocampus, globus pallidus, deep cerebellar nuclei and certain thalamic nuclei (32).

However, there are many areas where Kv3.2 transcripts do not overlap with the products of the other Kv3 genes (22). Similar to Kv3.1, Kv3.3 transcript levels were also highest in the cerebral cortex and spinal cord (22). This overlap of transcript expression was expected since Kv3.1 and Kv3.3 transcripts are coexpressed in several neuronal subpopulations, including most auditory central processing neurons (15). Finally, Kv3.4 transcript levels were detected only in those neurons which expressed other Kv3 genes (15).

Brain and spinal cord distribution of Kv3 proteins

Recently, we have characterized the distribution of Kv3.1, Kv3.3, and Kv3.4 proteins throughout the central nervous system of the adult rat and notable differences have been found relative to transcript studies (37). The data from this study will be presented in greater detail in Specific Aim 2 of this dissertation. There are also additional studies evaluating Kv3.1 protein levels with contradictory findings. Data from the group of M. Weiser demonstrated that Kv3.1 protein levels were higher in the cerebellum compared to that of the thalamus, cerebral cortex and hippocampus (38). Other studies showed that high levels of Kv3.1 protein were detected in the hippocampus (39,40) and cerebral cortex (39).

Ablation of Kv3.1 and Kv3.3 channels

The ablation of Kv3 genes leads to a variety of physiological and behavioral phenotypes ranging from subtle to severe. For example, studies indicated that mice

lacking the Kv3.1 channel displayed an increased motor drive and required less sleep (41). Studies also demonstrated that Fast Spiking (FS) neurons of Kv3.1 knock-out mice displayed action potential broadening, as well as diminished firing frequency (42). In contrast, Kv3.3 deficient mice exhibited impaired motor function, as well as muscle twitches (43). Since Kv3.1 and Kv3.3 are coexpressed in the same neurons of the central nervous system, it has been suggested that the moderate phenotypic alterations observed in either single mutant are the result of functional redundancy of the Kv3.1 and Kv3.3 genes (44). Kv3.1/Kv3.3 double mutant mice (DKO) displayed severe ataxia, tremulous movements, myoclonus and hypersensitivity to ethanol (44). In spite of these debilitating motor deficits, Kv3.1/Kv3.3 deficient mice displayed no obvious learning or memory deficits (44).

The Kv1 channel subfamily

Kv1 channels are another main subfamily of voltage-gated K⁺ channels (16). A total of seven mammalian genes have been identified which belong to the Kv1 family: Kv1.1, Kv1.2, Kv1.3, Kv1.4, Kv1.5, Kv1.6 and Kv1.7 (45). These Kv channels are typically noninactivating or slowly inactivating with the exception of Kv1.4 and Kv1.7, which are fast inactivating channels (46-51). Six of the Kv1 channels, Kv1.1-Kv1.6 are expressed in mammalian brain with Kv1.1, Kv1.2 and Kv1.4 being the most abundant (16). The Kv1 channels are also expressed in excitable tissues such as smooth muscle and heart, as well as nonexcitable tissues and cell types including: colon, kidney, endothelial cells, epithelial cells, adipocytes, T cells and granulose cells (52-57). The Kv1 channels,

with the exception of Kv1.6 contain a highly conserved N-glycosylation site within the first (S1-S2) extracellular loop (16). Earlier studies demonstrated that the N-glycosylation site of the Kv1.1, Kv1.2 and Kv1.4 proteins were occupied by sialylated glycan structures in rat brain (16,58-60). Given these observations, it was of further interest to our laboratory to characterize these sialyl linkages. Our sialyl linkage studies are presented in Specific Aim 3 of this dissertation.

Biological roles of oligosaccharides

Nearly all membrane proteins are N-glycosylated (61). This co-translational and post-translational modification may serve as a primary determinant in the biosynthesis, folding, trafficking and stabilization of membrane proteins (62). Since all cells are covered with oligosaccharides, it has been predicted that specific functions of oligosaccharides at the cell surface are cell adhesion, interactions between cells and ligands, and between cells and microbes (61). Cell surface oligosaccharides are also critical determinants of cell-cell interactions (61). Furthermore, modulatory effects of glycosylation on the function of proteins has previously been suggested, and therefore will be a focal point in this dissertation with regard to the Kv3.1 channel protein heterologously expressed in B35 cells.

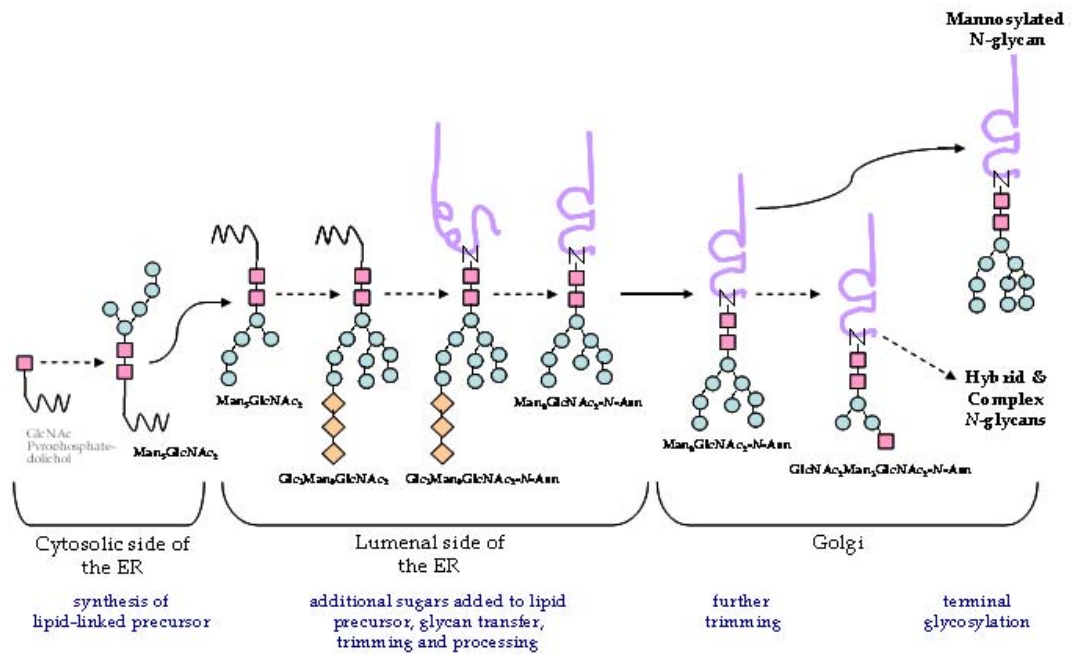
The N-glycosylation pathway

The biosynthesis of N-linked oligosaccharides begins on the cytoplasmic side of the endoplasmic reticulum (ER) with the formation of the lipid linked monosaccharide

GlcNAc-pyrophosphatedolichol (63) (Figure 1). Subsequent formation of this lipid linked monosaccharide, one GlcNAc and five mannose residues are attached in a stepwise fashion (63). The $\text{Man}_5\text{GlcNAc}_2$ intermediate structure is then translocated by flippase from the cytoplasmic side to the luminal side of the ER, where four mannose and three glucose residues are added (64). This common precursor oligosaccharide ($\text{GlcNAc}_2\text{Man}_9\text{Glc}_3$) is then transferred to selected asparagine acceptor sites located within the recognition tripeptide Asn-Xxx-Ser/Thr (where X can be any amino acid except for proline) of nascent polypeptides (63). This step is catalyzed by the membrane associated oligosaccharyl transferase (OST) complex (65). Previous studies showed that the asparagine acceptor sites must be spaced a minimum distance from the membrane surface in order to reach the active site of OST for efficient glycosylation of membrane proteins (66). Immediately after coupling to the polypeptide chain, the precursor N-glycan is then subjected to processing in the ER by the trimming of three glucose residues and one mannose residue which is catalyzed by specific glycosidases (63). This glycoprotein intermediate is then directed to the cis, medial and trans compartments of the Golgi for maturation where specific glycosidases and glycosyltransferases catalyze the removal and addition of specific sugar residues (67). In the trans-Golgi apparatus sialic acid residues are added to generate complex type N-glycans (68).

Figure 1. The N-linked glycosylation pathway

Pink squares indicate N-acetylglucosamine (GlcNAc); blue circles indicate mannose (Man); peach diamonds indicate glucose (Glc); purple lines indicate the polypeptide chain and black curvy lines indicate dolichylphosphate.

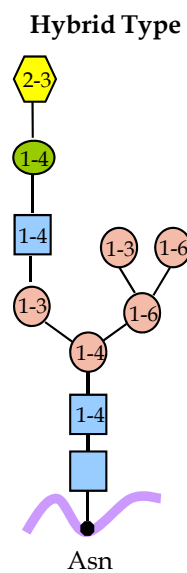
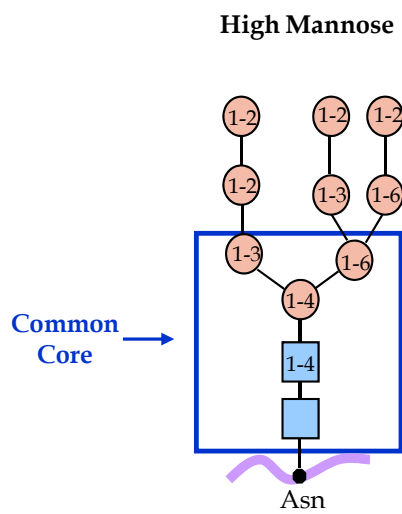


N-Linked oligosaccharide structures

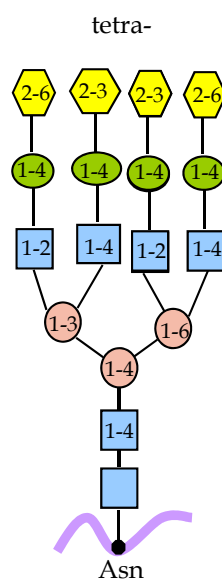
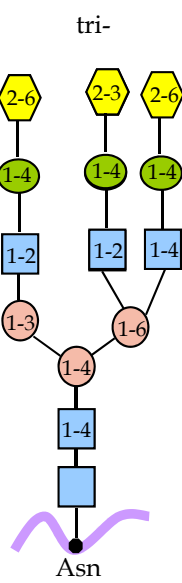
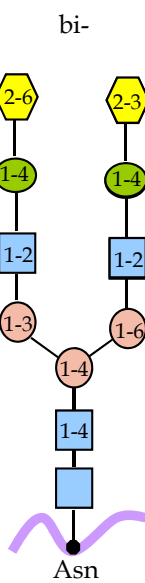
Asparagine-linked oligosaccharides are classified into three subgroups: high mannose, complex and hybrid (Figure 2). N-Linked high mannose oligosaccharides contain two to six additional mannosyl residues linked to the core pentasaccharide and may form branches (67). Complex type N-linked oligosaccharides bear two or more branches containing at least one GlcNAc, one galactose and one sialic acid residue (67). These N-glycans are often highly branched and can be di-, tri- or tetraantennary (67). Previous studies on the structure of sialylated N-glycans in the adult rat brain revealed that di-, tri- and tetraantennary N-glycans with either one or two sialyl residues are the most abundant (69,70). Hybrid N-linked oligosaccharides contain structural elements of both high mannose and complex type sugar chains (67). In the hybrid structure the α 1-6-linked core mannose has only mannose residues attached to it (similar to the high mannose type) (71). Additionally, the α 1-3-linked core mannose has one or more GlcNAc initiated antennae attached to it (similar to the complex type) (71). In general, both high mannose and hybrid type N-glycans materialize as intermediates along the processing pathway, while complex type N-glycans denote the mature form of N-linked oligosaccharides (67). However, not all N-glycans are processed to complex type due to orientation and placement in the ER and Golgi membrane, as well as the folding state which may prevent access to glycotransferases.

Figure 2. Schematic structures of different N-glycans

Different structures of high mannose, hybrid and complex type N-linked oligosaccharides. All N-linked glycoproteins have a common pentasaccharide core as outlined in dark blue. Light blue squares indicate N-acetylglucosamine (GlcNAc); green ovals indicate galactose (Gal); pink circles indicate mannose (Man); yellow hexagons indicate sialic acid (Sia); and purple curved lines indicate the polypeptide chain.



Complex Type



Diseases and disorders associated with N-linked glycosylation

N-Glycosylation is an essential process required for eukaryotic cell survival (64). Inhibition of protein N-glycosylation provokes the accumulation of unfolded proteins in the ER, and therefore induces ER stress (72). ER stress has been suggested to be involved in several neurodegenerative diseases (72,73). Furthermore, defects in the assembly of the oligosaccharide substrate or processing of oligosaccharides after they are transferred to proteins in the ER have also been shown to result in severe disorders (63,74). These disorders have profound systemic effects including psychomotor retardation, low muscle tone, incomplete brain development, impaired vision, coagulation disorders, endocrine abnormalities and dysmorphic features (75,76). These carbohydrate related genetic disorders are characterized by the absence of N-glycans or structurally abnormal N-glycans on many glycoproteins, and therefore are termed congenital disorders of glycosylation (CDG, formerly named carbohydrate deficient glycoprotein syndrome) (64).

To date, four types of CDG (types I through IV) have been identified based on the abnormal pattern of N-glycans of serum transferrin (65). CDG type I is associated with defects in monosaccharide synthesis, glycotransferases, synthesis of a dolichyl phosphate bound monosaccharide and chaperone like proteins (63). CDG type II results from defects in glycosyltransferases, glycosidases and transporters (65). The enzymatic defects for CDG type III and type IV have not yet been identified (65).

The *Mgat-I* null mouse embryo

A reduction of complex N-glycan synthesis in humans is debilitating (77,78). The gene product of *Mgat-I*, GlcNAc-TI transferase is essential for catalyzing the conversion of high mannose N-glycans to hybrid and complex N-glycans (79). Studies demonstrated that mouse embryos lacking GlcNAc-T1 activity and complex N-linked oligosaccharide synthesis do not survive past 10.5 days after fertilization (80-82). A morphological analysis of these *Mgat-I* null mouse embryos revealed several abnormalities including defects in neural tube formation and vascularization, as well as impaired determination of left-right body plan symmetry (80-82). Studies using these mutants showed that complex N-linked oligosaccharides provide crucial information during mouse embryogenesis.

N-Glycosylation modifies Kv channel function and trafficking

Despite progress in the electrophysiological characterization of N-glycosylation processing of voltage-gated K^+ channels, most studies have only been conducted in nonexcitable cells. Findings from earlier studies conducted in our laboratory demonstrated that the absence of simple type N-glycans on Kv3.1 channels, when expressed in *Spodoptera frugiperdae*, Sf9 cells, caused slower activation rates, and furthermore, a slight positive shift in voltage dependence compared to its glycosylated form (35). Further studies showed that the gating properties of Kv1.1 (58,83), Kv1.2 (84) and Kv10.1 (85) channels were altered by N-glycosylation. These functional differences included a positively shifted $V_{1/2}$ (83,84), a shallower slope for the conductance versus voltage relationship (83,84), a dramatic decrease in current density (85), slowed

activation kinetics (84,85) and decreased deactivation kinetics (84). Moreover, the absence of N-glycosylation lead to diminished trafficking of Kv 10.1 (85), Kv1.2 (84) and Kv1.4 (86) channels to the cell surface, but had little or no effect on Kv1.1 channels (86). Also, it has been shown that when N-glycosylation of HERG was abolished, currents were greatly reduced and cell surface membrane expression was virtually absent (87).

Sialylated brain N-glycans

The N-glycan pool of mammalian brain contains surprisingly elevated levels of sialylated N-glycans with atypical structures (69). Studies demonstrated that sialic acid enrich N-linked oligosaccharides account for at least 40% of the total N-glycan population in the adult mammalian brain (69,88). Sialic acids are a family of acidic 9-carbon amino sugars containing over 50 members (89,90) which occupy the non-reducing terminal position of glycan chains on many cell surface glycoproteins and glycolipids (90-92). This terminal position, as well as their net negative charge at physiological pH, explains the functional importance of sialic acid in many ligand-receptor and cell-cell interactions (89,93). The sialylation of glycoproteins and glycolipids has also played a prominent role during development, regeneration and pathogenesis (93,94).

Typical glycosidic bonds for sialic acid residues include α 2,3- and α 2,6-linkages (69,95). Sialic acid residues with α 2,3-ketosidic linkages are abundant in mammalian brain (69,95). A unique glycosidic bond for sialic acid residues is α 2,8-linkage which gives rise to di/oligo/polysialic acid units (96). These α 2,8-linked di/oligo/polysialic acid

units are primed by an initiating α 2,3-linked sialic acid attached to the terminal ends of the N-glycans (96,97). In mammalian brains, the first two glycoproteins which were identified to contain polymers of 8 or more α 2,8-linked sialic acid residues were neural cell adhesion molecules (NCAMs) (88,97-99) and the α -subunit of the voltage sensitive sodium channel (98). Since these initial findings, four additional polysialylated bearing proteins have been identified (90,100-102) Further studies demonstrated that in mammalian brain there are more α 2,8-linked disialic acid (70) and oligosialic acid chains on glycoproteins than previously thought; however the proteins have yet to be identified (88,97,98). An additional unique glycosidic bond is sialyl residues linked to internal residues of the carbohydrate chains of sialoglycoconjugates (103,104). Prior to the present investigation, this unusual glycosidic bond for sialyl residues had only been identified in gangliosides, not N-glycans (103,104).

Furthermore, evidence has suggested that the attachment of negatively charged sialyl residues to N-linked oligosaccharide chains of Kv channels plays a role in regulating channel activity. Electrophysiological studies demonstrated that reducing the sialic acid content of the Kv1.1 and Kv1.2 channels had significant functional effects on their activation parameters (83,84). Our laboratory was the first to demonstrate that sialyl residues were linked to internal carbohydrate residues of the Kv1.1, Kv1.2, and Kv1.4 N-glycans, as well as the Kv3.1, Kv3.3, and Kv3.4 N-glycans. This same investigation also showed that Kv3 and Kv1 channels contained N-linked glycoconjugates with di/oligo/polysialyl units. Until now, this linkage was not shown to be associated with K⁺

channels. The results of this study are discussed extensively in Specific Aim 3 of this dissertation.

Specific Aims of this Investigation

Asparagine-linked glycosylation is a co-translational and post-translational protein modification which is initiated in the lumen of the ER (105). The addition of N-glycan structures to proteins promotes proper folding, assembly, stability and intracellular trafficking (61). Glycoproteins displayed on the cell surface also play a vital role in cell recognition events and in cell–cell interactions (61). In recent years, the biological importance of N-linked glycan biosynthesis to mammalian physiology has been dramatically illustrated by the identification of congenital disorders of glycosylation (CDG) in humans (63,64). The biological role of complex N-linked oligosaccharides in mammalian development has also been illustrated by the generation of mouse embryos which lack a functional *Mgat-I* gene (81). Additionally, recent studies suggested that altered N-glycosylation occupancy provoked by ER stress may lead to several neurodegenerative diseases (73). N-Glycoproteins have also been shown to influence Kv1.1 (58,83), Kv1.2 (84) and Kv10.1 (85) channel function. Elegant experiments previously conducted in our laboratory demonstrated that Kv3.1 channels with unoccupied sites had slower activation kinetics and a slight positive voltage shift for channel activation compared to Kv3.1 channels occupied with N-glycans of simple type (35). Taken together, the primary goal of this dissertation was to characterize the N-glycan structures of Kv3 and Kv1 glycoproteins in the adult rat brain, as well as to

determine how neuronal N-glycosylation processing regulates the function of the Kv3.1 voltage-gated K⁺ channel in B35 neuroblastoma cells. To address this central goal, a set of four specific aims each representing a single published unit were devised and listed in the text beneath:

Specific Aim 1: To demonstrate that both absolutely conserved N-glycosylation sites of Kv3.1, Kv3.3, and Kv3.4 channels are fully occupied by complex oligosaccharides in rat brain.

Specific Aim 2: To demonstrate that sialylated N-glycan structures attached to Kv3.1, Kv3.3, and Kv3.4 channels are different throughout the central nervous system of the adult rat.

Specific Aim 3: To determine the different linkages of sialyl residues associated with N-glycans attached to Kv3.1, 3.3, 3.4, 1.1, 1.2 and 1.4 channels in rat brain, as well as a rat neuroblastoma cell line.

Specific Aim 4: To determine whether atypical sialylated N-glycans associated with the Kv3.1 protein modulated channel activity.

The experimental design employed to study these four specific aims entailed immunoband shift assays and functional measurements. Immunoband shifts generated by various glycosidase treatments of brain and spinal cord membranes, as well as immunoaffinity purified Kv3.1 protein from various transfected B35 cells, were utilized to evaluate Kv3 and Kv1 N-glycan occupancy, type, and composition. Moreover, this assay was utilized to identify specific Kv3 glycoforms. Metabolic radiolabeling of sugars combined with immunoband shifts of glycosidase digestion reactions were also employed

to determine whether the N-glycan structures of the Kv3 glycoproteins were composed of an oligo/polysialyl unit. Functional measurements were conducted in the whole cell mode of the patch clamp technique for glycosylated (wild type), unglycosylated (N220Q/N229Q), and partially glycosylated (N220Q and N229Q) Kv3.1 channels heterologously expressed in stable transfected B35 neuroblastoma cells. Activation, inactivation, and deactivation kinetics, along with current density and current type for the glycosylated (wild type Kv3.1) and each of the glycosylated mutant (N220Q/N229Q, N220Q, N229Q) Kv3.1 channels were determined and compared for statistical analysis.

CHAPTER 2 - THE PATCH CLAMP TECHNIQUE

Mastering the patch clamp technique

The patch clamp technique is a laboratory technique in electrophysiology which was originally developed in 1976 by Neher and Sakmann to study ion currents through single channels in cell membranes (106). Since then this technique has been widely used over the past three decades to investigate the role of how ion channels function under both physiological and pathological conditions in excitable and nonexcitable cells. The basic principle underlying the patch clamp technique involves using a fine-tipped glass micro-pipette. The interior of the glass micro-pipette is filled with an electrolyte which in the case of the whole cell recording mode may match the ionic composition of the cytoplasm. An electrode or chloride silver wire is placed in contact with this solution and is connected to an amplifier. In the case of the cell-attached configuration of the patch clamp technique, this electrode is used for both the passage of voltage and the recording of current. An additional chloride silver wire is placed in the bath chamber and serves as the ground electrode.

Once the electrode within the glass micro-pipette makes contact with the cell of interest, which in my case is kept in a low K^+ bath solution with the appropriate osmolarity, a brief soft suction is applied to achieve a gigaohm seal between the glass micro-pipette and the membrane. As the gigaohm seal begins to form, the horizontal lines of the current trace collapse. After forming a tight seal on the cell membrane, vertical "peaks" appear in the current trace due to the glass micro-pipette capacitance. The amplifier is then used to compensate for the glass micro-pipette capacitance from the

current recording. After electrically removing the glass micro-pipette capacitance, the vertical spikes recede.

In order to break into the whole cell recording mode of the patch clamp technique, additional soft suction is applied. This soft suction is critical in breaking the membrane and establishing electrical access into the interior of the cell. Moreover, the intracellular solution of the micro-pipette diffuses into the cytoplasm. Once electrical access into the interior of the cell has been achieved both whole cell capacitance and series resistance are compensated for by using the amplifier. Once the micro-pipette solution has diffused into the cytoplasm, whole cell currents are stimulated by numerous voltage protocols.

Although the patch clamp technique is well utilized for determining ion channel functionality, it is notoriously laborious and requires great expertise. Therefore, mastering the patch clamp technique, along with employing it to study Kv3.1 channel activity, was the major focus of specific aim 4. By measuring whole cell currents in the whole cell configuration of the patch clamp technique, I have shown that the attachment of atypical sialylated N-glycans to the Kv3.1 channel is critical for channel transitions.

CHAPTER 3 - MATERIALS AND METHODS

Brain, spinal cord and heart membrane extracts

Cerebellum, hypothalamus, cerebral cortex, hippocampus, spinal cord, thalamus, stripped brain and heart from adult Sprague-Dawley rats were purchased from Pel Freez Biological (Rogers, AR, USA). Tissues were collected from 3-18 different rats. Liquid nitrogen frozen hippocampus, spinal cord and thalamus were homogenized in 10 mL of ice-cold lysis buffer (4 mM HEPES (pH 7); 320 mM sucrose; 5 mM EDTA; protease inhibitor cocktail set III (100 mM AEBSF, Hydrochloride; 80 μ M Aprotinin, Bovine, Lung, Crystalline; 5 mM Bestatin; 1.5 mM E-64, Protease; 2 mM Leupeptin, Hemisulfate; and 1 mM Pepstatin A) 1:500 (Calbiochem, San Diego, CA, USA). In the case of cerebellum, hypothalamus, cerebral cortex, stripped brain and heart the tissues were ground to a fine powder under liquid nitrogen prior to homogenization. Subsequent to centrifugation of the homogenate at 2,000 x g in an Eppendorf F-45-30-11 rotor (Eppendorf, Westbury, NY, USA) for 10 min at 4 °C, the supernatant was stored on ice. The low speed pellet was resuspended in up to 10 mL lysis buffer, homogenized and centrifuged as described above. The resulting supernatants were pooled and then centrifuged at 197,568 x g in a TH-641 rotor (Sorvall, Newtown, CT, USA) for 1 h at 4 °C to produce a pellet containing tissue membranes. After resuspending pellets in 5 mL lysis buffer, protein concentrations were determined by the modified method of Lowry (107). Samples were then stored at -80 °C until needed. In some cases, an aliquot of each sample was combined with reducing SDS sample buffer (2X), heated at 80 °C for 3 min and analyzed by immunoblotting. In order to assess the Kv3 protein levels, as well as

identify the various Kv3 glycoforms throughout the adult rat central nervous system, SDS-PAGE gels were loaded with either 25 $\mu\text{g}/\text{well}$ of brain membrane proteins or with adjusted amounts to generate immunobands of equal intensities.

Endoglycosidase N reactions

Membrane proteins (5 g/L) or an aliquot of partially M2 immunoaffinity purified Kv3.1 protein from B35 cells (50 μL) was digested with recombinant endoglycosidase N (Endo N; 33 or 65 $\mu\text{g}/\text{mL}$) in 50 mM sodium phosphate (pH 7.5), 0.1 M sodium chloride, and protease inhibitor cocktail set III. Recombinant Endo N was expressed and isolated as previously described (108). For control reactions, 50 mM sodium phosphate (pH 7.5), 0.1 M sodium chloride was substituted for Endo N. Reactions were incubated overnight at 37 °C and processed for western blotting as described below.

Peptide N-glycosidase F (PNGase F) reactions

Membrane proteins (4-5 g/L) were digested with PNGase F (4-31 U/ μL or 12.5 U/ μL) (New England Biolabs, Ipswich, MA, USA) in a reaction mixture containing 50 mM sodium phosphate (pH 7.5), and protease inhibitor cocktail set III, plus or minus 0.8% NP-40 (Calbiochem, San Diego, CA, USA). In some cases, (Figures 9 and 12 of manuscript 2) membrane proteins (4-5 g/L) were treated with denaturation buffer (0.5 % SDS and 0.04 mol/L DTT) (New England Biolabs, Ipswich, MA, USA) at 90 °C for 10 min prior to digestion with PNGase F. Digestion reactions were allowed to proceed overnight at 37°C. For “partial” PNGase F digestions, 1 μL of diluted enzyme (25-, 80-

and 100-fold) was added to membrane proteins followed by incubation for 30 min at 37 °C. All enzyme control reactions were performed in parallel by substituting PNGase F with 50 mM sodium phosphate (pH 7.5). For immunoblot analysis, 15-60 µg (Figures 9 and 12 of manuscript 2) or 25-50 µg (Figures 5 and 6 of manuscript 1) of PNGase F digestion reactions were loaded per well on SDS-PAGE gels.

Sialidase A, C, S, and neuraminidase reactions

Sialidase A, C, and S were purchased from Glyko, San Leandro, CA, USA. Sialidase A (*A. ureafaciens*) removes α 2,3-, α 2,6-, and α 2,8-linked sialyl residues from the non-reducing termini of carbohydrate chains, as well as sialyl residues linked to internal residues of oligosaccharide chains (109-111). Sialidase C (*C. perfringens*) removes α 2,3-, and α 2,6-linked sialyl residues from the non-reducing termini of carbohydrate chains (112) while sialidase S (*S. pneumoniae*) only removes α 2,3-linked sialyl residues from the ends (113). Neuraminidase (*C. perfringens*) from New England Biolabs, Ipswich, MA, USA is identical to sialidase C however, much more concentrated. At a much higher concentration this exoglycosidase will remove α 2,8-linked sialyl residues, along with α 2,3- and α 2,6-linked sialyl residues, from the non-reducing termini of carbohydrate chains. Sialidase A (0.2-0.5 mU/µL), sialidase C (0.5-1.0 mU/µL), or sialidase S (0.2-0.5 mU/µL) were added to membrane proteins (5 g/L) in 50 mM sodium phosphate (pH 6.0) and protease inhibitor cocktail set III. Neuraminidase (1-8 U/µL) was added to membrane proteins (5 g/L) in 50 mM sodium citrate (pH 6.0) plus protease inhibitor cocktail set III. Mock digestions lacking the enzymes sialidase A, sialidase C,

sialidase S or neuraminidase were performed as controls by substituting the appropriate enzymes with either 50 mM sodium phosphate (pH 6.0) or 50 mM sodium citrate (pH 6.0). Membrane proteins were digested overnight at 37 °C. For immunoblot analysis, 15-60 µg (Figures 9 and 13 of manuscript 2) or 25-50 µg (Figure 7 of manuscript 1) of neuraminidase digestion reactions were loaded per well on SDS-PAGE gels.

Sialidase C and endoglycosidase N double digestion reactions

Sialidase C (0.5-1.0 mU/µL) and Endo N (33 or 65 µg/mL) were added to membrane proteins (5 g/L) with 50 mM sodium phosphate (pH 6.0) and protease inhibitor cocktail set III. Enzyme control reactions contained all of the above constituents except 50 mM sodium phosphate (pH 7.5) was substituted for the various glycosidases. Glycosidase digestion reactions were incubated overnight at 37 °C.

Double digestion reactions with PNGase F and either sialidase A or neuraminidase

Different combinations of PNGase F (6 U/µL or 12.5 U/µL), sialidase A (0.4 mU/µL) or neuraminidase (2 U/µL or 10-20 U/µL) were added to membrane proteins (4-5 g/L) in 50 mM sodium phosphate (pH 7.5), plus protease inhibitor cocktail set III. For control reactions, equivalent amounts of 50 mM sodium phosphate (pH 7.5) were substituted for PNGase F, sialidase A or neuraminidase. All digestions were allowed to proceed overnight at 37 °C.

Endoglycosidase H (Endo H) digestions

Membrane proteins (5 g/L), after denaturing for 10 min at 90 °C in denaturation buffer (0.5 % SDS and 0.04 mol/L DTT) were incubated with Endo H (38 U/ μ L) (New England BioLabs, Ipswich, MA, USA) in 50 mM sodium citrate containing protease inhibitor cocktail set III and NP-40 for overnight at 37 °C. In some instances, an aliquot of partially M2 immunoaffinity purified Kv3.1 protein from B35 cells was digested with Endo H (50 U/ μ L) without denaturing. Membrane proteins and partially M2 immunoaffinity purified Kv3.1 protein from B35 cells were mock treated by substituting Endo H for dH₂O. To verify the activity of Endo H a control digestion was performed in which partially purified Kv3.1 heterologously expressed in an insect cell line, Sf9 cells was supplemented to rat brain membranes. This cell line adds simple type N-glycans to Kv3.1 (35). Subsequent to these digestions 25-50 μ g (Figure 5 of manuscript 1) of membrane proteins were loaded per well on SDS-PAGE gels for immunoblot analysis.

Construction of recombinant expression vectors

Kv3.1 recombinant pcDNA3.1 mammalian expression vectors 3'FLAG-Kv3.1-pcDNA3.1, 3'FLAG-N220Q/N229Q-pcDNA3.1, 3'FLAG-N220Q-pcDNA3.1 and 3'FLAG-N229Q-pcDNA3.1 were constructed for heterologous expression in rat B35 neuroblastoma cells. Each of these constructs generate either single or double mutants in which either one or both native N-glycosylation sites at positions 220-222 (NKT) and 229-231 (NGT) of Kv3.1 were abolished (Figure 22A). Single mutants were generated by site-directed mutagenesis while the double mutant was constructed by PCR overlap

extension. The FLAG epitope tagged Kv3.1 cDNA molecules were acquired from our previous study in Sf9 cells (35). Each of the respective Kv3.1 cDNA molecules were removed from their respective Baculovirus expression vectors 3'FLAG-Kv3.1-pACSG2 by EcoRI (New England BioLabs, Ipswich, MA, USA) digestion. The isolated EcoRI fragments were then ligated into the prepared pcDNA3.1 (EcoRI) mammalian expression vector. The products of the ligation reaction were then transformed into *Escherichia coli* DH5 α TM competent cells (Invitrogen, Carlsbad, CA, USA). The resultant transformants were then screened for orientation of the Kv3.1 cDNA insert by SmaI (New England BioLabs, Ipswich, MA, USA) restriction enzyme analysis. One clone of 3'FLAG-Kv3.1-pcDNA3.1, 3'FLAG-N220Q/N229Q-pcDNA3.1, 3'FLAG-N220Q-pcDNA3.1 and 3'FLAG-N229Q-pcDNA3.1 confirmed correct orientation and was isolated and sequenced. Standard procedures were followed for DNA amplification and isolation, as well as subcloning (114).

B35 neuroblastoma cell culture

B35 cells (rat central nervous system, derived) were obtained from American Type Culture Collection (Manassas, VA, USA) and maintained in DMEM (Mediatech Inc., Manassas, VA, USA) supplemented with 10% fetal bovine serum (Invitrogen, Carlsbad, CA, USA), penicillin (50 U/mL) (Invitrogen, Carlsbad, CA, USA), and streptomycin (50 μ g/mL) (Invitrogen, Carlsbad, CA, USA) at 37 °C under 5% CO₂. B35 cells were plated on uncoated 60 mm dishes (Fisher Scientific, Suwanee, GA, USA)

every 4 days after a brief trypsin-EDTA (Invitrogen, Carlsbad, CA,USA) treatment and the cell culture medium was changed every 2-3 days.

Transient and stable transfection assay

For the production of transient and stable cell lines expressing the various forms of the Kv3.1 protein, B35 cells of 75-80% confluency were transfected with neomycin selectable pcDNA3.1 expression plasmids encoding wild type Kv3.1, N220Q/N229Q, N220Q or N229Q Kv3.1 mutants using LipofectamineTM 2000 (Invitrogen, Carlsbad, CA, USA) according to the manufacturer's protocol. In brief, FBS and antibiotic free B35 cell culture media (1 mL) containing approximately 6 or 8 µg of recombinant vector and 11.5 or 15 µL of LipofectamineTM 2000 (Invitrogen, Carlsbad, CA, USA) was added to each dish. Following an incubation of 5 h with the DMEM-DNA-lipid transfection solution, each dish of B35 cells was re-fed with 3 mL of serum and antibiotic containing DMEM medium. B35 cells were selected for stable transfectants by the addition of 1.0 g/L of Geneticin[®] (Invitrogen, Carlsbad, CA, USA) to the cell culture medium 48 h after transfection. Distinct, antibiotic-resistant, individual colonies appeared after 2-3 weeks and were dissociated into small clumps of B35 cells, and transferred into a 60 mm dish. B35 cells were then expanded into two 60 mm dishes and continuously propagated in the presence of Geneticin. Stable B35 cells expressing wild-type Kv3.1, N220Q/N229Q, N220Q, or N229Q Kv3.1 mutants were seeded onto small glass chips (Fisher Scientific, Suwanee, GA, USA) in a 35 mm dish (Fisher Scientific, Suwanee, GA, USA) and kept under culturing conditions for approximately 15 h before electrophysiological

investigations. For electrophysiological investigations, small glass chips with attached stable transfected B35 cells expressing wild-type Kv3.1, N220Q/N229Q, N220Q or N229Q glycosylation mutants were transferred to a recording chamber (Warner Instruments, Hamden, CT, USA).

Metabolic radiolabeling of sialylated N-glycans in B35 cells

For metabolic radiolabeling experiments, 1.5 mL of complete medium, plus 1.5 mL of complete medium containing acetyl-D-mannosamine, N-[6-³H] (31 μ Ci/mL) (American Radiolabeled Chemicals, St. Louis, MO, USA) was added to each dish of B35 cells following a 5 h incubation with the DMEM-DNA-lipid transfection solution. Acetyl-D-mannosamine, N-[6-³H] is a precursor of sialic acid and is commonly used to radiolabel sialylated N-glycans (115). After 22-24 h the unradiolabelled and radiolabeled transient transfected B35 cells were harvested and Kv3.1 was immunoaffinity purified as described in the text below. Unradiolabelled samples were loaded on 12% SDS gels and Western blotted using the method described below. Radiolabelled proteins were separated on 10% SDS gels using *N,N'*diallyltartardiamide (DATD) (Bio-Rad, Hercules, CA, USA) as the crosslinker, instead of bis-acrylamide. Gel slices of interest were excised between the 150 and 75 kDa KaleidoscopeTM markers (Bio-Rad, Hercules, CA, USA). This region contained the heterologously expressed Kv3.1 protein with complex N-glycans as determined by Western blotting of transfected B35 membranes separated on 10% SDS gels using DATD as a crosslinker. Surprisingly, the Kv3.1 protein ran much faster on this type of gel and was just above the 100 kDa marker. Excised gel slices were

placed in 2% sodium periodate solution (0.5-1 mL) (Aldrich Chemical Co., Inc., Milwaukee, WI, USA) and incubated on a shaker at ambient temperature. After 2-4 h, scintillation fluid (5 mL) (Fisher Scientific Co., Hampton, NH, USA) was added to each sample. Samples were then refrigerated for approximately 1 h before radioactivity was measured by scintillation counting for 20 min to reduce the margin of error to less than 5%.

M2 immunoaffinity purified Kv3.1 protein and glycosidase digestion reactions

Wild type Kv3.1, N220Q/N229Q, N220Q and N229Q stable transfected B35 cells (4, 60 mm plates per sample) were resuspended in lysis buffer (50 mM Na₂HPO₄; 0.3 M KCl, pH7.5 and 0.5% Triton X-100) and then sonicated at a power setting of 3 with short pulses till solubilized. After centrifugation at 500 x g in an Eppendorf F-45-30-11 rotor (Eppendorf, Westbury, NY, USA) for 15 min at 4°C, supernatants were collected and M2-Flag® resin (40-50 µL, 1:1 gel slurry) (Sigma-Aldrich, St. Louis, MO, USA) was added. Next, samples were rotated for 1 h at room temperature and centrifuged at 400 x g in an Eppendorf F-45-30-11 rotor (Eppendorf, Westbury, NY, USA) for 3 min at 4 °C. The resin was then washed twice in 50 mM Na₂HPO₄; 0.3 M KCl, pH7.5 followed by two additional washes with PBS. In some instances, partially purified wild type, N220Q/N229Q, N220Q, and N229Q Kv3.1 proteins were combined with reducing SDS sample buffer (2X) and analyzed by western blotting as described in the text below. For neuraminidase digestion reactions, the resin was washed an additional time in 50 mM sodium citrate (pH 6.0) followed by resuspension. Equal volumes of resuspended resin

were then split into two separate tubes. Neuraminidase (0.83 U/ μ L) (New England Biolabs, Ipswich, MA, USA), was then added to the appropriate tube while 50 mM sodium citrate (pH 6.0) was added to the control reaction. For “partial” PNGase F digestions, 1 μ L of diluted enzyme (10-, 20-, 40- and 80-fold) was added to resin washed and resuspended in 50 mM sodium phosphate in a total reaction volume of 50 μ L. For metabolic radiolabeling experiments control and Endo N reactions were washed an additional time with 1 mL PBS, while the neuraminidase reaction was washed once more with 1 mL of 50 mM sodium citrate (pH 6.0). Endo N (33 or 65 μ g/mL) or neuraminidase (10 U/ μ L) was then added to the appropriate tubes while PBS was added to the control reaction. All glycosidase digestion reactions were allowed to proceed overnight at 37 °C.

B35 cell membrane isolation

Nontransfected B35 cells (about 11×10^7) were homogenized (70-90 strokes) in 2 mL of lysis buffer (10 mM Tris (pH 7.4)); 250 mM sucrose, 5mM EDTA; protease inhibitor cocktail set III 1:500 (Calbiochem, San Diego, CA, USA), and subsequently centrifuged at 2,000 x g in an Eppendorf F-45-30-11 rotor (Eppendorf, Westbury, NY, USA) for 10 min at 4°C. The supernatant was then centrifuged at 197,568 x g in a TH-641 rotor (Sorvall, Newtown, CT, USA) for 1 h at 4 °C. The high speed pellet was resuspended in about 1 mL lysis buffer and the protein concentration was determined by the method of Lowry. Samples were then stored at -80 °C until needed. In some cases an aliquot of each sample was combined with reducing SDS sample buffer (2X) and analyzed by western blotting.

Western blotting

For preparation of immunoblots, reducing SDS sample buffer (2X) was added to all undigested and digested reactions of membrane proteins, partially M2 immunoaffinity purified Kv3.1 protein samples, as well as B35 membranes, and was subjected to electrophoresis for 100 min at 20 mAmps on SDS-PAGE gels in a Mini Protean® Cell (Bio-Rad, Hercules, CA, USA). 10% SDS-PAGE gels were used for Kv3 and N-CAM proteins while 12% and 15% were utilized for Kv1 and transferrin proteins, respectively, unless otherwise indicated. Separated proteins were transferred to Immobilon-P PVDF (Millipore, Billerica, MA, USA) membranes for 1-1.5 h at 175 mAmp using a Mini Trans-Blot[®] Cell (Bio-Rad, Hercules, CA, USA) containing CAPS buffer (10 mM 3-cyclohexylamino-1-propane sulfonic acid, 10% methanol; pH 11). However, nitrocellulose (Invitrogen, Carlsbad, CA, USA) membranes were utilized for the anti-Kv1.2 antibody. Next, blotted membranes were blocked by incubation for 30 min in membrane blocking buffer (PBS, 3% BSA with 0.1% Tween 20). Blotted membranes were then incubated with commercially available anti-Kv1 (NeuroMab, Davis, CA, USA), anti-Kv3 (Alamone Labs, Jerusalem, Israel), anti-N-CAM (Cell Signaling Technology, Danvers, MA, USA), or anti-transferrin (Santa Cruz Biotechnology, Inc., Santa Cruz, CA, USA) antibodies for 2 h at room temperature. However, the incubation of the anti-Kv1.2 antibody with heart membrane proteins was allowed to proceed overnight at 4 °C. The Kv antibodies are specific for: rat Kv1.1 (accession no. P10499), EEDMNSIAHYRQANIRTG; rat Kv1.2 (accession no. P63142), EGVNNSNEDFRENLKTA; rat Kv1.4 (accession no. P15385),

NSHMPYGYAAQARARERERLAHSR; rat Kv3.1b (accession no. P25122), CKESPVIKYMPTTEAVRT; rat Kv3.3 (accession no. Q01956), KSPITPGSRGRYSRDRAC; and rat Kv 3.4 (accession no. Q63734), EAGDDERELALQRLGPHEG(C). The specificities of the anti-Kv1 (59) and anti-Kv3 (35,37,116) antibodies have been previously described. Following incubation, blotted membranes were washed three times with PBS plus 0.1% Tween 20 and then treated with their specific alkaline phosphate conjugated secondary antibody for 2 h. In some cases, the incubation proceeded overnight at 4 °C. Following three washes with PBS plus 0.1% Tween 20, bound antibodies were detected by Immuno alkaline phosphatase substrate (MP Biomedicals, Irvine, CA, USA).

Western blot analysis

The level of each Kv3 protein in the various tissues tested was determined by comparing the intensity and surface area of the immunobands when equal amounts were loaded. Alternatively, Western blots were subjected to quantitative analysis using UNSCANIT computer software (Silk Scientific, Inc., Orem, UT, USA) for parametric tests. Immunobands were digitized and the total number of pixels for each of the designated immunobands was counted. Background intensity was subtracted from each of the designated band intensities. Values of intensity differences were normalized using the net intensity of stripped brain. Relative molecular masses (Mr) for the Kv3 proteins were estimated by plotting the log of the molecular masses for each of the Kaleidoscope marker (Bio-Rad, Hercules, CA, USA) bands as a function of their relative mobilities. A

linear equation derived from the least-squares method was then used to generate the apparent molecular mass. To enhance protein separation, the dye front was permitted to run off the gel, therefore the relative mobility (Rf) is defined as the distance migrated by the immunoband divided by the length of the separating gel. Differences in the relative electrophoretic mobility ($\Delta R_f \times 100$) represent the electrophoretic mobility shifts induced by the various glycosidase treatments for each of the glycoproteins. Group data were presented as mean \pm S.E. (n represents the number of Western blots). When comparing the significance of two groups, the unpaired Student's t test was utilized. All experiments involving comparisons between multiple groups were analyzed using a one-way ANOVA followed by Bonferroni's post hoc-tests. A value of $P < 0.05$ was considered significant.

Whole cell recordings

Electrophysiological measurements were obtained from stable transfected B35 cells using the whole cell configuration of the patch clamp technique. Whole cell K^+ currents were recorded at room temperature with an Axopatch 200B amplifier (Axon Instruments, Sunnyvale, CA, USA) controlled by CLAMPEX 9.0 software (Axon Instruments, Sunnyvale, CA, USA) running on a Dell Optiplex GX270 Pentium desktop computer using a Digidata 1322A analog-to-digital interface (Axon Instruments, Sunnyvale, CA, USA). Whole cell recordings were primarily conducted in pairs to reduce possible differences due to passage number and cell treatment. These differences were minimized by conducting the cell transfections and whole cell recordings in parallel for each pair. The two pairs were wild type Kv3.1 and N220Q/N229Q channels, and the two

single mutant channels, N220Q and N229Q. In some cases, whole cell recordings of either wild type Kv3.1 or N220Q/N229Q were conducted along side the single mutants. The external bath solution utilized during recordings had the following composition (in mM): 5 potassium aspartate, 135 sodium aspartate, 1 MgCl₂ hexahydrate, 10 Mes, 60 mannitol (pH 6.3). The measured osmolarity of the external bath solution was 295-312 mOsm. Borosilicate glass tubing (Sutter Instruments, Novato, CA, USA) was pulled with a P-97 Flaming-Brown micropipette puller (Sutter Instruments, Novato, CA, USA) and fire polished with a MF-830 microforge (Narishige, McHenry, IL, USA) to obtain patch pipettes with a resistance of 4-9 M Ω when filled with intracellular solution. The intracellular solution contained (in mM): 140 potassium aspartate, 10 EGTA, 5 MgCl₂ hexahydrate, 10 Hepes, 50 mannitol (pH 7.2). The measured osmolarity of the internal pipette solution was 320-340 mOsm. For comparative reasons, the solutions were similar to those previously used to examine the functional role of simple type glycans attached to the Kv3.1 channel in Sf9 cells (35). The only difference between the solutions was the slightly higher osmolarity for the mammalian cells. Both cell capacitance and series resistance was compensated for throughout the course of experiments. The patch pipette silver/silver chloride wire was connected to the input of an Axopatch 200B amplifier through a salt bridge (plastic pipette tip filled with 3% Agarose in 0.3M KCl). All Kv3.1 currents were sampled at 10 kHz subsequent filtering at 1 kHz. Whole cell current recordings were accepted during these experiments only if membrane seal resistance was $\geq 1\text{G}\Omega$, minimum current amplitudes were ≥ 400 pA and minimal cell capacitance was displayed after compensation. Of note, the endogenous current was minor in

nontransfected B35 cells (the mean maximum current amplitude was 37.9 ± 4.2 pA with a mean capacitance of 11.6 ± 1.6 pF, $n = 21$) compared to the Kv3.1 transfected B35 cells (Table 1). Whole cell recordings were acquired from several voltage clamp protocols. For the activation protocols, K^+ currents were elicited by depolarizing pulses (100 ms and 2 s) from -40 mV to +80 mV in 10 mV increments at a holding potential of -50 mV. Currents were evoked from deactivation protocols by stepping to +40 mV (25 ms) and then stepping from -110 mV to 0mV (200 ms) in 10 mV increments from a holding potential of -50 mV.

Current analysis

Digitized whole cell current recordings from stable transfected B35 cells were analyzed using the CLAMPFIT 9.0 analysis program (Axon Instruments, Sunnyvale, CA, USA). Graphs were generated using Origin 7.5 (OriginLab Corporation, Northampton, MA, USA). Normalized conductance-voltage relationships were constructed by normalizing conductance to maximal conductance and were fitted with a Boltzmann equation of the form: $G = G_{\max}/[1 + \exp(V_{0.5} - V_m)/q]$ where q represents the slope factor, V_m stands for the test potential, $V_{0.5}$ is the potential at which the conductance was half maximal, G is the conductance and G_{\max} is the maximal conductance. For activation kinetics, whole cell current recordings were analyzed by both rise times and activation time constants. Rise times represent the time required for the current to rise from 10% to 90% of its peak current at a given applied test potential. Activation time constants were fitted with a single exponential function at +40 mV. The mean deactivation time constant

(tau) was determined by fitting the current at -60 mV with a single exponential. For inactivation kinetics the percentage of current decay at +40 mV and +60 mV was determined by dividing the peak current amplitude by the current remaining near the last 10 ms of the +40 mV and +60 mV sweep. The peak current amplitude was determined from 3 ms of data points for inactivating currents and noninactivating currents without transient peaks, as well as from 1 ms for noninactivating currents with transient peaks. Current density was calculated by dividing the maximum current amplitude for each stable transfected B35 cell by the cell capacitance. Data are presented as the mean \pm S.E. and n represents the number of cells tested. Student's t -test was utilized to evaluate the statistical comparisons. One-way ANOVA was used to evaluate statistical significance when more than two groups were compared. Statistical significance was considered at $P < 0.05$ or $P < 0.01$ as indicated in the figure legends.

CHAPTER 4 - COMPLEX OLIGOSACCHARIDES ARE N-LINKED TO KV3

VOLTAGE-GATED K⁺ CHANNELS IN RAT BRAIN

Tara A. Cartwright, Melissa J. Corey, Ruth A. Schwalbe

Biochimica et Biophysica Acta 1770 (2007) 666-671

Abstract

Neuronal Kv3 voltage-gated K^+ channels have two absolutely conserved N-glycosylation sites. Here, it is shown that Kv3.1, 3.3, and 3.4 channels are N-glycosylated in rat brain. Digestion of total brain membranes with peptide N glycosidase F (PNGase F) produced faster migrating immunobands than those of undigested membranes. Additionally, partial PNGase F digests showed that both sites are occupied by oligosaccharides. Neuraminidase treatment produced a smaller immunoband shift relative to PNGase F treatment. These results indicate that both sites are highly available and occupied by N-linked oligosaccharides for Kv3.1, 3.3, and 3.4 in rat brain, and furthermore that at least one oligosaccharide is of complex type. Additionally, these results point to an extracytoplasmic S1–S2 linker in Kv3 proteins expressed in native membranes. We suggest that N-glycosylation processing of Kv3 channels is critical for the expression of K^+ currents at the surface of neurons, and perhaps contributes to the pathophysiology of congenital disorders of glycosylation.

Introduction

The Kv3 channel family is part of the large super gene family of voltage gated K⁺ (Kv)¹ channels. These channels play an essential role in enabling neurons to fire repetitively at high frequencies (14). There are four different Kv3 genes: Kv3.1, 3.2, 3.3 and 3.4, and by alternative splicing encode for multiple protein isoforms with divergent C termini(15,18,31-33). Hydropathy plots predict that Kv3 channels possess six transmembrane segments (S1–S6) with cytoplasmic amino-and carboxyl-termini (Figure 3). The Kv3 multiple protein isoforms have two absolutely conserved sites for N-glycosylation which lie within the S1–S2 extracytoplasmic loop. Amino acid sequence identity of the S1–S2 linker is 100% identical for the Kv3.1 protein of: rat, human, mouse, rabbit and cattle, and greater than 95% for the Kv3.4 protein (Figure 4). Sequence identity is also highly conserved for Kv3.2 and Kv3.3 proteins.

Attachment of N-linked oligosaccharides to newly synthesized membrane proteins is the most ubiquitous protein co-translational modification in the lumen of the endoplasmic reticulum (ER) (105). The required protein consensus sequence is AsnXxxSer/Thr, where Xxx can be any amino acid except for proline. Maturation of the glycoprotein occurs in the lumen of the ER and Golgi apparatus. The importance of the N-glycosylation process has been indicated in congenital disorders of glycosylation (CDG) (64) and mice mutants (80,81,117,118). Of recent, endoplasmic reticulum (ER) stress has been suggested to be associated with neurodegenerative diseases (73).

N-Glycosylation of K⁺ channels has been shown to influence: folding, trafficking, and function (35,58,83,86,119). It has also been used as an extracellular marker to verify

Figure 3. Topological model of Kv3 channels

The Kv3 monomeric unit in a lipid bilayer. Transmembrane segments (S1–S6) are represented by cylinders in the lipid bilayer. The first transmembrane segment (S1) to the sixth transmembrane segment (S6) proceed counter clockwise. Black circles denote the Asn of the two native N-glycosylation consensus sequences for Kv3 channels. Branched structures represent N-linked oligosaccharides.

Figure 3
Cartwright et al., 2006

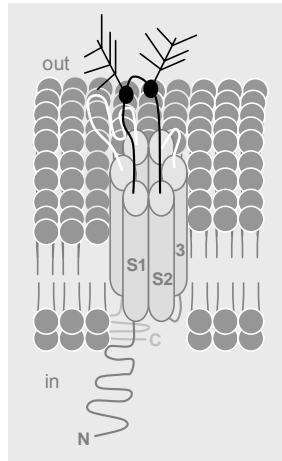


Figure 4. Amino acid sequence alignments of the S1–S2 linker of Kv3 channels

Alignments of available amino acid sequences of the S1–S2 linker for Kv3 channels in: rat, human, mouse, rabbit, and cattle. Conserved, native N-glycosylation sites are shown as underlined, enlarged font. The italicized number indicates the first residue of the S1–S2 linker. The shaded regions represent amino acids which are non-identical. Accession numbers are as follows: Kv3.1 Rat P25122, Human P48547, Mouse P15388, Rabbit AAX23602, Cattle AAX23601; Kv3.2 Rat P22462, Human AAO89503, Mouse NP_001020752; Kv3.3 Rat Q01956, Human Q14003, Mouse Q63959, Rabbit AAN15930; Kv3.4 Rat Q63734, Human Q03721, Mouse NP_666034, Rabbit AAM46839, Cattle XP_613047.

Figure 4
Cartwright et al., 2006

Kv3.1	Rat	210	ETHERFNPIV <u>NKTE</u> IEIENVR <u>NGT</u> QVRYRYREAETEAFPTY
Kv3.1	Human	210	ETHERFNPIV <u>NKTE</u> IEIENVR <u>NGT</u> QVRYRYREAETEAFPTY
Kv3.1	Mouse	210	ETHERFNPIV <u>NKTE</u> IEIENVR <u>NGT</u> QVRYRYREAETEAFPTY
Kv3.1	Rabbit	210	ETHERFNPIV <u>NKTE</u> IEIENVR <u>NGT</u> QVRYRYREAETEAFPTY
Kv3.1	Cattle	210	ETHERFNPIV <u>NKTE</u> IEIENVR <u>NGT</u> QVRYRYREAETEAFPTY
Kv3.2	Rat	249	ETHEAFNIVK <u>NKTE</u> EPVI <u>NGT</u> SAVLQYEIETDPALTY
Kv3.2	Human	249	ETHEAFNIVK <u>NKTE</u> EPVI <u>NGT</u> SVVLQYEIETDPALTY
Kv3.2	Mouse	253	ETHEAFNIVK <u>NKTE</u> EPVI <u>NGT</u> SPVLQYEIETDPALTY
Kv3.3	Rat	311	ETHEGFIHIS <u>NKT</u> VTQASPIPGAPPE <u>NI</u> TNVEVETEPFLTY
Kv3.3	Human	310	ETHEGFIHIS <u>NKT</u> VTQASPIPGAPPE <u>NI</u> TNVEVETEPFLTY
Kv3.3	Mouse	310	ETHEGFIHIS <u>NKT</u> VTQASPIPGAPPE <u>NI</u> TNVEVETEPFLTY
Kv3.3	Rabbit	312	ETHEGFIHIS <u>NKT</u> VTQASPIPGAPPE <u>NV</u> TNVEVETEPFLTY
Kv3.4	Rat	249	ETHEAFNIDR <u>NVTE</u> IHRVG <u>NI</u> TSVFRREVETEPILTY
Kv3.4	Human	248	ETHEAFNIDR <u>NVTE</u> ILRVG <u>NI</u> TSVFRREVETEPILTY
Kv3.4	Mouse	252	ETHEAFNIDR <u>NVTE</u> IHRVG <u>NI</u> TSVFRREVETEPILTY
Kv3.4	Rabbit	72	ETHEAFNIDR <u>NVTE</u> IHRVG <u>NI</u> TSVFRREVETEPILTY
Kv3.4	Cattle	243	ETHEAFNIDR <u>NVTE</u> IHRVG <u>NT</u> TSVFRREVETEPILTY

topological K⁺ channel structure (35,120-123). Here we have evaluated utilization of the N-glycosylation consensus sequences of Kv3.1, 3.3, and 3.4 in rat brain. Western blots of total brain membranes demonstrated that Kv3.1, 3.3, and 3.4 proteins were expressed in rat brain. When total brain membranes were treated with peptide N glycosidase F (PNGase F) or neuraminidase, immunobands of Kv3.1, 3.3, and 3.4 migrated faster than those from untreated membranes. Endoglycosidase H (Endo H) treatment of total membranes did not alter the immunoband patterns of Kv3.1, 3.3, and 3.4 from those of untreated samples. Based on enzyme specificities and electrophoretic migration patterns, our results indicate that both N-glycosylation sites are highly available and occupied by N-linked oligosaccharides of either hybrid or complex types. In addition, these results indicate that the S1-S2 loop is extracytoplasmic in native membranes. Given the above observations, the high conservation of N-glycosylation sites, and CDG diseases, we suggest that N-glycosylation processing of the Kv3 channels is critical in regulating the expression of K⁺ currents at the surface of neurons.

Results

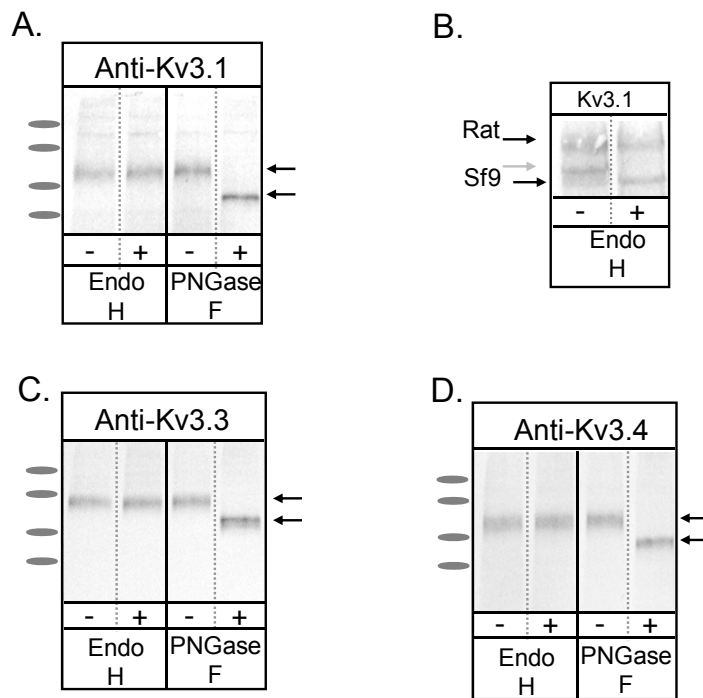
N-Glycosylation of Kv3 channels

Two absolutely conserved N-glycosylation consensus sequences of Kv3 proteins are located between the first two transmembrane segments (S1-S2; Figure 3). The first site is predicted to be 10 amino acid residues from the C-terminus of the S1 segment, the last site is at least 12 amino acid residues from the N-terminus of the S2 segment, and the number of amino acid residues between the sites is at least 4 (Figure 4). Membranes were isolated from total brain of an adult female rat. Total brain membranes were digested with EndoH (an endoglycosidase which removes high mannose oligosaccharides) [23], and PNGase F (an amidase which removes high mannose, hybrid, and complex oligosaccharides) (124) and then analyzed by Western blots (Figure 5). When brain membrane proteins separated on a 10% SDS gel were transferred to blotting membranes and probed with anti-Kv3.1b antibodies, a diffused immunoband which migrated to about 110 kDa was observed (Figure 5A). The electrophoretic mobility of this band remained unchanged when membrane proteins were treated with Endo H. However, when membrane proteins were digested with PNGase F, the immunoband migrated much faster to about 84 kDa, as we have previously shown (35). The relative molecular weight of the Kv3.1 protein was much larger than the calculated molecular weight of 66 kDa. To demonstrate that the Kv3.1 immunoband did not shift as a result of inactive Endo H under the reaction conditions, partially purified Kv3.1 heterologously expressed in Sf9 cells was added to total rat brain membranes prior to Endo H digestion (Figure 5B). Previously, we showed that Kv3.1 expressed in infected Sf9 cells has both sites occupied

Figure 5. Kv3 proteins are N-glycosylated in rat brain tissue

Total rat brain membranes were untreated (-) or treated (+) with Endo H or PNGase F as indicated, subjected to SDS-PAGE and immunoblotted using anti-Kv3.1b (A), anti-Kv3.3 (C), and anti-Kv3.4 (D) antibodies. As a control Endo H digestion was carried out in total rat brain membranes supplemented with partially purified Kv3.1 from infected Sf9 cells (B). The black arrows point to glycosylated (upper arrow) Kv3 protein derived from rat brain or unglycosylated (lower arrow) Kv3 proteins from rat brain or infected Sf9 cells for each panel. The gray arrow represents glycosylated Kv3.1 protein expressed in infected Sf9 cells(B).Ovals represent Kaleidoscope™ protein standards (top to bottom in kDa): 250, 150, 100, and 75.

Figure 5
Cartwright et al., 2006



by simple type N-glycans (35). This result is verified when Kv3.1 protein derived from Sf9 cells is digested in the presence of total rat brain membranes. Of note, the Kv3.1 protein derived from rat brain shows a similar electrophoretic migration as undigested samples. Taken together, these results indicate that the N-glycans attached to Kv3.1 in the rat brain are hybrid or complex types, not simple type.

Similar sets of experiments were performed using either anti-Kv3.3 (Figure 5C) or anti-Kv3.4 (Figure 5D) antibodies to probe blotting membranes. In both cases the immunobands migrated faster when total brain membranes were digested with PNGase F, but not Endo H. Relative molecular weights of Kv3.3 and Kv3.4 proteins in total rat brain membranes were about 131 kDa and 121 kDa, respectively. When samples were treated with PNGase F, relative molecular weights of Kv3.3 and Kv3.4 proteins were about 107 kDa and 102 kDa, respectively. In all cases, the relative molecular weights were quite large compared to their calculated molecular weights of 94 kDa for Kv3.3 and 68 kDa for Kv3.4. Previous studies are in agreement that Kv3.1b (38-40,125), Kv3.3 (126) and Kv3.4 (127) proteins migrate much slower than their calculated molecular weights when expressed in native tissue. However, it was not demonstrated in these studies whether the slower migration patterns were due to N-glycosylation. Our results indicate that Kv3.1, 3.3 and 3.4 channel proteins have N-linked oligosaccharides of hybrid or complex types, and furthermore that the channels are following the N-glycosylation processing route for delivery of functional channels to the plasma membrane. Additionally, these results show that the expression of Kv3.4 protein is easily detected, like Kv3.1 and 3.3, even though the transcript levels have been reported to be relatively low (22).

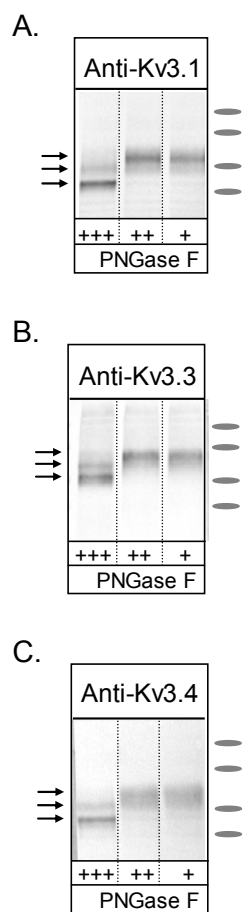
Occupancy of both conserved N-glycosylation sites

To show that both native N-glycosylation consensus sequences were indeed occupied by oligosaccharides, partial PNGase F digestions were conducted (Figure 6). When membranes were digested with the two lower amounts of PNGase F, an immunoband corresponding to the Kv3.1 immunoband identified in untreated membranes was observed (Figure 6A). However, this immunoband was much broader and occurred in the downward direction. The Kv3.1 immunoband broadening appeared much like a diffused doublet, and suggested the removal of one of the N-linked oligosaccharides. Indeed this was the case, the lower band of the doublet became quite defined at the highest level of PNGase F, the upper band disappeared, and furthermore an even faster migrating band was observed (Figure 6A). The upper band corresponded to the fully glycosylated Kv3.1 protein and was similar to Kv3.1 identified in membranes which were not digested with PNGase F (Figure 5A). The fastest migrating band corresponded to the unglycosylated Kv3.1 protein which was identified by complete digestion with PNGaseF as shown in Figure 5A. The middle band was assigned to Kv3.1 with one site occupied by N-linked oligosaccharide. These results demonstrate the Kv3.1 protein has both sites utilized in native tissue, similar to that previously shown when Kv3.1 was expressed in *Spodoptera frugiperda* (Sf9) cells (35). When partial PNGase F digestions were carried out with Kv3.3 (Figure 6B) and Kv3.4 (Figure 6C) proteins, the findings were similar to that of the Kv3.1 channel. As the amount of PNGase F was increased, the upper immunoband or the fully glycosylated forms of both Kv3.3 and 3.4 channels disappeared, while two distinct lower bands could be observed. In both cases, the lowest band

Figure 6. Utilization of both N-glycosylation sites for Kv3 proteins

Total rat brain membranes were treated with various dilutions of PNGase F (25-fold, +++; 80-fold, ++; and 100-fold, +). After digestions, samples were analyzed by Western blots using anti-Kv3.1b (A), anti-Kv3.3 (B), and anti-Kv3.4 (C) antibodies. The upper arrow represents fully glycosylated Kv3 proteins, the center arrow is one glycosylation site of the Kv3 protein occupied, and the lowest arrow is unglycosylated Kv3 protein. Ovals represent molecular weight standards (top to bottom in kDa): 250, 150, 100, and 75.

Figure 6
Cartwright et al., 2006



corresponded to unglycosylated Kv3.3 or 3.4 proteins, while the middle band represented occupancy of one glycosylation site, and the upper band was occupancy of both glycosylation sites.

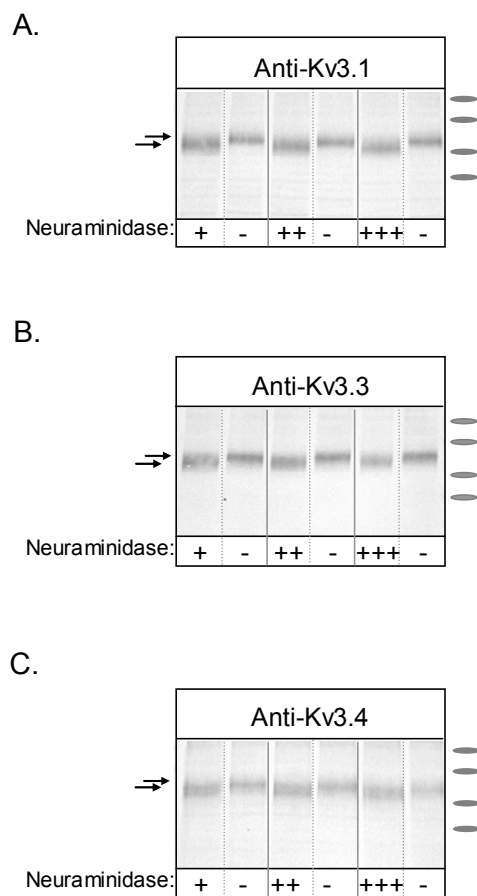
N-Linked oligosaccharides are of complex type

Neuraminidase, an enzyme which removes $\alpha 2-3$, $\alpha 2-6$, and $\alpha 2-8$ linked sialic acid residues from oligosaccharides (79), was utilized to determine whether the N-glycans of Kv3.1, 3.3 and 3.4 were of complex type. Total brain membranes were treated with three different amounts of neuraminidase, and then Kv3.1b (Figure 7A), Kv3.3 (Figure 7B), and Kv 3.4 (Figure 7C) proteins were identified by Western blotting. In all cases, a downward shift of the immunobands was observed in the samples treated with neuraminidase. The shift was much more dramatic for Kv3.1 and Kv3.3 proteins than that of the Kv3.4 protein. These results indicate that at least one N-linked oligosaccharide is of complex type for Kv3.1, 3.2, and 3.4.

Figure 7. N-Linked oligosaccharides of Kv3 proteins are of complex type

Total rat brain membranes were untreated (-) or treated with increasing amounts (+, ++, +++) of neuraminidase, and immunoblotted using anti-Kv3.1b (A), anti-Kv3.3 (B), and anti-Kv3.4 (C) antibodies. The upper arrows represent the native Kv3 glycoform and the lower arrow represents Kv3 protein with various amounts of sialic acid residues removed. Ovals are Kaleidoscope™ protein standards (top to bottom in kDa): 250, 150, 100, and 75.

Figure 7
Cartwright et al., 2006



Discussion

Here the results show that the two absolutely conserved N-glycosylation sites of Kv3.1 (NKT, amino acid residues at positions 220–222 and NGT, amino acid residues at positions 229–231), Kv3.3 (NKT, amino acid residues at positions 221– 223 and NIT, amino acid residues at positions 237–239), and Kv3.4 (NVT, amino acid residues at positions 259–261 and NIT, amino acid residues at positions 268–270) are occupied by large hydrophilic oligosaccharides in rat brain. Occupancy of these sites provides evidence that the S1–S2 linkers of Kv3.1, 3.3 and 3.4 channels are fairly flexible and in an aqueous environment (Figure 3). This finding is in agreement with glycosylation of the S1–S2 linker of other Kv channels (35,86,123,128-130). However, it is quite different from the X-ray structure of a Kv channel from *Aeropyrum pernix* (KvAP) which suggested the S1–S2 linker resides in the membrane for all Kv channels (131).

Secondly, these results show that virtually all of the Kv3.1, 3.3, and 3.4 channel proteins are N-glycosylated in total rat brain membranes indicating the availability of sites to the oligosaccharyltransferase is high. Occupancy of N-glycosylation sites is also regulated by enzyme kinetics and substrate levels in the ER (132). Therefore, it is plausible that certain cell types of the brain, which have either lower enzyme activities or lower levels of substrate, may generate some Kv3 protein with vacant N-glycosylation sites.

CDG group I patients have unoccupied N-glycosylation sites due to defective enzymes involved in the biosynthesis of the lipid-linked core oligosaccharide (64). Based on high occupancy of the Kv3.1, 3.3, and 3.4 channels in total brain, it would be very

likely that occupancy of Kv3.1, 3.3, and 3.4 channels would be lower in CDG group I patients than normal individuals. Previously, we have shown that unglycosylated Kv3.1 channels expressed in Sf9 cells have slower activation kinetics than glycosylated Kv3.1 channels (35). Taken together, it could be suggested that the Kv3 channels contribute to abnormal brain development, and aberrant function of the nervous system in CDG group I patients.

CDG diseases emphasize the importance of occupied N-glycosylation sites and distinct N-linked oligosaccharide structures for mammalian physiology (64). The influence of N-glycosylation on the initiation and development of human neuronal diseases are unknown. However, it has recently been suggested that ER stress contributes to some human neurodegenerative diseases (73). Future studies are needed to determine whether environmental factors or infections which cause ER stress alter occupancy or N-linked oligosaccharide structure of neuronal proteins such as the Kv3 channels.

**CHAPTER 5 - NOVEL KV3 GLYCOFORMS DIFFERENTIALLY EXPRESSED
IN ADULT MAMMALIAN BRAIN CONTAIN SIALYLATED N-GLYCANS**

Ruth A. Schwalbe, Melissa J. Corey and Tara A. Cartwright

Biochemistry and Cell Biology 86 (2008) 21-30

Abstract

The N-glycan pool of mammalian brain contains remarkably high levels of sialylated N-glycans. This study provides the first evidence that voltage-gated K⁺ channels, Kv3.1, 3.3, and 3.4, possess distinct sialylated N-glycan structures throughout the central nervous system of the adult rat. Electrophoretic migration patterns of Kv3.1, 3.3, and 3.4 glycoproteins from: spinal cord, hypothalamus, thalamus, cerebral cortex, hippocampus, and cerebellum membranes digested with glycosidases were used to identify the various glycoforms. Differences in the migration of Kv3 proteins were attributed to the desialylated N-glycans. Expression levels of the Kv3 proteins were highest in cerebellum, whereas those of Kv3.1 and Kv3.3 were much lower in the other five regions. The lowest level of Kv3.1 was expressed in the hypothalamus, whereas the lowest levels of Kv3.3 were expressed in both thalamus and hypothalamus. The other regions expressed intermediate levels of Kv3.3, with spinal cord expressing the highest. The expression level of Kv3.4 in the hippocampus was slightly lower than that in cerebellum, and was closely followed by the other four regions, with spinal cord expressing the lowest level. We suggest that novel Kv3 glycoforms may endow differences in channel function and expression among regions throughout the central nervous system.

Introduction

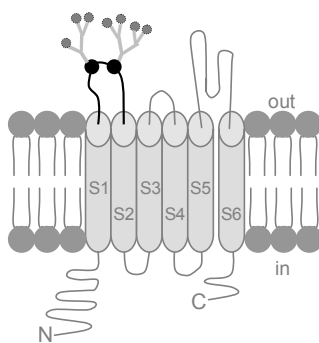
Kv3 channels belong to the super gene family of voltage gated K⁺ (Kv)¹ channels and are present in both axonal and somatodendritic compartments of neurons, where they regulate the intrinsic electrical excitability (16). Four mammalian genes have been identified which belong to the Kv3 family: Kv3.1, Kv3.2, Kv3.3 and Kv3.4. Expression levels of Kv3.1 and 3.3 transcripts are higher than those of Kv3.2 and Kv3.4 in adult rat brain (22,32,36). The amino acid sequence of the Kv3 proteins has revealed two N-glycosylation consensus sequences that lie within the first extracellular loop. Previously, these two absolutely conserved N-glycosylation sites of Kv3.1, 3.3, and 3.4 proteins were shown to be utilized in adult rat brain (Figure 8) (116).

N-Glycosylation of nascent membrane proteins is the most ubiquitous protein co-translational modification (105). Inside the cell this modification has been shown to be involved in protein folding and assembly, as well as intracellular protein sorting (61,133). Outside the cell the oligosaccharides have been shown to be involved in: cell adhesion, as well as cell-ligand, cell-cell, and cell-microbe interactions (61,133). A more recent view of N-glycosylation is the role of N-linked oligosaccharides in the modulation of protein function (133). In the past decade, the biological importance of the N-glycosylation pathway in mammalian physiology has been emphasized by the identification of congenital disorders of glycosylation (CDG) in humans (134) and mutant glycosylation mice (80,81,117,118,135-137). Additionally, it has been suggested that ER stress, which would most likely alter N-glycosylation occupancy, may lead to several neurodegenerative diseases (73).

Figure 8. Topological model of a Kv3 monomeric unit with sialylated N-glycans

The six transmembrane segments (S1-S6) are represented by cylinders in the lipid bilayer. Both N- and C- termini are localized in the cytoplasm. Black circles denote the Asn residues of the two native N-glycosylation consensus sequences for Kv3 channels. Branched structures signify N-sialylated glycans occupying the two native N-glycosylation sites. The gray circles correspond to sialic acid residues which terminate the N-linked oligosaccharides.

Figure 8
Schwalbe *et al.*, 2007



To date there are few studies that have characterized the importance of N-glycosylation of potassium channels. However, N-glycosylation of Kir1.1 stabilizes the opening state of the channel (119). Additionally, the activation kinetics of the Kv3.1 channel with simple type N-glycans was faster compared to its unglycosylated counterpart heterologously expressed in *Spodoptera frugiperdae*, Sf9 cells (35). Here we show that Kv3.1, Kv3.3, and Kv3.4 glycoproteins are expressed in: hypothalamus, cerebral cortex, cerebellum, hippocampus, spinal cord, and thalamus of the adult rat. Moreover, we show that the protein expression patterns of these various regions are different for each of the Kv3 proteins. Immunoband shift assays of cerebellum, hypothalamus, cerebral cortex, thalamus, hippocampus and spinal cord membranes, both treated and untreated with various glycosidases, were used to identify different Kv3.1, 3.3, and 3.4 glycoforms throughout the central nervous system. Additionally, the results indicated that the sialylated N-glycan structures of Kv3.1, 3.3 and 3.4 differed by their neutral N-glycan structures which give rise to the sialylated structures.

Results

N-Glycans of neuronal Kv3 channels contain sialic acid residues

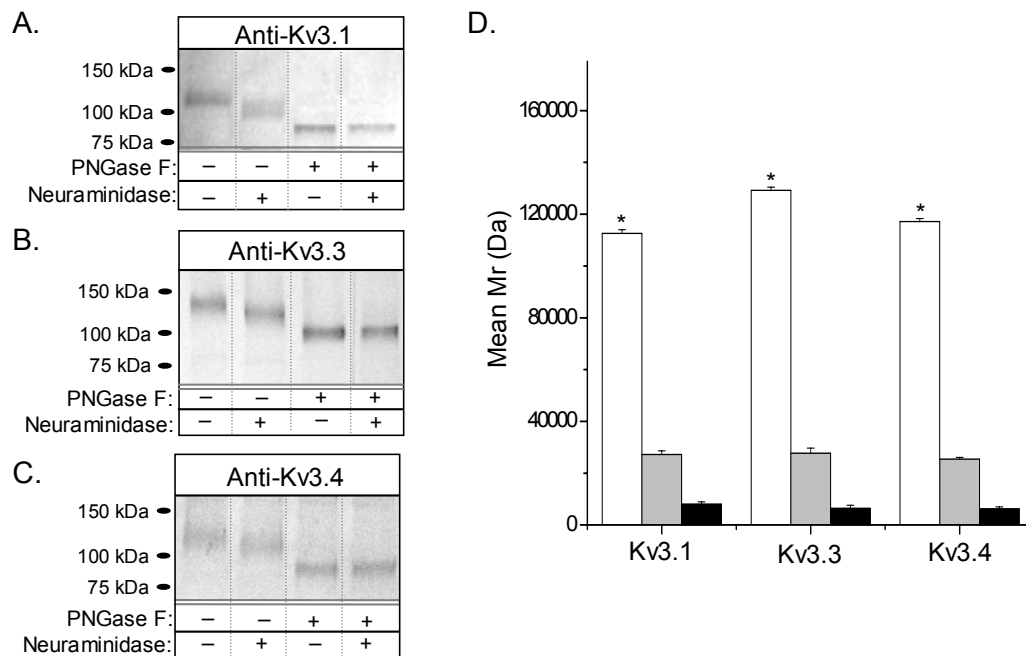
The two N-glycosylation sites in the first extracytoplasmic loop of Kv3.1, 3.3 and 3.4 channels were shown to be utilized in rat brain (35,116). To directly demonstrate that the N-glycans of Kv3 channels were composed of sialyl residues, stripped brain membranes were treated with and without different combinations of PNGase F and neuraminidase under nondenaturing conditions (Figure 9). PNGase F is an amidase which removes high mannose, hybrid, and complex N-linked oligosaccharides (124). Neuraminidase (*Clostridium perfringens*) is an exoglycosidase which removes sialyl residues with α 2,3- α 2,6- and α 2,8-linkages (79). Upon treatment of stripped brain membranes with PNGase F, there were large shifts in the electrophoretic mobilities of Kv3.1 (Figure 9A), Kv3.3 (Figure 9B), and Kv3.4 (Figure 9C) proteins. This result was similar to PNGase F digestions performed previously under denaturing conditions for these Kv3 channels (116). The immunoband shifts produced by neuraminidase were smaller than those generated by PNGase F treatment by approximately 75%. When membranes were treated with PNGase F and neuraminidase simultaneously the electrophoretic mobility shifts of Kv3.1 (Figure 9A), Kv3.3 (Figure 9B) and Kv3.4 (Figure 9C) were virtually identical to those treated solely with PNGase F. These results directly demonstrated that the N-glycans of Kv3.1, 3.3, and 3.4 glycoproteins contain sialic acid residues.

The values for the M_r for all three Kv3 proteins were greater (Kv3.1, $112,578 \pm 1,397$ Da, $n=30$ blots; Kv3.3, $129,236 \pm 1,166$ Da, $n=32$ blots; and Kv3.4, $117,149 \pm$

Figure 9. N-Linked oligosaccharides of Kv3.1, Kv3.3, and Kv3.4 proteins are composed of sialic acid residues

Western blots of brain membrane proteins untreated (-) or treated (+) with various combinations of PNGase F and neuraminidase were probed with (A) anti-Kv3.1, (B) anti-Kv3.3, and (C) anti-Kv3.4 antibodies. Ovals represent the KaleidoscopeTM protein molecular mass standards, as indicated. (D) The mean M_r values (in Da) for the Kv3 immunobands (white bars) were as follows: Kv3.1, $112,578 \pm 1,397$ ($n=30$ blots); Kv3.3, $129,236 \pm 1,166$ ($n=32$ blots); Kv3.4, $117,149 \pm 1,185$ ($n=31$ blots). The asterisk indicates statistical significance between the neighboring white bars; $p < 0.05$. The mean M_r values for the N-glycans (gray bars) were as follows: Kv3.1, $27,241 \pm 1,408$ ($n=11$ blots); Kv3.3, $27,724 \pm 1,901$ ($n=10$ blots); Kv3.4, $25,395 \pm 707$ ($n=11$ blots). These values represent the difference between the M_r for the Kv3 proteins with and without PNGase F treatment. The mean M_r values for the sialic acid residue content (black bars) were as follows: Kv3.1, $8,019 \pm 929$ ($n=10$ blots); Kv3.3, $6,376 \pm 1,245$ ($n=7$ blots); Kv3.4, $6,200 \pm 777$ ($n=9$ blots). These values denote the difference between M_r values for the Kv3 samples treated and untreated with neuraminidase.

Figure 9
Schwalbe *et al.*, 2007



1,185 Da, $n=31$ blots) than their calculated molecular masses deduced from amino acid sequences (Kv3.1, 66 kDa; Kv3.3, 94 kDa; and Kv3.4, 68 kDa) (Figure 9D, white bars). The mean M_r values for the Kv3 protein with the N-glycans removed were also higher (Kv3.1, $85,300 \pm 1,373$ Da, $n=11$ blots; Kv3.3, $105,562 \pm 1,632$ Da, $n=10$ blots; and Kv3.4, $95,350 \pm 2,607$ Da, $n=11$ blots). In all cases, the neighbors were statistically different from one another, supporting the specificity of the various Kv3 antibodies. In part the larger apparent molecular mass resulted from the N-glycans. However, other factors also appeared to influence the slower electrophoretic migration of these membrane proteins relative to the globular protein standards (116).

The electrophoretic migration of the two N-linked oligosaccharides was determined by the difference between the means of the M_r for each Kv3 protein in the absence and presence of PNGase F. Interestingly, N-glycans were remarkably similar for all three Kv3 proteins (Kv3.1, $27,241 \pm 1,408$ Da, $n=11$ blots; Kv3.3, $27,724 \pm 1,901$ Da, $n=10$ blots; and Kv3.4, $25,395 \pm 707$ Da, $n=11$ blots) (Figure 9D, grey bars). The percent of the N-glycan shift resulting from sialic acid residues was also quite similar for all three Kv3 proteins (Kv3.1, $8,019 \pm 929$ Da, $n=10$ blots; Kv3.3, $6,376 \pm 1,245$ Da, $n=7$ blots; and Kv3.4, $6,200 \pm 777$ Da, $n=9$ blots) (Figure 9D, black bars). This calculation was determined by the difference between the electrophoretic migration of the respective Kv3 protein treated and untreated with neuraminidase. The relatively large electrophoretic mobility shift produced by neuraminidase treatment of all three Kv3 proteins prior to N-glycan removal suggested that the sialic acid content of the N-glycans was remarkably high. Hence, our results directly showed that the N-glycans are capped with at least

several sialic acid residues for Kv3.1, 3.3, and 3.4 glycoproteins (Figure 8). They also confirmed that the Kv3 glycoproteins expressed in brain were of different sizes.

Protein levels of Kv3.1, Kv3.3, and Kv3.4 throughout the central nervous system

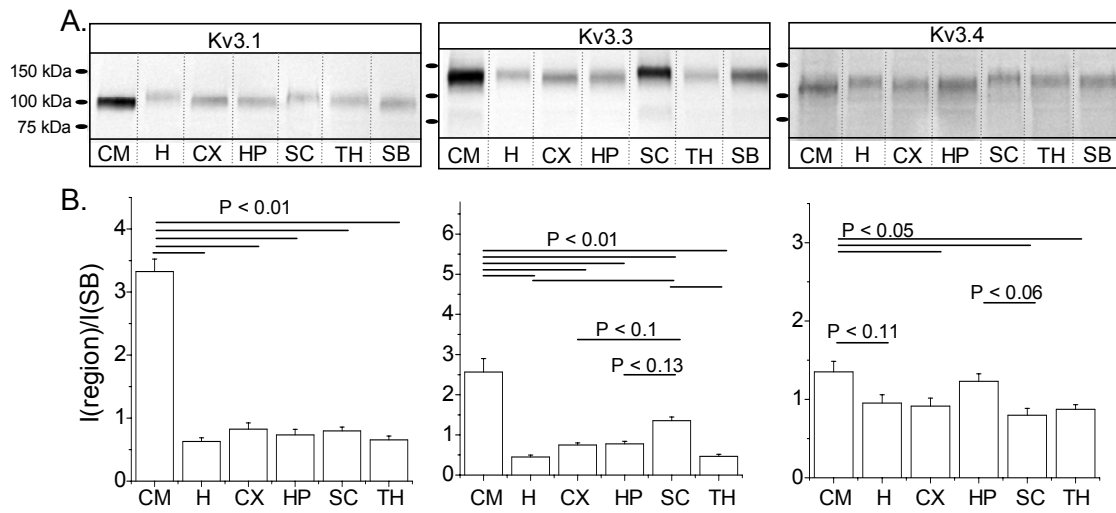
When equal amounts of membrane protein were loaded per well, the amount of Kv3.1 (Figure 10A, left panel) protein in cerebellum was much higher than in: hypothalamus, cerebral cortex, hippocampus, spinal cord, or thalamus. It was also higher than that in stripped brain which correlates with the lower amounts in the other regions of brain. The Kv3.1 band in cerebellum was darker than those in the other regions on eleven out of eleven Western blots. The lightest band was detected in hypothalamus seven out of eleven times while differences were not observed between the other four regions. Statistical analysis supported the observation that Kv3.1 protein levels were highest in cerebellum but not that hypothalamus expressed the lowest level (Figure 10B, left panel).

Kv3.3 protein levels in various regions of the central nervous system could be divided into four categories based on the Kv3.3 band intensities (Figure 10A, middle panel). Like Kv3.1, the Kv3.3 protein was found to be most highly expressed in cerebellum. The next darkest band was in the spinal cord which was followed by the bands in hippocampus and cerebral cortex. The lightest bands were observed in the thalamus and hypothalamus. In all cases, the ranking of the band intensities is supported by ten out of ten Western blots. Parametric tests agreed that cerebellum expressed the highest level of Kv3.3 protein whereas spinal cord had the second highest level (Figure

Figure 10. Differences in the Kv3.1, Kv3.3, and Kv3.4 protein expression levels in the various regions of the central nervous system

(A) For the Kv3.1, Kv3.3, and Kv3.4 Western blots, respectively, 50, 25, and 60 μg of cerebellum (CM), hypothalamus (H), cerebral cortex (CX), hippocampus (HP), spinal cord (SC), thalamus (TH) and stripped brain (SB) membrane proteins were loaded into wells. Ovals represent the Kaleidoscope protein molecular mass standards, as indicated. (B) The protein levels were: CM, 3.3259 ± 0.1958 ; H, 0.6311 ± 0.0563 ; CX, 0.8240 ± 0.0998 ; HP, 0.7333 ± 0.0892 ; SC 0.7973 ± 0.0608 ; TH, 0.6540 ± 0.0602 for Kv3.1 ($n=11$ blots, left panel); CM, 2.5636 ± 0.3369 ; H, 0.4494 ± 0.0481 ; CX, 0.7485 ± 0.0510 ; HP, 0.7766 ± 0.0660 ; SC, 1.3531 ± 0.0925 ; TH, 0.4671 ± 0.0491 for Kv3.3, ($n=10$ blots, middle panel); CM, 1.3514 ± 0.1338 ; H, 0.9525 ± 0.1059 ; CX, 0.9141 ± 0.1024 ; HP, 1.2301 ± 0.0971 ; SC, 0.7990 ± 0.0861 ; TH 0.8743 ± 0.0566 for Kv3.4 ($n=9$ blots, right panel). $I_{\text{region}}/I_{\text{stripped brain}}$ represents the intensity of each given region divided by the intensity of stripped brain. Each line indicates the two regions being compared and the statistical significance is indicated above the line(s).

Figure 10
Schwalbe *et al.*, 2007



10B, middle panel). Moreover, the tests suggested that the lowest Kv3.3 protein expression occurred in hypothalamus and thalamus

Kv3.4 protein levels in the various regions could also be ranked into four groups according to the band intensities from ten different Western blots. However, the ranking of the groups was different (Figure 10A, right panel) from that observed for Kv3.3 (Figure 10A, middle panel). On all ten Western blots, the darkest Kv3.4 band was observed in cerebellum while hippocampus was the next darkest on nine blots. The spinal cord expressed the lightest Kv3.4 band six out of ten blots. Bands observed in cerebral cortex, thalamus and hypothalamus were darker than spinal cord but lighter than those in either cerebellum or hippocampus. Statistical analysis favored the highest protein level in cerebellum, followed by hippocampus, and the lowest expression in the spinal cord. Taken together, our results showed that each of the Kv3.1, 3.3, and 3.4 proteins were expressed in the various regions of the central nervous system, and furthermore reported differences in the protein expression patterns for these Kv3 channels.

Different Kv3.1, Kv3.3, and Kv3.4 glycoforms identified throughout the central nervous system

When equal amounts of brain membrane protein samples were loaded per well, the electrophoretic migrations of all three Kv3 proteins in the various brain regions were slightly different from those in stripped brain (Figure 10A, left, middle and right panels). These small shifts in electrophoretic migration were also observed when reduced levels of brain membrane protein were loaded to give similar immunoband intensities (Figure

11A, left, middle and right panels). The relative speed of electrophoretic migration of the Kv3.1 protein from the various membranes was as follows: spinal cord and hypothalamus < thalamus < hippocampus and cerebral cortex < cerebellum membranes (Figure 11A, left panel). A similar migration pattern was observed on nine other Western blots. The mean M_r values for the Kv3.1 immunobands from the various membranes also suggested a similar size ranking (Figure 11B, left panel). However, statistical analysis failed to identify the Kv3.1 glycoform in the cerebellum as the smallest.

Similar electrophoretic migration patterns were observed for both Kv3.3 and 3.4 proteins on the representative Western blots (Figure 11A, middle and right panels), plus twelve and ten blots, respectively. Statistical analysis also supports the assigned sizes of the immunobands in the various regions (Figure 11B, middle and right panels). Overall, these results show that the Kv3.1, 3.3, and 3.4 proteins are modified in a different manner throughout the adult rat central nervous system.

Treating samples with and without PNGase F demonstrated that small differences in the electrophoretic migration of Kv3.1, Kv3.3, and Kv3.4 glycoproteins were due to N-glycosylation, and not another type of protein modification (Figure 12). Similar to the observations above (Figures 10 and 11), Kv3 proteins expressed in the various membrane samples showed dissimilarities in their electrophoretic migration when they were not treated with PNGase F (Figure 12A and B). On the contrary, when samples were treated with PNGase F the immunobands migrated to similar positions for Kv3.1, 3.3 and 3.4 in: cerebral cortex, hypothalamus, cerebellum, and stripped brain membranes (Figure 12A). The migration of deglycosylated Kv3.1, Kv3.3, and Kv3.4 proteins in thalamus,

Figure 11. The M_r values for Kv3 proteins are different in the various brain regions and spinal cord

(A) Western blots of the Kv3 proteins, as indicated, with relatively similar immunoband intensities in the various regions. Ovals represent the Kaleidoscope protein molecular mass standards, as indicated. (B) The mean M_r values (in Da) of Kv3 proteins were determined as follows. Kv3.1 ($n=15$ blots, left panel): CM, $110,386 \pm 1,151$; H, $120,077 \pm 934$; CX, $113,324 \pm 990$; HP, $112,738 \pm 1,345$; SC, $121,540 \pm 1,130$; and TH, $116,328 \pm 1,049$. Kv3.3 ($n=13$ blots, middle panel) CM, $125,034 \pm 1,062$; H, $131,322 \pm 1,194$; CX, $125,300 \pm 1,105$; HP, $125,492 \pm 1,022$; SC, $132,761 \pm 1,176$; and TH, $128,637 \pm 1,089$. Kv3.4 ($n=11$ blots, right panel) CM, $112,527 \pm 1,050$; H, $123,002 \pm 1,559$; CX, $116,025 \pm 1,412$; HP, $116,947 \pm 1,437$; SC, $128,086 \pm 1,865$; and TH, $121,530 \pm 1,300$. CM, cerebellum; H, hypothalamus; CX, cerebral cortex; HP, hippocampus; SC, spinal cord; TH, thalamus; SB, stripped brain.

Figure 11
Schwalbe *et al.*, 2007

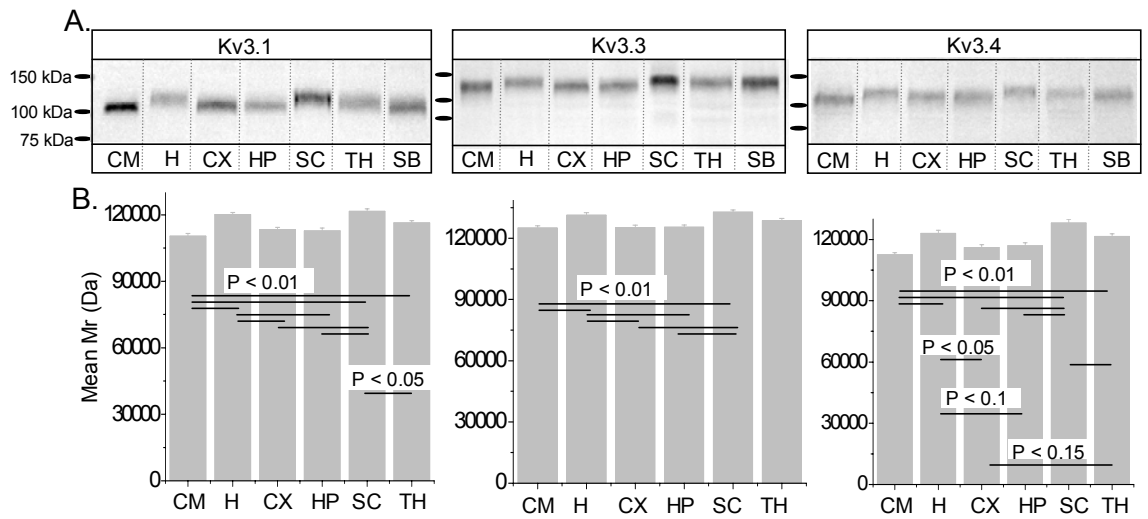
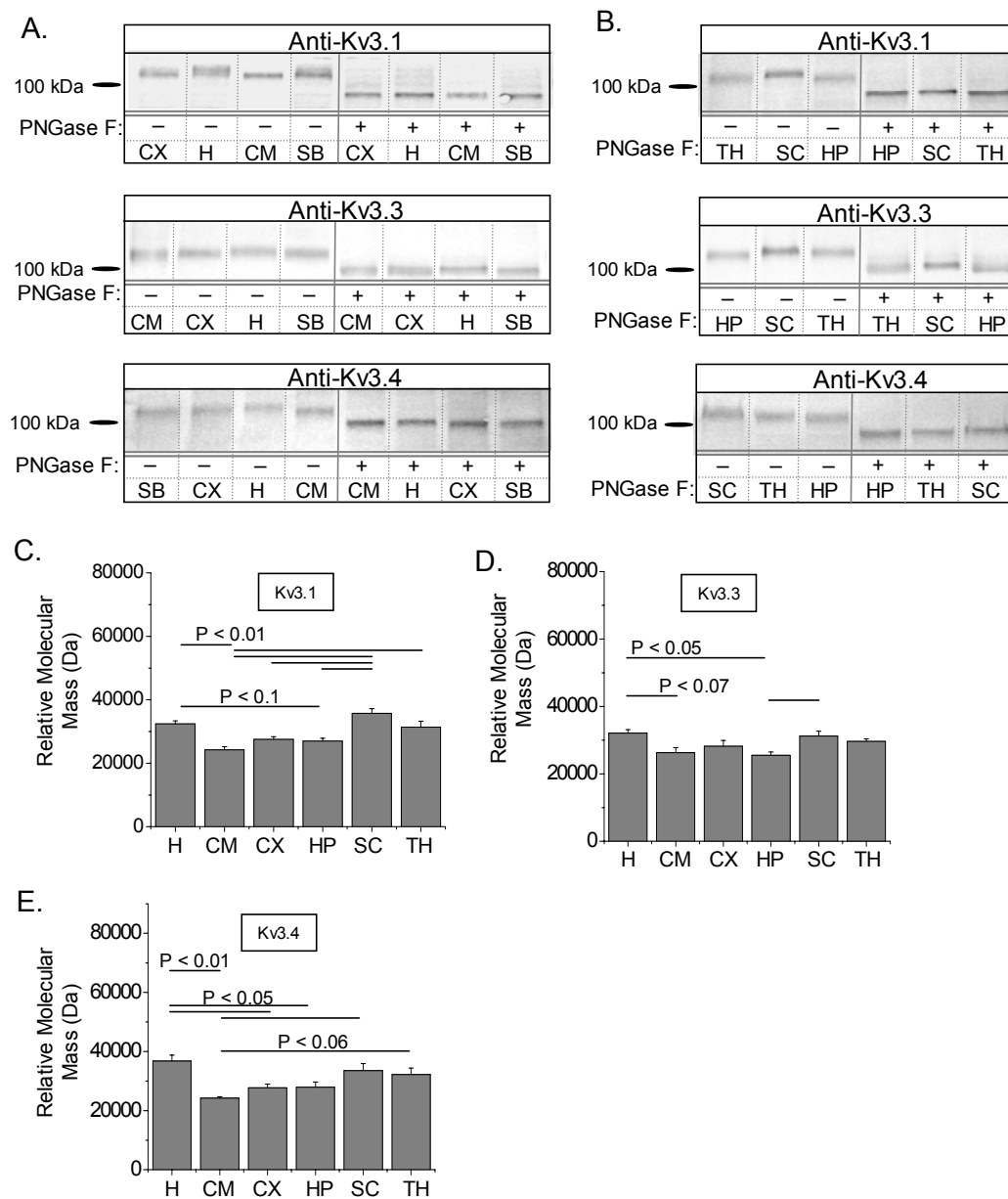


Figure 12. Differences in M_r values for the Kv3 proteins are due to N-glycosylation

Western blots of CM, H, CX, and SB membranes (A), and HP, SC and TH membranes (B) were untreated (-) or treated (+) with PNGase F. The oval represents the 100 kDa protein standard. (C) The mean values (in Da) for the Kv3 proteins were determined as follows. Kv3.1 ($n=5$ blots): CM, $26,994 \pm 1,598$; H, $36,310 \pm 2,095$; CX, $29,074 \pm 1,577$; HP, $27,033 \pm 827$; SC, $35,725 \pm 1,498$; and TH $31,396 \pm 1,886$. Kv3.3 ($n=5$ blots) CM, $27,887 \pm 2,289$; H, $31,858 \pm 3,016$; CX, $29,240 \pm 2,822$; HP, $24,194 \pm 1,304$; SC, $30,480 \pm 2,035$; and TH, $28,333 \pm 1,646$. Kv3.4 ($n=4$ blots) CM, $24,247 \pm 480$; H, $36,775 \pm 1,994$; CX, $27,722 \pm 1283$ ($n=5$ blots); HP, $27,968 \pm 1,708$; SC, $33,446 \pm 2,379$; and thalamus (TH), $32,219 \pm 2,137$. CM, cerebellum; H, hypothalamus; CX, cerebral cortex; HP, hippocampus; SC, spinal cord; TH, thalamus; SB, stripped brain

Figure 12
Schwalbe *et al.*, 2007



hippocampus, and spinal cord were also relatively similar to those determined from stripped brain (Figure 12B). However, slight differences in the migration pattern of Kv3.1, 3.3 and 3.4 deglycosylated forms from spinal cord compared to thalamus and hippocampus could be observed but failed to be supported statistically.

Different mobility shifts, which were attributed to the N-linked oligosaccharides of the Kv3 proteins in the various regions were represented as the mean M_r of the N-glycans (Figure 12C, D and E). The M_r values of the N-glycans were determined by the differences in the migration of the Kv3 proteins treated and untreated with PNGase F. These values were found to be higher in: hypothalamus, spinal cord and thalamus, and lower in: hippocampus, cerebral cortex, and cerebellum. These two groups correlated with the high and low M_r groups identified for the Kv3 immunobands in these regions (Figure 11). The N-linked oligosaccharides produced the smallest effect on the electrophoretic migration of both Kv3.1 (Figure 12C) and 3.4 (Figure 12D) proteins in cerebellum while the effect on the Kv3.3 protein (Figure 12E) in cerebellum was similar to that in cerebral cortex and hippocampus. The N-glycan produced the largest effect on the migration of the Kv3.1 (Figure 12C) protein in spinal cord, whereas a difference in the migration of the Kv3.3 (Figure 12D) and 3.4 (Figure 12E) proteins in this region were not apparent. Taken together, these results showed that the shifts in electrophoretic mobility of the Kv3 proteins in the different membranes of the adult rat central nervous system were due to the attachment of unique N-glycan structures to Kv3.1, 3.3, and 3.4 glycoproteins.

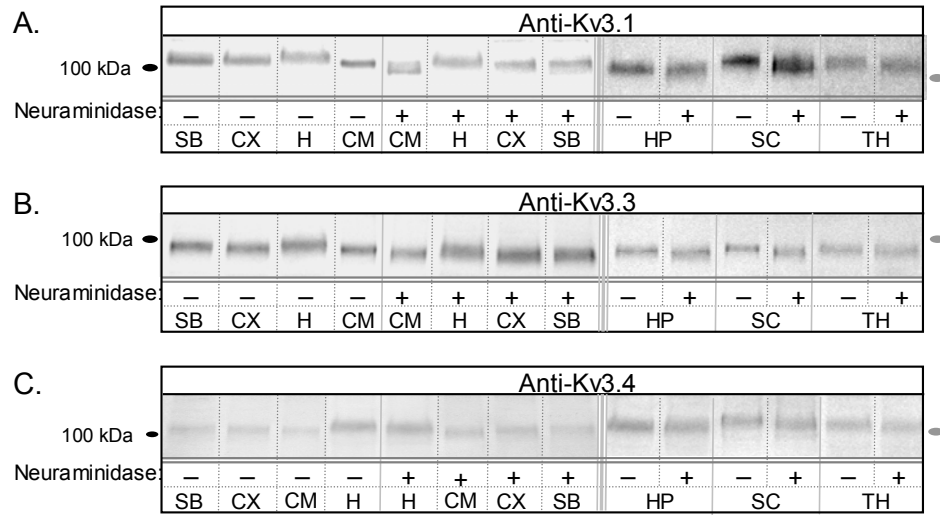
Differentially expressed Kv3 glycoforms contain sialylated N-glycans

To ascertain whether the Kv3 glycoforms were sialylated in all six regions, membrane samples were treated with neuraminidase and analyzed by Western blotting (Figure 13). Again, all three Kv3 proteins appeared to migrate differently than stripped brain in the untreated membranes. In all cases, Kv3 proteins of various membranes treated with neuraminidase migrated slightly faster than their corresponding untreated proteins. Additionally, the immunoband patterns for Kv3.1, 3.3, and 3.4 proteins in the various membranes were mostly retained for neuraminidase treated samples, indicating that the differences in electrophoretic mobility were not primarily due to the sialic acid content. These results demonstrated that the N-glycans of Kv3 proteins were sialylated in: hypothalamus, cerebellum, cerebral cortex, hippocampus, spinal cord and thalamus, and agree with the analysis of Kv3 proteins in stripped brain. The results also indicated that the differences in electrophoretic migration were primarily due to the neutral N-glycan structures which give rise to the sialylated N-glycans.

Figure 13. Sialylated N-glycans of Kv3.1, Kv3.3 and 3.4 channels were detected in the spinal cord and different brain regions

Western blots of cerebellum (CM), hypothalamus (H), cerebral cortex (CX), hippocampus (HP), spinal cord (SC), thalamus (TH), and stripped brain (SB) membranes were untreated (-) or treated (+) with neuraminidase. Antibodies used for Western blots, as indicated. The oval represents the 100 kDa protein standard.

Figure 13
Schwalbe *et al.*, 2007



Discussion

Previously, it was shown that both N-glycosylation sites of Kv3.1, 3.3, and 3.4 proteins were occupied by N-linked oligosaccharides in adult rat brain (116). The data presented here directly demonstrated that the N-glycans were sialylated for these Kv3 proteins in adult rat brain (Figure 9). Removal of sialic acid residues from the N-glycans caused glycosylated Kv3 proteins to migrate 25% of the distance of their deglycosylated counterparts. Moreover, sialylated N-glycans were present in all tested regions of the central nervous system (Figure 13). Therefore, these results showed that the N-glycans of Kv3.1, 3.3, and 3.4 proteins were capped with several sialyl residues in various regions of the central nervous systems (Figure 8).

We have demonstrated that the expression patterns of Kv3.1, 3.3, and 3.4 proteins were different from one another throughout the central nervous system of the adult rat. Kv3.1 protein levels in cerebellum were much higher than those in other examined regions (Figure 10, left panels). In agreement with our study, Kv3.1 protein levels were much higher in cerebellum than thalamus, cerebral cortex, and hippocampus (38). Additionally, relatively high levels of Kv3.1 protein were detected in hippocampus (39,40) and cerebral cortex (39). However, contrary to our results, Kv3.1 protein levels (38), as well as Kv3.1 transcript levels (22,32,36), have been found to be higher in thalamus than those in: cerebral cortex and hippocampus. Moreover, very little if any Kv3.1 protein was observed in cerebral cortex and hippocampus (38). Additionally, Kv3.1 protein could not be detected in hypothalamus (39), and Kv3.1 mRNA molecules appeared absent in most of the neurons of the hypothalamus (22). An explanation of the

discrepancy between the protein expression pattern and the transcript expression pattern (22,32,36) of Kv3.1 in the various brain regions indicates that transcript levels do not adequately represent the protein levels, and although explanations of the discrepancies among protein levels were unclear, the discrepancies may have resulted from: the number of observations, purification procedure, detection method, or perhaps variability in the rats utilized for each of the independent studies.

Kv3.3 protein levels were highest in cerebellum followed by that in spinal cord (Figure 10A and B, middle panels), similar to the Kv3.3 transcript levels (22). On the other hand, Kv3.3 protein was detected in hypothalamus, and it was more prominent in hippocampus and cerebral cortex than that in thalamus, which is unlike Kv3.3 transcript levels (38). Kv3.4 protein levels were highest in cerebellum, high in hippocampus, low in hypothalamus, cerebral cortex and thalamus, and lowest in spinal cord (Figure 10A and 10B, right panels). In contrast, Kv3.4 transcript levels were much lower in: hypothalamus, cerebral cortex and hippocampus than in thalamus and spinal cord (22).

The data presented here provides the first evidence for different Kv3 glycoforms in the adult central nervous system of rat (Figures 10, 11, 12, and 13). Overall, the size rankings of the Kv3.1, 3.3 and 3.4 glycoforms in the spinal cord and various regions of the brain were remarkably similar. The electrophoretic migrations of the Kv3.1 glycoforms in cerebellum, cerebral cortex, and thalamus (Figure 11A and B, left panels) were in agreement with a previous study (38). However, the differences in migration were unsolved in the earlier study. In contrast, Kv3.1 proteins migrated much faster in cerebral cortex than cerebellum and hippocampus (39).

According to the electrophoretic migration shifts produced by the N-glycans of the Kv3 proteins (Figure 12), the N-glycan structures of the Kv3 proteins appear to be similar in identical regions of the central nervous system. This finding is in agreement with earlier reports, indicating that occupancy and structure of N-linked oligosaccharides are cell type specific (132). Moreover, we suggest that the Kv3.1, 3.3, and 3.4 glycoproteins contain these distinct N-glycan structures in: spinal cord, hypothalamus, thalamus, cerebral cortex, hippocampus, and cerebellum of both human and mouse brains because the N-glycan structures from identical mammalian organs are conserved (138).

Based on hydropathy plots of Kv3 channels, as well as other Kv channels, the S1-S2 linker was predicted to be extracytoplasmic (Figure 8). Moreover, we directly demonstrated that both N-glycosylation sites of Kv3.1 which lie within the S1-S2 linker were utilized (35,116). The highly acidic N-glycans attached to neuronal Kv3 proteins, and their removal under non-denaturing conditions (Figure 9) indicates that the linker is in a hydrophilic environment and at the protein surface. These findings are incompatible with the linker residing in the membrane, along with the placement and orientation of the transmembrane segments, as proposed by the bacterial KvAP channel x-ray crystal structure (131).

The Kv1 gene family, except for the Kv1.6 gene, is another gene family of voltage-gated K⁺ channels which contains an N-glycosylation consensus sequence within the S1-S2 linker. Kv1.1, 1.2, and 1.4 proteins were shown to contain sialylated N-glycans in rat brain membranes (16,58-60). Immunoband shifts produced by neuraminidase (*Vibrio cholerae*) treatment for Kv1.1, 1.2, and 1.4 glycoproteins (59) were not as

dramatic as the immunoband shifts for Kv3.1, 3.3, and 3.4 glycoproteins (Figure 9 and 13), suggesting that sialyl residues were more abundant in Kv3 glycoproteins than the Kv1 glycoproteins. It would be of interest to further characterize the N-glycan structures of Kv1 and Kv3 glycoproteins and determine whether these structures can influence the transport of these proteins to either axonal or somatodendritic domains of neurons.

Overall, this study has demonstrated that Kv3.1, 3.3, and 3.4 glycoproteins are expressed in: hypothalamus, cerebral cortex, cerebellum, hippocampus, spinal cord, and thalamus of adult rat. Additionally, it was observed that the protein expression pattern throughout the central nervous system was different for each Kv3 protein, and we directly demonstrated that the N-glycans of Kv3.1, 3.3, and 3.4 proteins were terminated with sialic acid residues (Figure 8). The results also revealed that different Kv3.1, 3.3, and 3.4 glycoforms were expressed throughout the central nervous system, and that they differed in their desialylated N-glycan. Future studies will entail examining the linkage of the sialic acid residues. Furthermore, it will be of great interest to examine the specific roles that the diverse N-linked sialoligosaccharides at the highly conserved N-glycosylation sites of the Kv3 glycoproteins in function, expression at the cell surface of either axonal or somatodendritic domains, and in cellular recognition events.

**CHAPTER 6 - ATYPICAL SIALYLATED N-GLYCAN STRUCTURES ARE
ATTACHED TO NEURONAL VOLTAGE-GATED POTASSIUM CHANNELS**

Tara A. Cartwright and Ruth A. Schwalbe

Bioscience Reports (2008) In press

Abstract

Mammalian brains contain relatively high amounts of common and uncommon sialylated N-glycan structures. Sialic acid linkages were identified for voltage-gated potassium channels, Kv3.1, 3.3, 3.4, 1.1, 1.2, and 1.4, by evaluating their electrophoretic migration patterns in adult rat brain membranes digested with various glycosidases. Additionally, their electrophoretic migration patterns were compared to those of N-CAM, transferrin, and the Kv3.1 protein heterologously expressed in B35 neuroblastoma cells. Metabolic labeling of the sugars combined with glycosidase digestion reactions were utilized to show that the N-glycan of recombinant Kv3.1 protein was capped with an oligo/polysialyl unit. All three brain Kv3 glycoproteins, like N-CAM, were terminated with α 2,3-linked sialyl residues, as well as atypical α 2,8-linked sialyl residues. Additionally, at least one of their antenna was terminated with an oligo/polysialyl unit, similar to recombinant Kv3.1 and N-CAM. In contrast, brain Kv1 glycoproteins consisted of sialyl residues with α 2,8-linkage, as well as sialyl residues linked to internal carbohydrate residues of the carbohydrate chains of the N-glycans. This type of linkage was also supported for Kv3 glycoproteins. To date, such sialyl linkage has only been identified in gangliosides, not N-linked glycoproteins. We conclude that all six Kv channels contribute to the atypical sialylated N-glycan pool in mammalian brain. Identification of these novel sialylated N-glycan structures implicate a connection between potassium channel activity and atypical sialylated N-glycans in modulating and fine tuning the excitable properties of neurons in the nervous system.

Introduction

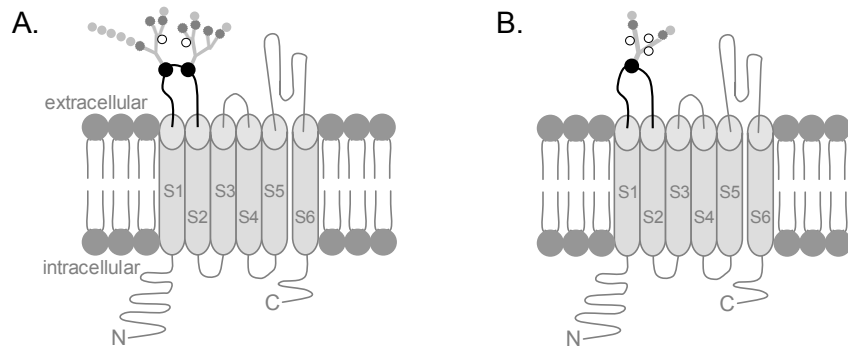
The N-glycan pool of mammalian brain contains remarkably high levels of sialyl residues and presents them in an atypical manner (69). Sialyl residues are commonly found at the outermost ends of carbohydrate chains (139). The common types of glycosidic bonds for sialyl residues include α 2,3- and α 2,6-linkages with the former being more prevalent in mammalian brain (69,95). An unusual glycosidic bond for sialyl residues is α 2,8-linkage which gives rise to di/oligo/polysialic acid units (139). These structural units are attached to α 2-3-linked sialyl residues on non-reducing terminal ends of N-glycans (97,139). In adult mammalian brain, there are only six proteins identified which have these homopolymers of 8 or more sialyl residues (88,90,98-102,140). Additionally, there are more α 2,8-linked disialic acids (70,141) and oligosialic acid chains on glycoproteins than previously thought (88,97,98). Another unusual type of linkage is sialyl residues linked to internal residues of carbohydrates which has only been identified for gangliosides (103,104). Clearly, identification of these carriers is the first step in defining the roles of these unusual sialylated N-glycans.

Kv1 and Kv3 channels belong to the super gene family of voltage-gated K⁺ (Kv)¹ channels, and are responsible for the repolarization and shape of action potentials (5). The Kv1 channels, except Kv1.6 (59,86,123,129,130) , as well as the Kv3 channels (35,116) have one or two utilized N-glycosylation sites, respectively, between the first and second transmembrane segments (Figure 14). In the adult rat central nervous system, the Kv3 N-glycan structures have been shown to be quite diverse (37). Additionally, the

Figure 14. Biochemically-derived sialic acid linkages of the N-glycans attached to Kv channels

Topological models of the Kv3 (A) and Kv1 (B) α -subunits have two and one utilized N-glycosylation sites, respectively, within the S1-S2 linker. The Asn residues of these sites are signified by black circles. Cylinders represent the six transmembrane segments (S1-S6) within the lipid bilayer with amino and carboxyl-termini exposed to the cytoplasm. Branched tree structures correspond to the desialylated N-linked oligosaccharides. Sialyl residues of the carbohydrate chains with α 2,3-linkage and α 2,8-linkage are depicted by dark grey circles and light grey circles, respectively. Additionally, one chain is terminated with an oligosialyl unit with internal α 2,8-linkages (row of light grey circles). The N-glycans also contain sialyl residues linked to internal residues of the carbohydrate chains (white-filled circles).

Figure 14
Cartwright and Schwalbe, 2008



gating properties of Kv1.1 (58,83), 1.2 (84), and 3.1 (35) channels, as well as protein trafficking of the Kv1.2 (84) and 1.4 channels (84,86), were altered by the presence and type of N-glycan structures. Congenital disorders of glycosylation in humans (134), along with mutant glycosylation mice (80,81,117,118,135-137) also emphasize the importance of N-glycosylation in mammalian neuronal physiology. In this study, immunoband shift assays of glycosidase treated adult rat brain membranes were utilized to identify unique α 2,8-linked sialylated N-glycans of Kv3 and Kv1 channels. The results also supported that the Kv3.1 glycoprotein heterologously expressed in B35 cells, as well as brain Kv3.1, 3.3, and 3.4 glycoproteins, have an oligo/polysialyl unit attached to their N-glycans. Additionally, sialyl residues were shown to be linked to internal carbohydrate residues of the Kv1 N-glycans. Kv3 N-glycans also appeared to have branched sialyl residues. Previously, the occurrence of branched sialyl residues was unrecognized in N-glycosylated proteins.

Results

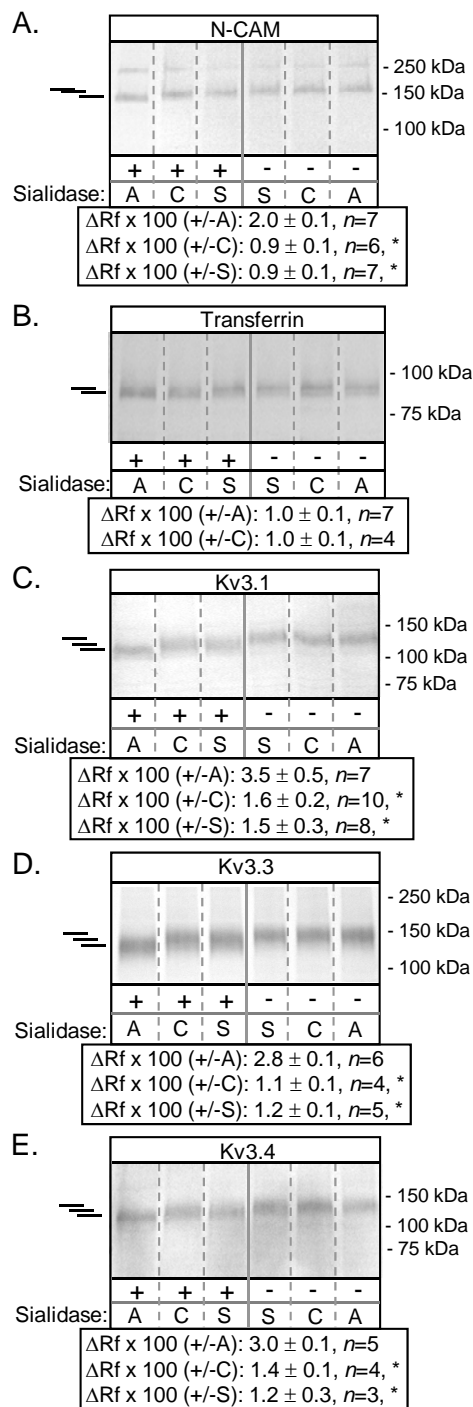
Neuronal Kv3 proteins are associated with α 2,3-, α 2,8-linked sialylated N-glycan structures

Previous studies have shown that N-CAM and sodium channels, along with other unidentified N-glycosylated proteins, in adult mammalian brain are bearers of di/oligo/polysialyl units (69,70,88,90,97-102,140,141). Generally, these units consist of an initial α 2,3-linked sialyl residue followed by α 2,8-linked sialyl residues (97,139). Kv3.1, 3.3, and 3.4 channels expressed in adult rat brain and spinal cord have sialylated N-glycans (37,116). Additionally, we showed that the type of N-glycan attached to each of the Kv3 proteins is different in the various regions of the adult rat brain (37). To further examine these sialylated N-glycans is quite challenging because expression levels of the Kv3 proteins are quite low. However, we have evaluated the sialic acid linkages of these neuronal Kv3 and Kv1 glycoproteins by utilizing a sialic acid linkage analysis kit combined with Western blots. Two sialylated N-glycosylated proteins, neuronal cell adhesion molecule (N-CAM) and transferrin were used as controls. Additionally, removal of sialic acid residues due to initial rates of hydrolysis was eliminated by prolonged incubation of the digestion reactions (111). Stripped brain membranes were treated with either sialidase A (specific for the cleavage of branched, α 2,3-, α 2,6-, and α 2,8-linked sialic acid), sialidase C (specific for the cleavage of α 2,3-, and α 2,6-linked sialic acid), or sialidase S (specific for the cleavage of α 2,3-linked sialic acid) under nondenaturing conditions. Samples were then denatured in reducing SDS-PAGE sample buffer and analyzed by Western blotting (Figure 15). A predominant immunoband (167 kDa) was detected in stripped brain membranes for N-CAM (Figure 15A). A fainter immunoband

Figure 15. Removal of sialic acid residues from Kv3 glycoproteins

Stripped brain membranes were digested (+) or undigested (-) with sialidase A, C, or S. Western blots were probed with: anti-N-CAM (A), anti-transferrin (B), anti-Kv3.1 (C), anti-Kv3.3 (D), and anti-Kv3.4 (E) antibodies. Membrane proteins were separated on 10% SDS gels for detection of Kv3 and N-CAM proteins while 15% SDS gels were utilized for transferrin. Upper lines correspond to fully sialylated glycoproteins while lower lines denote the desialylated glycoproteins. Middle lines represent partially desialylated glycoproteins. Molecular weight standards (kDa) are as indicated for each immunoblot. The relative electrophoretic mobility difference ($\Delta R_f \times 100$ values) between undigested (-) and digested (+) transferrin, N-CAM and Kv3 proteins are listed below their respective Western blots. *n* corresponds to the number of Western Blots. Asterisks denote significant difference from the sialidase A immunoband shift.

Figure 15
Cartwright and Schwalbe, 2008



(193 kDa) could also be detected but was not rigorously characterized due to its light intensity. These two immunobands corresponded to those previously identified (142-144). Sialidase A treatment produced a larger immunoband shift than those produced by either sialidase C and S for the faster migrating species. Similar electrophoretic mobility shifts were observed on 6-7 Western blots (*n*). This is shown in the text box below the Western blot (Figure 15A) which reports the difference in the relative electrophoretic mobility ($\Delta R_f \times 100$) for each treatment. Immunoband shifts produced by both sialidase C and S treatments were not significantly different while they were significantly different from those produced by sialidase A, as indicated by the asterisks. These results indicated that sialyl residues with $\alpha 2,3$ -linkage could be detected for the N-CAM glycoprotein, while those with $\alpha 2,6$ -linkage could not be identified. They also suggested that $\alpha 2,8$ -linked sialyl residues could be detected for the N-CAM glycoprotein. It is unlikely that the immunoband shift is greater for sialidase A treatment than either sialidase C or S treatments as a result of kinetic selectivity or N-glycan resistance because reactions were allowed to proceed overnight. Additionally, sialidase C removes $\alpha 2,3$ -linked sialic acid at a faster rate than $\alpha 2,6$ -linked sialic acid (145) while sialidase A removes $\alpha 2,6$ -linked sialic acid at a faster rate than $\alpha 2,3$ -linked sialic acid (111). The largest immunoband shift produced by sialidase A treatment could also suggest the presence of branched-sialylated structures. However, branched-sialylated structures have only been identified for gangliosides (103,104), not N-glycans. Taken together, the immunoband shift assays support that $\alpha 2,3$ - and $\alpha 2,8$ -linked sialic acids were attached to the N-glycans of N-CAM, as previously shown (98,146).

The electrophoretic migration of transferrin (94 kDa) from untreated membranes (Figure 15B) was similar to previous reports (147,148). Moreover, we observed that the electrophoretic migration of transferrin synthesized in liver was virtually identical to that in brain (not shown). Identical immunoband shifts were detected for both sialidase A and C treatments while an immunoband shift was not detected for sialidase S treatment. The small immunoband shifts induced by the various treatments were replicated on 4-7 Western blots (*n*) as indicated by the difference in the relative electrophoretic mobility ($\Delta R_f \times 100$) (Figure 15B). These results revealed that the sialylated N-glycans of transferrin from brain consisted solely of $\alpha 2,6$ -linked sialyl residues, similar to transferrin from blood (148,149) and semen (150).

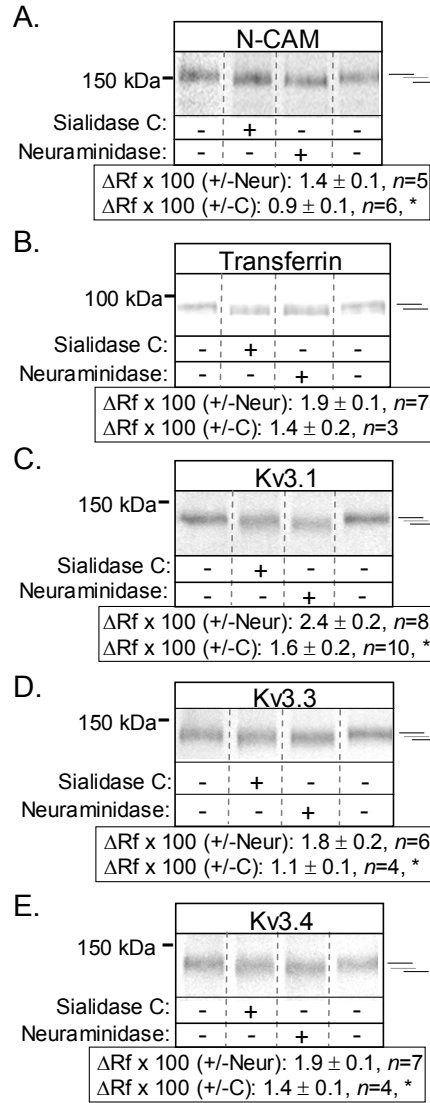
In all cases, the immunobands for the Kv3.1 glycoprotein migrated faster for treated brain membranes than those of untreated membranes (Figure 15C). The electrophoretic migration of the Kv3.1 proteins treated with sialidase S was similar to that produced by sialidase C while that produced by sialidase A treatment was largest. The reproducibility of these immunoband shifts are summarized by the change in the electrophoretic mobility shifts from 7-10 Western blots (Figure 15C). These results were similar to those of the control, N-CAM, in that $\alpha 2,3$ -sialylated structures could be detected for the Kv3.1 glycoprotein, as was $\alpha 2,8$ - sialylated structures. Patterns of the immunoband shifts produced by the various sialidase treatments for the Kv3.3 (Figure 15D) and Kv3.4 (Figure 15E) glycoproteins were similar to that of Kv3.1. Therefore, the results supported that all three Kv3 glycoproteins have $\alpha 2,3$ - and $\alpha 2,8$ -sialylated structures, similar to the N-CAM glycoprotein.

To further examine the presence of α 2,8-linked sialylated N-glycans for N-CAM, transferrin, Kv3.1, 3.3, and 3.4 proteins, stripped brain membranes were digested with either neuraminidase or sialidase C (Figure 16). Neuraminidase is identical to sialidase C. The reason we refer to the same enzyme with two distinct names is because they were purchased from two different companies. Of note, the concentration of neuraminidase is at least 1000-fold higher in the reaction mixtures than sialidase C. At this high concentration, the enzyme can remove α 2,8-linked sialyl residues from sialoglycoconjugates but has a much greater preference for α 2,3- and α 2,6-linked sialyl residues, as indicated in the company literature accompanying the product. The immunoband shift generated by neuraminidase treatment of N-CAM was significantly larger than that produced by sialidase C (Figure 16A) while those of transferrin were virtually identical (Figure 16B). It is unlikely that the difference in the amount of sialic acids removed from N-CAM were due to initial rates of hydrolysis because reactions were incubated for prolonged periods. It is also unlikely that N-glycan resistance resulted in the difference in immunoband shifts because the immunoband shift of N-CAM produced by sialidase A treatment was also larger than that produced by sialidase C (Figure 15A). Additionally, immunoband shifts produced by transferrin were identical (Figure 16B). Taken together, the immunoband shift assay confirms the presence of α 2,8-sialylated N-glycans for N-CAM (98,146). Moreover, our results for N-CAM and transferrin support that the immunoband shifts are due to the removal of sialic acid residues, not initial rates of hydrolysis, N-glycan resistance, proteolysis or other glycosidase activities.

Figure 16. Sialyl residues with α 2,8 linkages are present on neuronal Kv3 glycoproteins

Stripped brain membranes were treated (+) or untreated (-) with either sialidase C or with neuraminidase. Anti-N-CAM (A), anti-transferrin (B), anti-Kv3.1 (C), anti-Kv3.3 (D), and anti-Kv3.4 (E) antibodies were used for Western blots. Upper black lines represent immunobands of untreated brain membranes for the Kv3, N-CAM and transferrin proteins. Lower black lines signify removal of α 2,6-linked sialyl residues for transferrin, and removal of α 2,3- and α 2,8-linked sialyl residues for N-CAM and the Kv3 glycoproteins. Middle gray lines denote removal of α 2,3-linked sialyl residues for N-CAM and the Kv3 glycoproteins. Differences in the relative electrophoretic mobility ($\Delta R_f \times 100$ values) for the Kv3, N-CAM and transferrin glycoproteins are beneath their respective Western blots. *n* refers to the number of Western Blots. Asterisks indicate immunoband shifts significantly different from those produced by neuraminidase treatment.

Figure 16
Cartwright and Schwalbe, 2008



Immunoband shifts produced by neuraminidase treatment of the Kv3.1 (Figure 16C), 3.3 (Figure 16D), and 3.4 (Figure 16E) glycoproteins were markedly greater than those produced by sialidase C treatment. These larger electrophoretic migrations produced by neuraminidase treatment were observed on 4-10 Western blots (Figure 16C, 16D, 16E). Additionally, the difference between the electrophoretic mobility shifts produced by neuraminidase and sialidase C were significantly different. These results revealed that the N-glycans of the Kv3.1, 3.3, and 3.4 proteins are similar to N-CAM in that they contain α 2,8- sialylated N-glycans.

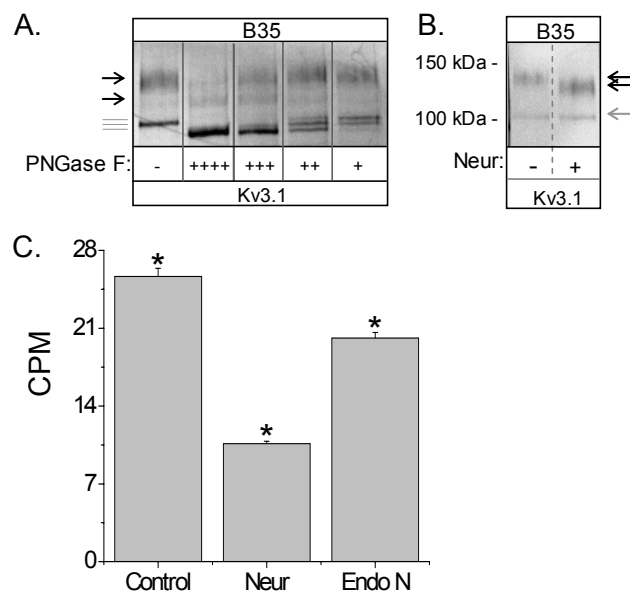
N-Glycan of Kv3.1 protein is heavily sialylated in neuroblastoma cells

Recombinant Kv3.1 was partially purified from transfected rat B35 neuroblastoma cells, and subsequently treated with various amounts of PNGase F (Figure 17A). Kv3.1 protein heterologously expressed in B35 cells migrated as two dark immunobands. The upper immunoband corresponded to the Kv3.1 protein with processed N-glycans and migrated slightly faster than Kv3.1 glycoprotein in adult rat brain (not shown). The lower immunoband represented simple type N-glycans attached to Kv3.1 (not shown), similar to heterologously expressed N-glycosylated Kv3.1 protein in Sf9 cells (35). At the highest level of PNGase F, a predominant immunoband was detected, representing the unglycosylated Kv3.1 protein. However, at lower amounts of PNGase F additional immunobands were detected. The two immunobands directly above the aglycoform immunoband signified either one or two simple N-glycans. The two upper immunobands represented Kv3.1 protein with either one or two complex N-glycans.

Figure 17. The N-glycans of Kv3.1 protein expressed in neuroblastoma cells are composed of oligo/polysialyl units

Western blots of Kv3.1 digested with PNGase F (A) and neuraminidase (Neur) (B). Partially purified Kv3.1 protein from transfected B35 cells was digested (+) and undigested (-) with various dilutions (0-, 10-, 20-, 40- and 80-fold) of PNGase F. The number of pluses (+) represents increasing amounts of PNGase F, while the minus (-) signifies the absence of PNGase F. Partially purified Kv3.1 protein from transfected B35 cells metabolically labeled with a sialic acid precursor ($[^3\text{H}]\text{-N-acetyl mannosamine}$) were untreated (Control) or treated with either neuraminidase or Endo N, and subsequently separated on 10 % SDS gels with DATD as the crosslinker (C). Gel slices of heterologously expressed Kv3.1 with complex N-glycans were collected, and radioactivity was measured by scintillation counting. Counts per minute (CPM). A one-way ANOVA using Bonferroni comparison exhibited statistical differences ($P = 0.01$) between control ($n = 3$), Neur ($n = 2$) and Endo N ($n = 3$) as represented by asterisks. n represents the number of SDS gels.

Figure 17
Cartwright and Schwalbe, 2008



When partially purified Kv3.1 protein was treated with neuraminidase, the upper immunoband migrated much slower while the lower immunoband did not shift (Figure 17B). These results demonstrated that both N-glycosylation sites of Kv3.1 are fully occupied however not fully processed when heterologously expressed in B35 cells. Additionally, the fully processed N-glycans of Kv3.1 were heavily sialylated, like those in adult mammalian brain.

Oligo/polysialyl moieties are attached to neuronal Kv3 proteins

To demonstrate that an oligo/polysialyl moiety was attached to the N-glycan of the Kv3.1 protein, partially purified recombinant Kv3.1 protein was digested with Endo N (Figure 17C). This glycosidase cleaves internal α 2,8-linkages with a minimal length of 5 sialyl residues (99,151). In brief, B35 cells were transfected with Kv3.1 and then metabolically labeled with [³H]-N-acetyl mannosamine. Radiolabeled Kv3.1 protein partially immunoaffinity purified from transfected B35 cells was separated on 10% SDS gels in which bis-acrylamide was replaced with DATD. Gel slices were excised between the 75 and 150 kDa markers. This region of the gel contained the Kv3.1 protein with complex N-glycans as revealed by Western blot analysis. The amount of radioactivity in the gel slice was determined by scintillation counting. Gel slices from samples treated, with either neuraminidase or Endo N, had much less radioactivity than those from untreated samples. As expected, the radioactivity signal from samples treated with neuraminidase was smaller than that of Endo N treated samples. These results indicated

that an oligo/polysialyl unit is associated with the Kv3.1 glycoprotein heterologously expressed in B35 cells.

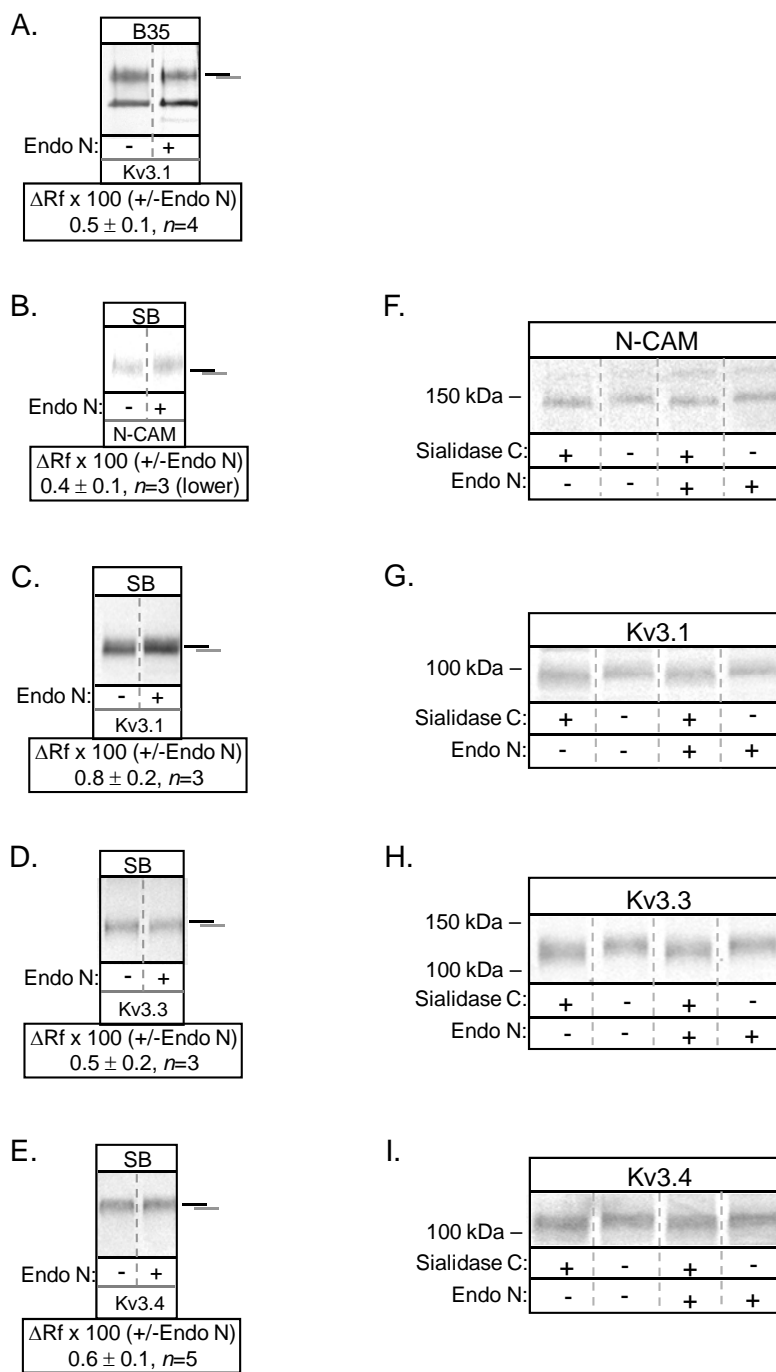
To determine whether the N-glycans of Kv3 proteins consisted of oligo/polysialyl moieties, membrane proteins were treated with and without Endo N (Figure 18). When partially purified Kv3.1 protein from B35 cells was treated with Endo N, the upper immunoband of Kv3.1 migrated slightly slower while the lower immunoband did not shift (Figure 18A). A similar result was also observed for N-CAM (Figure 18B) which has an oligo/polysialyl unit (98,146). The upward shift was surprising because sialidase A, sialidase C and neuraminidase produced downward shifts. However, this can be explained in that some of the N-glycan chains are terminated by α 2,3-linked sialyl residues and disialyl units, and removal of these residues generate a downward shift (Figure 14A). On the other hand, the chain terminated by an oligo/polysialyl unit produces an upward shift when it is removed. In other words, the oligo/polysialyl unit makes the glycoprotein more compact while the mono- and di-sialyl moieties make the glycoprotein less compact. This indeed appears to be the case as shown by the immunoband pattern of N-CAM treated with various combinations of Endo N and sialidase C (Figure 18F). The N-CAM immunoband from membranes treated with both Endo N and sialidase C migrated slightly further than the control but less than that from sialidase C treatment alone.

The immunoband patterns of the Kv3 glycoproteins were much like that of N-CAM. Immunobands shifted upward for Kv3.1 (Figure 18C), 3.3 (Figure 18D), and 3.4 (Figure 18E) proteins when brain membranes were treated with Endo N. In all cases, the

Figure 18. Brain Kv3 glycoproteins are composed of oligo/polysialyl units

B35 cells heterologously expressing Kv3.1 were partially purified, digested (+) and undigested (-) with Endo N, and analyzed by Western blotting utilizing the anti-Kv3.1 antibody (A). Stripped brain membranes digested (+) and undigested (-) with either Endo N, sialidase C or both were analyzed by Western blotting using: anti-N-CAM (B and F), anti-Kv3.1 (C and G), anti-Kv3.3 (D and H), and anti-Kv3.4 (E and I) antibodies. Beneath each respective Western blot are the differences in the relative electrophoretic mobility ($\Delta R_f \times 100$ values) for the Kv3 and N-CAM glycoproteins. *n* corresponds to the number of Western Blots.

Figure 18
Cartwright and Schwalbe, 2008



small upward immunoband shifts generated by Endo N were reproduced on at least three separate Western blots for each of the glycoproteins. Immunoband shifts produced by Endo N were neither detected for transferrin nor Kv1.1 glycoproteins (not shown). Additionally, treatment of the membranes with both Endo N and sialidase C produced immunobands for Kv3.1 (Figure 18F), 3.3 (Figure 18G), and 3.4 (Figure 18H) proteins which migrated in between those of the control and sialidase C treatment. These results support that brain Kv3.1, 3.3, and 3.4 proteins, like recombinant Kv3.1 protein and N-CAM (98), have an oligo/polysialyl unit attached to their N-glycans.

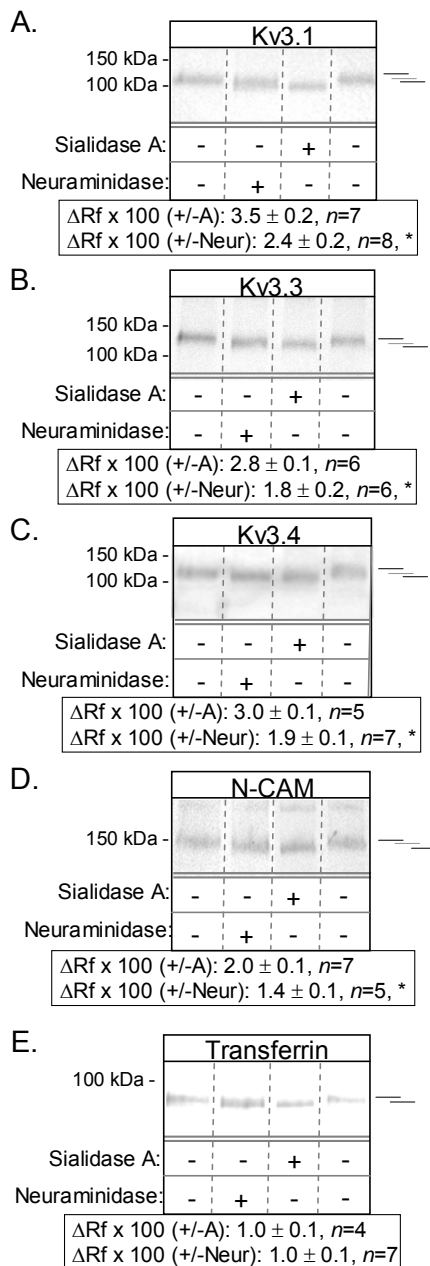
Detection of branched sialyl residues attached to Kv3 glycoproteins

To date, sialyl residues linked to internal carbohydrate residues have only been observed for gangliosides (103,104). To determine whether the N-glycans of the neuronal Kv3 proteins have this unusual type of linkage the immunoband shifts produced by neuraminidase and sialidase A treatments were examined. The specificities of neuraminidase and sialidase A are identical, except the latter can also remove branched sialyl residues. Immunoband shifts of stripped brain membranes treated with sialidase A were larger than those produced by neuraminidase for Kv3.1 (Figure 19A), Kv3.3 (Figure 19B), and Kv3.4 (Figure 19C) glycoproteins, as well as N-CAM (Figure 19D), on 5-8 Western blots, while the immunoband shifts were quite similar for transferrin on 4-7 Western blots (Figure 19E). Additionally, the larger electrophoretic mobility shift produced by sialidase A treatment compared to that produced by neuraminidase treatment was significantly different for all three Kv3 glycoproteins, as well as N-CAM, while they

Figure 19. Detection of branched sialyl residues attached to the N-glycans of Kv3 proteins

Stripped brain membranes were treated (+) or untreated (-) with either sialidase A or neuraminidase. Samples were immunoblotted with: anti-Kv3.1 (A), anti-Kv3.3 (B), anti-Kv3.4 (C), anti-N-CAM (D) and anti-transferrin (E) antibodies. Upper black lines represent fully sialylated glycoproteins. Lowest black lines denote completely desialylated glycoproteins. Middle gray lines signify partially desialylated glycoproteins. The relative electrophoretic mobility difference ($\Delta R_f \times 100$ values) for the transferrin, N-CAM and Kv3 glycoproteins are reported below each of their respective Western blots. *n* represents the number of Western Blots. Asterisks signify significant difference from the sialidase A immunoband shift.

Figure 19
Cartwright and Schwalbe, 2008



were not significantly different for transferrin. These results indicate that either neuronal Kv3.1, Kv3.3, Kv3.4 glycoproteins, as well as N-CAM, have sialyl residues linked to internal residues of the carbohydrate chains or that their sialylated N-glycans are more resistant to the action of neuraminidase than sialidase A.

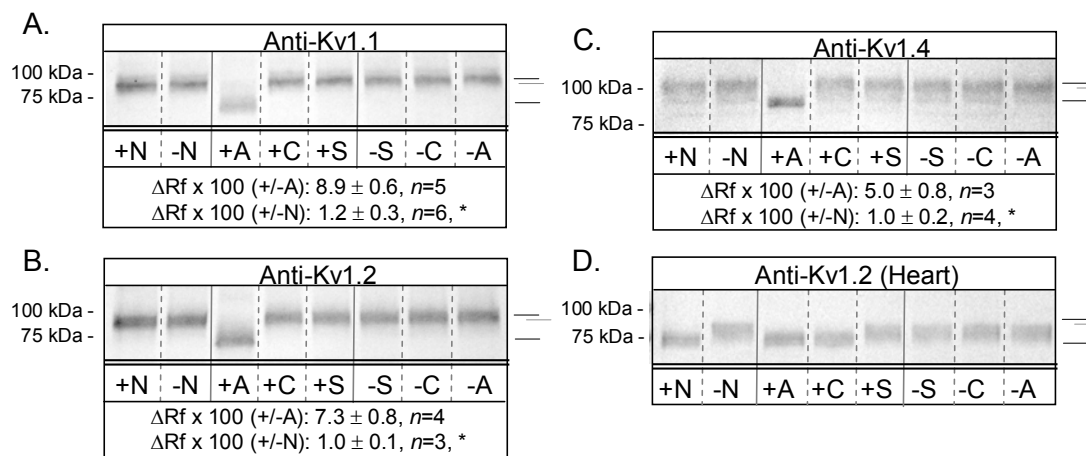
N-Glycans of Kv1.1, 1.2, and 1.4 proteins contain α 2,8-linked and branched sialyl residues

Earlier studies have shown that the sole N-glycosylation site of Kv1.1, 1.2, and 1.4 proteins are occupied by sialylated N-glycans in rat brain (59). However, the types of sialic acid linkage of their N-glycans have not been identified. Adult rat brain membranes were treated with neuraminidase, sialidase A, sialidase C, or sialidase S under nondenaturing conditions (Figure 20). The electrophoretic migrations of the Kv1.1 (87 kDa), Kv1.2 (92 kDa), and Kv1.4 (106 kDa) glycoproteins were much slower than anticipated from their amino acid sequences (Kv1.1, 65 kDa; Kv1.2, 65 kDa; and Kv1.4, 75 kDa). When stripped brain membranes were treated with either sialidase C or S, the immunobands for the Kv1.1 (Figure 20A), 1.2 (Figure 20B), and 1.4 (Figure 20C) glycoproteins migrated to virtually identical positions as those of untreated brain membranes. In contrast, the Kv1.1, 1.2, and 1.4 immunobands migrated slightly faster when membranes were treated with neuraminidase and much faster when treated with sialidase A. The immunoband shifts produced by neuraminidase and sialidase A were observed on 3-6 Western blots for all three of the Kv1 glycoproteins (Figure 20A, 20B, 20C). These results demonstrated the removal of α 2,8-linked sialyl residues from

Figure 20. Kv1.1, Kv1.2 and Kv1.4 glycoproteins in brain contain branched and α 2,8-linked sialyl residues

Western blots of stripped brain (A, B and C) and heart (D) membrane proteins untreated (-) or treated (+) with neuraminidase (N), sialidase A, C, or S were probed with: anti-Kv1.1, anti-Kv1.2, and anti-Kv1.4 antibodies. Upper black lines signify fully sialylated Kv1 glycoproteins. Lowest black lines represent the completely desialylated Kv1 glycoproteins. Middle gray lines denote partially desialylated Kv1 glycoproteins. Below each Western blot are the differences in the relative electrophoretic mobility ($\Delta R_f \times 100$ values) of the Kv1 glycoproteins. The number of Western blots is symbolized by *n*. Asterisks represent significant difference from the sialidase A immunoband shift.

Figure 20
Cartwright and Schwalbe, 2008



neuronal Kv1.1, 1.2, and 1.4 glycoproteins. They also suggested either the presence of sialic acids linked to internal residues of the carbohydrate chain or that the action of neuraminidase was hindered by the Kv1 glycoproteins.

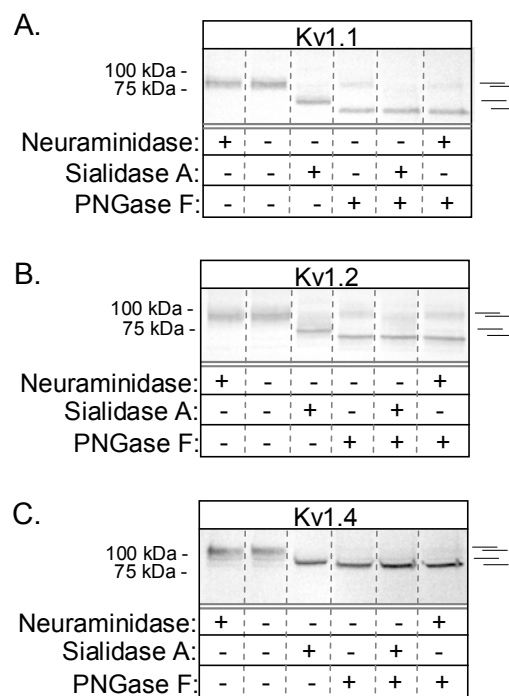
To determine whether the Kv1 proteins were preventing access of neuraminidase to the sialylated N-glycans, we examined the sialylated N-glycan of the Kv1.2 protein expressed in heart. The electrophoretic migration of the Kv1.2 protein (79 kDa) in heart was faster than that in brain (Figure 20D). When heart membranes were digested with neuraminidase and sialidase A, the immunoband shifts were identical. This result indicated that the Kv1.2 protein was not preventing the removal of sialic acid by neuraminidase. Additionally, our results indicated that both neuraminidase and sialidase A were efficient in removing sialic acid from the N-glycan of the Kv1.2 protein. The results also demonstrated that the N-glycan of the Kv1.2 protein from heart was different from that expressed in brain. For instance, identical immunoband shifts were generated by treatment of heart membranes with neuraminidase, sialidase A or sialidase C, while an immunoband shift was not observed when membranes were treated with sialidase S. This result indicated that Kv1.2 glycoprotein in heart was rich in α 2,6-linked sialic acid. Taken together, our results support that brain Kv1.1, 1.2, and 1.4 glycoproteins have α 2,8-linked sialic acids, as well as sialic acid residues linked to internal residues of the carbohydrate chains.

To directly demonstrate that the sialyl residues were removed from the N-glycans of the Kv1.1 (Figure 21A), 1.2 (Figure 21B), and 1.4 (Figure 21C) proteins, stripped brain membranes were digested with different combinations of neuraminidase, sialidase

Figure 21. Branched and α 2,8-linked sialic acid residues are attached to the N-linked oligosaccharides of Kv1.1, Kv1.2 and Kv1.4 proteins

Stripped brain membrane proteins were untreated (-) or treated (+) with various combinations of: neuraminidase, sialidase A and PNGase F, and then immunoblotted using anti-Kv1.1 (A), anti-Kv1.2 (B) and anti-Kv1.4 (C) antibodies. Uppermost lines correspond to fully sialylated Kv1 glycoproteins, upper middle line represents partially desialylated glycoproteins, lower middle lines signify fully desialylated glycoproteins, and the lowest lines denote unglycosylated Kv1 proteins.

Figure 21
Cartwright and Schwalbe, 2008



A and PNGase F. In all cases, Kv1 immunobands were shown to migrate slightly faster for samples treated with neuraminidase compared to those untreated. Additionally, they migrated even faster for those treated with sialidase A, and fastest for those treated with PNGase F. However, when samples were treated simultaneously with PNGase F and either neuraminidase or sialidase A, the Kv1 immunobands migrated to similar positions as those treated solely with PNGase F. Taken together, these results have directly shown that the N-glycans of the Kv1.1, 1.2, and 1.4 proteins, like Kv3 glycoproteins, were capped with α 2,8-linked sialyl residues, and have sialyl residues attached to internal residues of the carbohydrate chains.

Discussion

Here we have established an immunoband shift assay for detecting common and uncommon sialic acid linkages of native glycoproteins which are present in low amounts and difficult to purify. Changes in relative electrophoretic mobility due to the various sialidase treatments were interpreted as sialic acid removal, not proteolysis, or other glycosidase activities. Kinetic selectivity was eliminated by extending the incubation periods of the reactions (111). When sialylated N-glycans of the Kv3 (37) and Kv1 proteins (Figure 21) were absent, immunoband shifts produced by the various exosialidases were absent. These results demonstrated that proteolysis did not contribute to immunoband shifts. Contamination of different glycosidase activities in the various enzymes was also unlikely since the immunoband shift assays verified α 2,3- and α 2,8-linkages for N-CAM (98). To address N-glycan resistance, both sialidase A and neuraminidase were used to identify α 2,8-linked sialyl residues. Additionally, when heart Kv1.2 glycoprotein was treated with neuraminidase and sialidase A, the immunoband shifts were identical. This result indicated that the Kv1.2 protein was not hindering the action of neuraminidase, and therefore supported that sialyl residues were linked to internal residues of the carbohydrate chain of the neuronal Kv1 glycoproteins.

Utilization of this immunoband shift assay has demonstrated that the N-glycan chains were capped with α 2,3-linked sialyl residues for the Kv3.1, 3.3, and 3.4 proteins (Figure 14A) from adult rat brains. Sialyl residues with α 2,3- and α 2,6-linkage are common linkages with the former being more prevalent in adult rat brain (69). Secondly, sialylated N-glycans of the neuronal Kv3.1, 3.3, and 3.4 (37,116) and Kv1.1, 1.2, and 1.4

(59) glycoproteins were shown to have α 2,8-linked sialyl residues capping their carbohydrate chains (Figure 14). It was also found that Kv3.1, 3.3, and 3.4 glycoproteins, like N-CAM (98) and recombinant Kv3.1, have at least one of their carbohydrate chains capped with an oligo/polysialyl unit (Figure 14A). Moreover, our results supported a more compact glycoprotein when an oligo/polysialyl unit was attached and a less compact glycoprotein when mono/disialyl moieties were attached. Therefore, indicating the N-glycans were capped with monosialyl residues and disialyl units as showed in our proposed model of Kv3 glycoproteins. The results also supported that brain Kv1.1, 1.2, and 1.4 glycoproteins were capped with disialyl units (Figure 14B). As mentioned, sialyl residues with α 2,8-linkage give rise to di/oligo/polysialyl units which are primed by an α 2,3-linked sialyl residue (97). Less than 10% of sialylated glycoproteins in adult rat brain contain disialyl units (70). Moreover, it has been indicated that at least six glycoproteins contain oligosialyl units and about thirteen glycoproteins contain disialyl units in adult mammalian brains (88). The biological importance of the di/oligosialyl units of glycoproteins is unsolved. However, it may be that these di/oligosialyl units are involved in: cell adhesion, differentiation, and signal transduction, like gangliosides (88). Identification of six brain glycoproteins with di/oligosialyl units is the initial step in elucidating the roles of these atypical types of N-glycans.

An earlier study has shown that sialyl residues were linked to internal residues of the oligosaccharide moiety of gangliosides (103,104), and that sialidase A could cleave this type of linkage (109). To date, sialyl residues linked to internal residues of the carbohydrate chains of N-glycans has not been described. Here we have demonstrated

that the N-glycans of brain Kv1.1, 1.2, and 1.4 proteins (Figure 14B) have such branched sialyl residues. This finding is supported by the very large immunoband shift produced by sialidase A treatment relative to neuraminidase treatment for brain Kv1.1, 1.2, and 1.4 glycoproteins (Figure 20), along with the demonstration that the Kv1.2 protein did not interfere with neuraminidase activity in heart membranes. The Kv3.1, 3.3, and 3.4 glycoproteins (Figure 14A), as well as N-CAM, also appeared to have this novel type of sialic acid linkage.

Identification of these different Kv1 and Kv3 glycoforms and their unique sialic acid linkages suggest critical biological roles of their attached glycoconjugates. Additionally, the absolute conservation of the two N-glycosylation sites in the S1-S2 linker of the Kv3 proteins (35,37,116), along with the highly conserved site in the S1-S2 linker of the Kv1 subfamily members with the exception of Kv1.6 (16,59) argue the importance of the sialyloligosaccharides in regulating neuronal excitability. Previously, we showed that the activation kinetics was slowed in unglycosylated Kv3.1 channels compared to those with simple type N-glycans (35). The activation rates of the Kv10.1 channel was much slower for the aglycoform than the glycoform (85). Additionally, currents were greatly reduced when N-glycosylation of HERG was abolished as a result of diminished cell surface expression (87). Also, it was shown that glycosylation of the Kir1.1 channel can stabilize the open state (119). Secondly, sialyl residues of glycosylated Kv channels have been demonstrated to regulate ion channel activity. Removal of sialyl residues from Kv1.1 and 1.2 channels decreased their activation rates, and furthermore a greater positive potential was required for their activation (58,83,84).

Therefore, it may be that the attachment of atypical sialylated N-glycans to the Kv3 and Kv1 channels assists in regulating action potential waveforms by influencing the rates of repolarization. Future studies will entail determining the roles of these uncommon sialylated N-glycans on channel activities of the Kv3 and Kv1 glycoproteins.

Overall, this study has identified novel sialylated N-glycans for two classes of voltage-gated potassium channels. Six members from these classes were shown to contain glycoconjugates with α 2,8-linked sialyl residues which consist of di/oligo/polysialyl units. Additionally, sialyl residues linked to internal carbohydrate residues were shown to be components of the N-glycans of Kv1 glycoproteins, as well as Kv3 glycoproteins, which until now has only been identified in gangliosides (103,104). This unique N-glycan modification of branched sialyl residues was also identified for N-CAM. We speculate that these novel sialylated N-glycans of the Kv3 and Kv1 channels are important modifications in regulating channel function or channel expression at the cell surface of either axonal or somatodendritic domains. Additionally, the sialylated N-glycans of the Kv3 and Kv1 proteins may play a role in cellular recognition events which perhaps involve plasticity and synapse formation.

**CHAPTER 7 - NEURONAL N-GLYCOSYLATION PROCESSING REGULATES
VOLTAGE-GATED POTASSIUM CHANNEL ACTIVITY**

Tara A. Cartwright and Ruth A. Schwalbe

Cell Biochemistry and Biophysics (2009) In review

Abstract

Atypical sialylated N-glycans are attached to the Kv3.1 protein in adult rat brain, along with the heterologously expressed Kv3.1 protein in rat B35 neuroblastoma cells. Glycosylated (wild type), partially glycosylated (N220Q and N229Q), and unglycosylated (N220Q/N229Q) Kv3.1 proteins were characterized utilizing transfected B35 cells. Electrophoretic migration of partially glycosylated Kv3.1 proteins treated with neuraminidase showed that both N-glycans were sialylated. Whole cell current recordings showed that the glycosylated Kv3.1 protein favored a subpopulation of channels with fast activation and inactivation rates. In contrast, the predominant subpopulation of the aglycoform had slow activation and inactivation rates. Only the glycosylated Kv3.1 protein could produce the subpopulation of channels with fast activating and inactivating rates for the inactivating current type. Both glycosylated and partially glycosylated Kv3.1 channels could generate this subpopulation when expressing the noninactivating current type while this subpopulation for the aglycoform was seldom. The predominant effect resulting from the absence of an N-glycan at position 220 was a reduction in current density while at 229 was a shift in the threshold potential for channel activation. Thus, mammalian neuronal N-glycosylation processing of the Kv3.1 channel has a greater effect on activation and inactivation properties than when the Kv3.1 glycoprotein was processed in insect cells (35). Additionally, sialoglycoconjugates at the cell surface contribute to the uniform transmembrane electrical field detected by the voltage sensor of the channel. We propose that cell-specific N-glycosylation processing of glycosylated ion channels provides a universal cellular mechanism for regulating ion channel function.

Introduction

Voltage-gated potassium channels (Kv)¹ are essential components responsible for determining the intrinsic electrical excitability of neurons by repolarizing action potentials (5). The Kv3 channel subfamily members, Kv3.1-Kv3.4, localized in the axonal and somatodendritic compartments of neurons (16) have two absolutely conserved N-glycosylation sites within the S1-S2 extracytoplasmic linker (35). The Kv3.1 channel, a delayed rectifier, has unique functional characteristics when heterologously expressed in *Xenopus* oocytes (20-23) and CHO cells (28) which include slow inactivation rates, fast activation and deactivation rates, and channel activation at more depolarized potentials than other Kv channels. Expression of the Kv3.1 channel in mammalian cells also produced noninactivating currents with transient peaks which lacked saturation at more positive potentials (24,26,29), along with noninactivating currents without transient peaks (14,26,29).

The N-glycan structures of the Kv3 proteins are quite diverse in the various regions throughout the adult rat central nervous system (37). Of recent, it has been demonstrated that the Kv3.1 (Figure 22A), 3.3, and 3.4, and Kv1.1, 1.2, and 1.4 proteins of adult rat brain, as well as Kv3.1 heterologously expressed in B35 cells, contain atypical sialylated N-glycans (152). These unique N-glycans were shown to consist of sialyl residues with α 2,8-linkage. This type of linkage gives rise to di/oligo/polysialic acid units (69,70,97,139). It was also discovered that the atypical N-glycans had sialyl residues linked to internal residues of the carbohydrate chain (152) which previously was solely identified for gangliosides (103,104). The information on the cellular roles of these

unique sialyl linkages is very limiting, if not absent, as is the effect of neuronal N-glycosylation processing on voltage-gated K^+ channels. However, some studies of N-glycosylation processing on Kv channels have been conducted utilizing non-excitabile cell systems. Previously, we have presented evidence that the absence of simple type N-glycans on Kv3.1 channels when expressed in *Spodoptera frugiperdae* (Sf9) insect cells causes slower activation rates, and furthermore, a slight positive shift in voltage dependence relative to its glycosylated counterpart (35). Additional studies have also shown that N-glycans alter the gating function of Kv1.1 (58,83), Kv1.2 (84) and Kv10.1 channels (85), as well as influences proper trafficking of the Kv1.2 (84) and Kv1.4 channel (86).

The primary aim of this paper was to determine whether cell-specific N-glycosylation processing modulates Kv3.1 channel activity. Activation rates of the heterologously expressed wild type Kv3.1 glycoprotein in B35 cells were greater than those for the Kv3.1 glycoprotein heterologously expressed in Sf9 cells (35). Moreover, the ratio of the rise times at +40 mV of the unglycosylated Kv3.1 channel to that of the glycosylated Kv3.1 channel expressed in B35 cells compared to that in Sf9 cells was much greater in B35 cells. It was also shown that the wild type Kv3.1 channel expressed in B35 cells could have fast inactivation rates while this property was unobserved for the wild type Kv3.1 channel expressed in Sf9 cells (35). Of note, utilization of the two independent heterologous expression systems supports that both highly conserved mutations are not responsible for the observed differences in the Kv3.1 channel properties. Instead, our results support that the wild type Kv3.1 channel associated with

atypical sialylated N-glycans can favor subpopulations with fast activating rates and either fast or slow inactivating rates while the absence of N-glycans largely favored the slow activating and inactivating rates. Furthermore, the results indicated that cell-specific glycoconjugates at the cell surface could influence the voltage sensor of the Kv3.1 channel. Taken together, our results strongly highlight the concept that atypical sialic acid linkages present in mammalian brain (69,70,97) are critical in modulating K⁺ currents of neurons.

Results

Both N-Glycans of the Kv3.1 protein are sialylated in B35 neuroblastoma cells

Mammalian brain N-glycans of Kv3 and Kv1 channels have high contents of sialic acid residues and display them in an uncharacteristic manner (69). To our knowledge, atypical N-glycosylation of endogenous and heterologous Kv glycoproteins has not been established when evaluating channel function. Recently, it was shown that the Kv3.1 channel heterologously expressed in B35 cells generates Kv3.1 glycoprotein with uncommon sialylated N-glycans (152). Here we have utilized this same expression system to study the affect of neuronal N-glycosylation processing on Kv3.1 channel activity. Wild type Kv3.1 protein has two N-glycosylation sites (Figure 22A) which are occupied in native tissue (116) and a heterologous expression system (35). Kv3.1 N-glycosylation mutants were constructed by removing both sites (N220Q/N229Q) and one site at a time (N220Q and N229Q) (35). In all cases, the FLAG epitope was attached to the C-terminus of each Kv3.1 protein for purposes of isolation and identification. Kv3.1 proteins were M2 immunoaffinity purified from stable transfected B35 cells. Partially purified Kv3.1 samples were then analyzed by Western blots (Figure 22B and 22C). Wild type Kv3.1 migrated predominantly as the fully processed form (132 kDa) and a faster migrating immunoband (88 kDa) (Figure 22B). As previously shown, wild type Kv3.1 is associated with atypical sialylated N-glycans in B35 cells, and the electrophoretic migration of the fully processed form was slightly slower than that observed in rat brain (152). The faster immunoband had a similar electrophoretic migration as the Kv3.1 glycoprotein produced in Sf9 cells (35,116). Additionally, the faster migrating form was

Figure 22. Topological model of the Kv3.1 glycoprotein and immunoblot analysis of wild type and N-glycosylation mutants of Kv3.1 protein heterologously expressed in B35 cells

(A) Schematic of the predicted topology of the Kv3.1 α -subunit. The amino acid sequence of the S1-S2 linker from rat (P25122) with the two native N-glycosylation consensus sites, NKT (220 to 222) and NGT (229 to 231) underlined. Trees denote the attachment of oligosaccharides at native consensus sites. Sialyl residues of the carbohydrate chains with α 2,3-linkage and α 2,8-linkage are depicted by black-filled circles and grey-filled circles, respectively. One of the carbohydrate chains is terminated with an oligosialyl unit (row of light grey circles). The N-glycans also contain sialyl residues linked to internal residues of the carbohydrate chains (white-filled circles). (B) Immunoblot analysis of M2 immunoaffinity purified Kv3.1 proteins from B35 cells transfected with recombinant vectors containing wild type Kv3.1, N220Q/N229Q, N220Q, and N229Q cDNA molecules. Upper arrow and upper line represent both N-glycosylation sites occupied by complex and simple type N-glycans, respectively, while the lower arrow and middle line signify occupancy of one site. The lowest line denotes the unglycosylated Kv3.1 protein. (C) Immunoblot analysis of immunoaffinity purified N220Q and N229Q Kv3.1 mutant proteins from transfected B35 cells were digested (+) and undigested (-) with neuraminidase. Kaleidoscope[®] protein molecular mass standards are as indicated.

sensitive to Endo H digestion while the upper band was resistant (not shown). Of note the faster migrating form has both N-glycosylation sites occupied by simple type N-glycans, and therefore will be referred to as unprocessed N-glycans. When both sites were abolished (N220Q/N229Q), a single migrating species (81 kDa) was detected which corresponded to the unglycosylated Kv3.1 protein. Two immunobands for each of the single N-glycosylation Kv3.1 mutants with quite similar electrophoretic mobility were detected. The upper bands (N220Q, 106 kDa and N229Q, 107 kDa) will be referred to as processed N-glycans and the lower bands (N220Q, 83 kDa and N229Q, 85 kDa) as unprocessed N-glycans (Figure 22B). In both cases, the upper immunobands were sensitive to neuraminidase treatment while the lower immunobands were insensitive (Figure 22C). Additionally, the electrophoretic migration of the faster immunobands was similar to those detected for the single mutant proteins associated with simple type N-glycans expressed in Sf9 cells (35).

To evaluate whether endogenous Kv3.1, 3.3 and 3.4 proteins could be detected in B35 cells, nontransfected B35 membrane proteins, as well as partially purified Kv3.1 protein samples, were subjected to SDS-PAGE and immunoblotted using anti-Kv3 antibodies (not shown). In all cases, endogenous Kv3.1, 3.3, and 3.4 glycoproteins were not observed in nontransfected B35 cells, nor were endogenous Kv3.3 and 3.4 proteins found to form heteromultimers with the heterologously expressed Kv3.1 glycoprotein. Overall, these results have shown that both sites were occupied by sialylated N-glycans, and that the occupancy of these sites was independent of one another. Moreover, the removal of one or even both of these sites does not greatly influence Kv3.1 protein

expression in neuronal cells, similar to that described in Sf9 cells (35). Based on the Western blotting studies, wild type Kv3.1, N220Q/N229Q, and both N220Q and N229Q will be referred to as the glycosylated, unglycosylated, and partially glycosylated forms of the Kv3.1 channel, respectively, throughout the text.

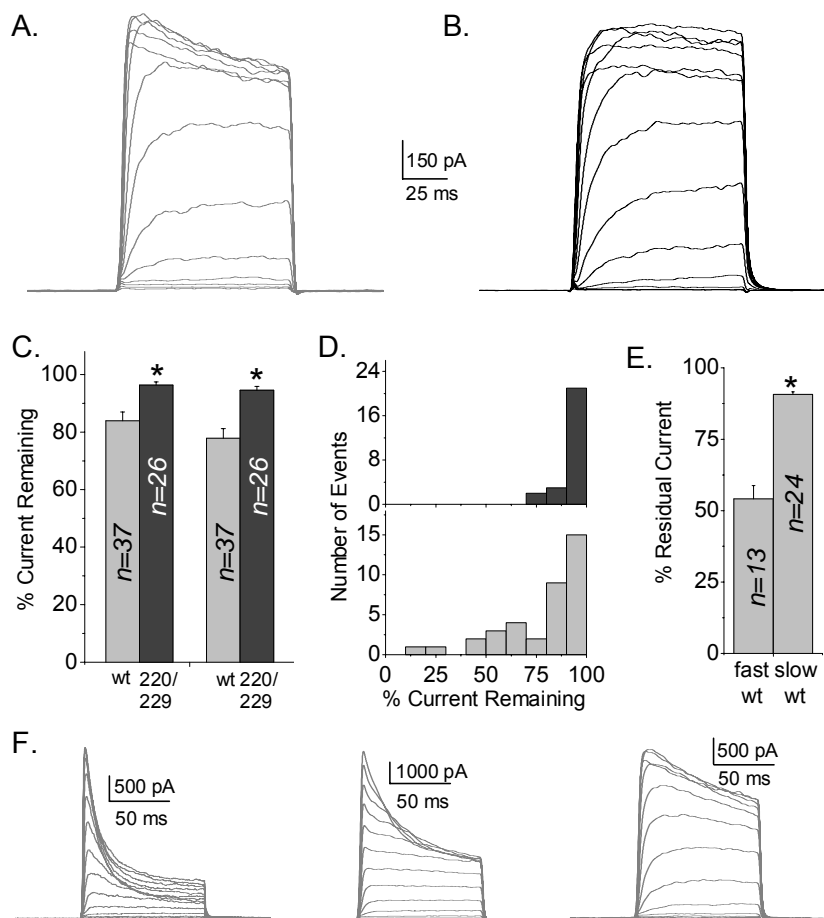
Glycosylated Kv3.1 channels have faster inactivation kinetics than their unglycosylated counterparts

To examine whether neuronal N-glycosylation processing affects Kv3.1 channel activity, current measurements were performed in the whole cell mode of the patch clamp technique. Whole cell currents of B35 cells heterologously expressing wild type Kv3.1 (Figure 23A) and N220Q/N229Q (Figure 23B) were detected when the applied test potential was greater than -30 mV, and furthermore began to saturate at about +40 mV. These whole cell current recordings were similar to those previously described for infected Sf9 cells (35), oocytes (20-22) and mammalian cells (40,153) heterologously expressing the Kv3.1 channel. This current pattern which saturates at more depolarized potentials will be defined as the inactivating current type. It was also noted that the inactivation of wild type Kv3.1 currents with respect to time appeared to be more dramatic than those from earlier reports. The whole cell currents of the wild type Kv3.1 channel could be observed to decrease with time at less depolarized potentials and to a greater extent than the N220Q/N229Q channel. The percent of current remaining at the end of the 100 ms sweep for wild type Kv3.1 was 13% and 18% smaller at +40 mV (gray and black bars on the left-side) and +60 mV (gray and black bars of the right-side),

Figure 23. Whole cell current recordings of wild type Kv3.1 and N220Q/N229Q channels display variations in the rate of inactivation

Exemplar currents mediated by wild type Kv3.1 (A) and N220Q/229Q (B) channels expressed in B35 cells. Currents were measured in the whole-cell configuration during 100 ms depolarizing test pulses from -40 to $+80$ mV from a holding potential of -50 mV. (C) Percentage of current remaining at $+40$ mV (left) and $+60$ mV (right) for wild type Kv3.1 (light gray, 83.9 ± 3.1 at $+40$ mV, 77.8 ± 3.4 at $+60$ mV) and N220Q/N229Q (dark gray, 96.3 ± 1.1 at $+40$ mV, 94.5 ± 1.4 at $+60$ mV) inactivating currents. (D) Frequency distribution histogram for percent current remaining at $+60$ mV for wild type Kv3.1 (light gray, $n=37$) and N220Q/N229Q (dark gray, $n=26$) inactivating currents. (E) Bar graph summarizing percent current remaining at $+60$ mV for fast (54.1 ± 4.6) and slow (90.7 ± 0.8) forms of the wild type Kv3.1 inactivating current type. (F) Representative tracings showing the broad distribution of fast inactivating currents for the wild type Kv3.1 channel. The percent of current remaining at $+60$ mV from left to right were: 19.7%, 43.9%, and 69.3%. Asterisks denote the level of significance against either wild type Kv3.1 ($P < 0.05$) or fast inactivating currents ($P < 0.01$). Data are expressed as mean \pm S.E. n corresponds to the number of cells tested.

Figure 23
Cartwright and Schwalbe, 2008



respectively, than those of the N220Q/N229Q channel (Figure 23C). These current remaining values are given in Table 1 which summarizes the whole current parameters for all four forms of the Kv3.1 channel. Taken together, these results showed that the glycosylated Kv3.1 channel has faster inactivation kinetics than its unglycosylated counterpart.

To further characterize the decrease of the currents with respect to time for the inactivating current type, frequency distribution histograms were constructed for the percent of current remaining at +60 mV for both wild type Kv3.1 (Figure 2D, lower panel) and N220Q/N229Q (Figure 23D, upper panel) channels. More than 80% of the N220Q/N229Q cells showed greater than 90% of current remaining while only about 40% of the wild type Kv3.1 cells displayed this slow inactivating behavior. It was also apparent that the number of wild type Kv3.1 cells showed a very broad range of inactivating kinetics while that of N220Q/N229Q cells was quite narrow. Therefore, the inactivating current type of the wild type Kv3.1 channel was further categorized by the time-dependence of current inactivation. We refer to these two time-dependent inactivating kinetic categories as the fast form and the slow form. The fast form included all wild type Kv3.1 transfected B35 cells which had percent current remaining values of less than 76% at +60 mV while the slow form encompasses the remainder of the wild type Kv3.1 transfected B35 cells. As shown, the percent of current remaining for the fast form was about 40% less than the slow form (Figure 23E). The wide range of current remaining values for the fast form is illustrated in the selected whole cell recordings (Figure 23F, percent of current residual at +60 mV: 19.7%, left panel; 43.9%, middle

panel; and 69.3 %, right panel). The inactivating rates for N220Q/N229Q transfected B35 cells were more like the slow form since all had greater than 76% current remaining (Figure 23D). However, the inactivating rates of the slow form of wild type Kv3.1 was significantly faster than those of N220Q/N229Q (Table 1 and 2). These results indicated that the wild type Kv3.1 protein associated with atypical sialylated N-glycans can express the inactivating current type with a broad spectrum of inactivation rates. They also support that both the fast and slow forms of the wild type Kv3.1 channel have faster inactivation rates than those of the N220Q/N229Q channel.

Inactivation kinetics of the wild type Kv3.1 (Figure 24A) and N220Q/N229Q (Figure 24B) channels were also examined using a similar voltage protocol, as above, except the duration (2 s) of the pulse was increased by about 20-fold. The whole cell recordings showed that initially the currents quickly increased with time, and then decreased as the duration of the pulse continued. Additionally, the decrease in current amplitudes at the end of pulses relative to the maximum current amplitudes was greater for the wild type Kv3.1 channel than the N220Q/N229Q channel. For example, the percent of current remaining for the wild type Kv3.1 channel was about 72% of the unglycosylated Kv3.1 channel when the test potential was +40 mV (Figure 24C). The frequency distribution histograms of both wild type Kv3.1 and N220Q/N229Q channels covered broad ranges (Figure 24D). However, the overall range of values for the wild Kv3.1 channel was lower than those of the N220Q/N229Q channel. The same cells expressing the fast and slow forms of the wild type Kv3.1 inactivating current type were used to characterize the inactivation kinetics of the longer pulse at +40 mV. The percent

Table I: Electrophysiological parameters of glycosylated, unglycosylated and partially glycosylated forms of the Kv3.1 channel in B35 cells

The biophysical parameters are shown for the inactivating current (inact i) and noninactivating current (noninact i) types. As defined, the former showed current saturation at more positive potentials while the latter lacked current saturation. The noninactivating current type was further grouped by the presence (w transient peak) or absence (w/o transient peak) of a transient peak. % I remaining, corresponds to the percent of current remaining near the last 10 ms of the indicated sweep relative to the peak current amplitude; RT stands for rise times; τ_{act} , activation time constant; $V_{1/2(peak)}$ and $V_{1/2(ss')}$, voltage at which 50% of activation is reached based on conductance-voltage curve determined from the current amplitude of the peak current (peak) or the last 10 ms of the sweep (ss'); $dV_{(peak)}$ and $dV_{(ss')}$, slope factor based on conductance-voltage curve; τ_{deact} , deactivation time constant of deactivation. Unpaired Student's t-test was used to compare wild type Kv3.1 and N220Q/N229Q transfected B35 cells, as well as N220Q and N229Q transfected B35 cells. A value of $P < 0.05$ was considered significant (*). N.S. indicates that N220Q and N229Q were not significantly different. To compare all four forms of the Kv3.1 protein one-way ANOVA followed by Bonferroni's post hoc-tests was utilized. A value of $P < 0.05$ indicated that the wild type transfected cells were considered significantly different from the Kv3.1 mutant transfected B35 cells (*). Values are given as mean \pm S.E. In all cases n corresponds to the number of cells tested.

Table I: Electrophysiological parameters of glycosylated, unglycosylated and partially glycosylated forms of the Kv3.1 channel in B35 cells

	Wild type	N220Q/N229Q	N220Q	N229Q
Kv (100 ms) protocol				
<i>Inactivation kinetics</i>				
% i remaining at +40 mV				
Inact i	83.9 ± 3.1 (n=37)	96.3 ± 1.1 (n=26)**	95.8 ± 1.0 (n=17) ^{NS*}	98.0 ± 0.8 (n=12)*
Noninact i	92.8 ± 0.8 (n=68)	98.6 ± 0.5 (n=13)**	94.0 ± 1.4 (n=10) ^{NS}	92.7 ± 1.0 (n=29)
w transient peak	90.0 ± 0.8 (n=44)	96.6 ± 0.7 (n=4)*	92.6 ± 1.3 (n=8) ^{NS}	90.6 ± 0.9 (n=22)
w/o transient peak	97.7 ± 1.1 (n=24)	99.6 ± 0.2 (n=9) ^{NS}	99.3 ± 0.1 (n=2) ^{NS}	99.4 ± 0.3 (n=7)
% i remaining at +60 mV				
Inact i	77.8 ± 3.4 (n=37)	94.5 ± 1.4 (n=26)**	94.7 ± 1.1 (n=17) ^{NS*}	96.7 ± 0.8 (n=12)*
Noninact i	87.8 ± 0.9 (n=68)	96.9 ± 1.2 (n=13)**	89.0 ± 1.5 (n=10) ^{NS}	87.8 ± 0.8 (n=29)
w transient peak	84.9 ± 0.6 (n=44)	90.8 ± 0.8 (n=4)**	87.4 ± 1.1 (n=8) ^{NS}	86.2 ± 0.7 (n=22)
w/o transient peak	93.1 ± 1.9 (n=24)	99.6 ± 0.2 (n=9)*	95.4 ± 4.3 (n=2) ^{NS}	93.1 ± 0.9 (n=7)
<i>Activation kinetics</i>				
RT at +40 mV (ms)				
Inact i	7.7 ± 0.6 (n=37)	16.2 ± 1.5 (n=26)**	10.7 ± 1.0 (n=17) ^{NS}	12.9 ± 1.5 (n=12)*
Noninact i	3.9 ± 0.3 (n=68)	9.6 ± 1.4 (n=13)**	3.3 ± 0.4 (n=10) ^{NS}	3.0 ± 0.1 (n=29)
w transient peak	3.0 ± 0.1 (n=44)	3.9 ± 0.2 (n=4)**	2.7 ± 0.04 (n=8) ^{NS}	2.8 ± 0.1 (n=22)
w/o transient peak	5.8 ± 0.7 (n=24)	12.2 ± 1.3 (n=9)**	5.8 ± 0.5 (n=2)*	3.7 ± 0.4 (n=7)
τ_{act} at +40 mV (ms)				
Inact i	3.1 ± 0.3 (n=37)	7.1 ± 0.7 (n=26)**	4.3 ± 0.3 (n=17)**	6.1 ± 0.8 (n=12)*
$V_{1/2}$ (peak) (mV)	10.1 ± 0.8 (n=37)	8.1 ± 0.6 (n=26)**	9.2 ± 0.8 (n=17)**	12.7 ± 0.9 (n=12)*
$V_{1/2}$ (ss') (mV)	5.7 ± 0.7 (n=37)	7.1 ± 0.6 (n=26)**	8.6 ± 0.8 (n=17)**	12.4 ± 0.9 (n=12)*
$dV_{(peak)}$	11.2 ± 0.5 (n=37)	9.6 ± 0.3 (n=26)**	9.9 ± 0.4 (n=17)**	9.5 ± 0.4 (n=12)*
$dV_{(ss')}$	9.8 ± 0.5 (n=37)	9.2 ± 0.4 (n=26)**	9.6 ± 0.5 (n=17)**	9.3 ± 0.5 (n=12)*
<i>Current density (pA/pF)</i>				
All I types				
	295 +/- 20 (n=105)	138 +/- 19 (n=39)**	199 +/- 34 (n=27)*	322 +/- 31 (n=41)
Inact i	163 +/- 24 (n=37)	88 +/- 13 (n=26)*	97 +/- 21 (n=17) ^{NS}	132 +/- 26 (n=12)
Noninact i	366 +/- 24 (n=68)	239 +/- 39 (n=13)*	373 +/- 50 (n=10) ^{NS}	401 +/- 33 (n=29)
<i>% Current type</i>				
Inact i	35% (n=105)	67% (n=39)	63% (n=27)	29% (n=41)
Noninact i	65% (n=105)	33% (n=39)	37% (n=27)	71% (n=41)
w transient peak	65% (n=68)	31% (n=13)	80% (n=10)	76% (n=29)
w/o transient peak	35% (n=68)	69% (n=13)	20% (n=10)	24% (n=29)
Kv(2sec) protocol				
% i decay at +40 mV				
Inact i	39.5 ± 2.8 (n=27)	55.2 ± 3.2 (n=18)**	60.2 ± 2.7 (n=14) ^{NS*}	65.0 ± 4.6 (n=9)*
Deactivation protocol				
τ_{deact} at -60 mV (ms)	1.29 ± 0.04 (n=31)	1.45 ± 0.04(n=19)**	1.29 ± 0.07 (n=11) ^{NS}	1.11 ± 0.05 (n=8)*

Table II: Comparison of the biophysical parameters for the fast and slow forms of the wild type Kv3.1 channel

Wild type (fast) and wild type (slow) denote B35 cells transfected with wild type Kv3.1 which expressed the inactivating current type with fast and slow inactivating currents with respect to time. If the percent of current remaining at +60 mV was less than 76% at the end of the pulse relative to the peak current amplitude then those were referred to as the fast form of wild type Kv3.1, and all others were referred to as the slow form. Asterisks denote statistical significance compared with the fast form of wild type Kv3.1 ($P < 0.05$) by unpaired Student's t test. Values are given as mean \pm S.E. In all cases n corresponds to the number of cells tested.

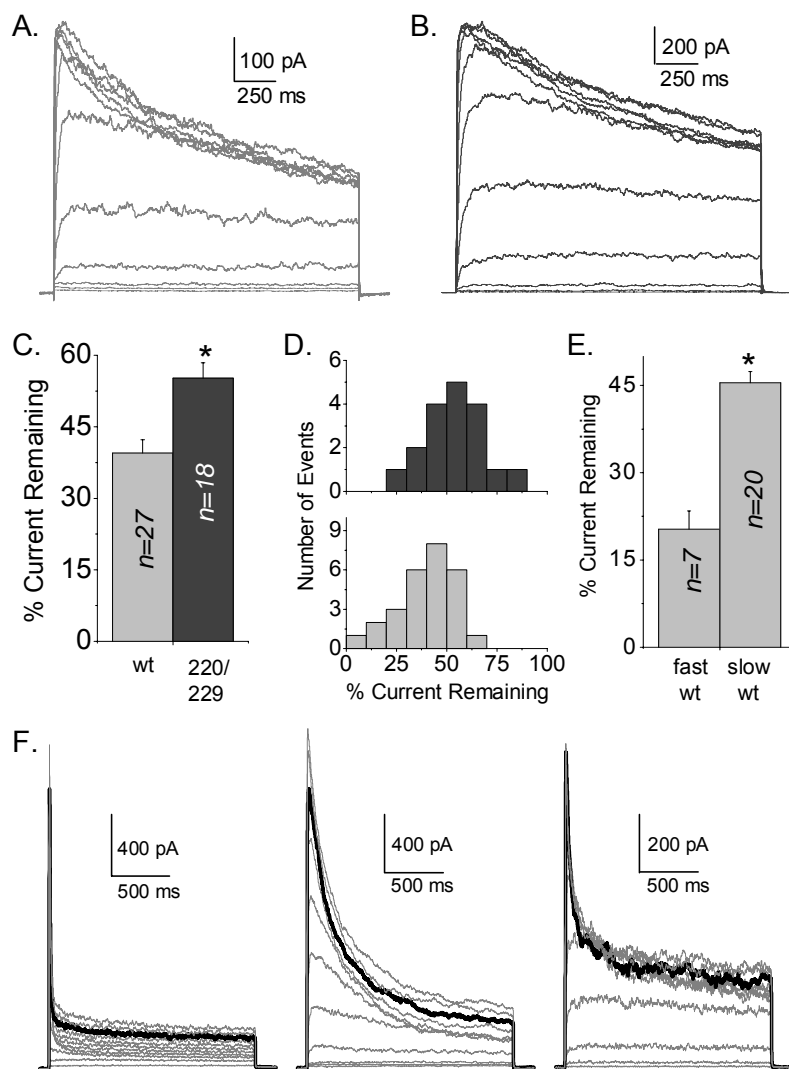
Table II: Comparison of the biophysical parameters for the fast and slow forms of the wild type Kv3.1 channel

	Wild type (fast)	Wild type (slow)
Kv (100 ms) protocol		
<i>Inactivation kinetics</i>		
% I remaining at +60 mV	54.1 ± 4.6 (n=13)	90.7 ± 0.8 (n=24)*
<i>Activation kinetics</i>		
RT at +40 mV (ms)	4.3 ± 0.4 (n=13)	9.6 ± 0.7 (n=24)*
τ_{act} at +40 mV (ms)	1.5 ± 0.2 (n=13)	3.9 ± 0.4 (n=24)*
$V_{1/2}$ (peak) (mV)	13.8 ± 1.5 (n=13)	9.0 ± 0.8 (n=24)*
$V_{1/2}$ (ss') (mV)	1.8 ± 1.0 (n=13)	7.6 ± 0.8 (n=24)*
dV _(peak)	14.0 ± 1.0 (n=13)	9.9 ± 0.5 (n=24)*
dV _(ss')	10.1 ± 0.8 (n=13)	9.4 ± 0.5 (n=24)
<i>Current Density (pA/pF)</i>	274 ± 53 (n=13)	103 ± 14 (n=24)*
Kv(2sec) protocol		
% i remaining at +40 mV	20.3 ± 3.1 (n=7)	45.5 ± 1.9 (n=20)*
Deactivation protocol		
τ_{deact} at -60 mV (ms)	1.28 ± 0.09 (n=10)	1.29 ± 0.04 (n=21)

Figure 24. Prolong depolarization steps enhance the differences in the inactivation rates of wild type Kv3.1 and N220Q/N229Q channels

A comparison of whole cell currents induced in B35 cells transfected with wild type Kv3.1 (A) and N220Q/N229Q (B) by 2 sec depolarizing steps from a -50 mV holding potential to potentials between -40 and 80 mV in 10 mV steps. (C) Percentage of current remaining at +40 mV for wild type Kv3.1 (light gray, 39.5 ± 2.8 at +40 mV) and N220Q/N229Q (dark gray, 55.2 ± 3.2 at +40 mV). (D) Histograms showing the frequency for occurrence of percent current remaining at +40 mV for wild type Kv3.1 (light gray, $n=27$) and N220Q/N229Q (dark gray, $n=18$) inactivating currents. (E) A summary bar graph illustrating the percent current remaining at +40 mV for the fast (20.3 ± 3.1) and slow (45.5 ± 1.9) forms of wild type Kv3.1 inactivating currents. (F) Whole cell recordings showing the broad range of the fast inactivation kinetics for the wild type Kv3.1 channel from left to right: 8.8%, 15.6%, and 28.6%. The thick black lines show the current response elicited at +40 mV. Statistically significant differences between wild type and N220Q/N229Q ($P < 0.05$) or fast and slow forms ($P < 0.01$) of the wild type Kv3.1 inactivating current type are indicated by asterisks. Data are expressed as mean \pm S.E. n corresponds to the number of cells tested.

Figure 24
Cartwright and Schwalbe, 2008



of current remaining for the fast form of wild type Kv3.1 was about 45% of the slow form (Figure 23E). Moreover, the percent of current remaining for the slow form of wild type Kv3.1 (Table 2) was about 20% less than that of N220Q/N229Q (Table 1). Representative whole cell recordings were selected to exemplify the broad range of the inactivation rates of the wild type Kv3.1 channel (Figure 24F, percent of current remaining at +40 mV: 8.8%, left panel; 15.6%, middle panel; and 28.6%, right panel). These results corroborated that the glycosylated Kv3.1 channel has a faster inactivation rate than the unglycosylated Kv3.1 channel. They also showed that wild type Kv3.1 expressed in B35 cells can generate Kv3.1 channels with a broad spectrum of inactivation rates. Taken together, these results indicate that neuronal N-glycosylation processing regulates Kv3.1 channel inactivation properties.

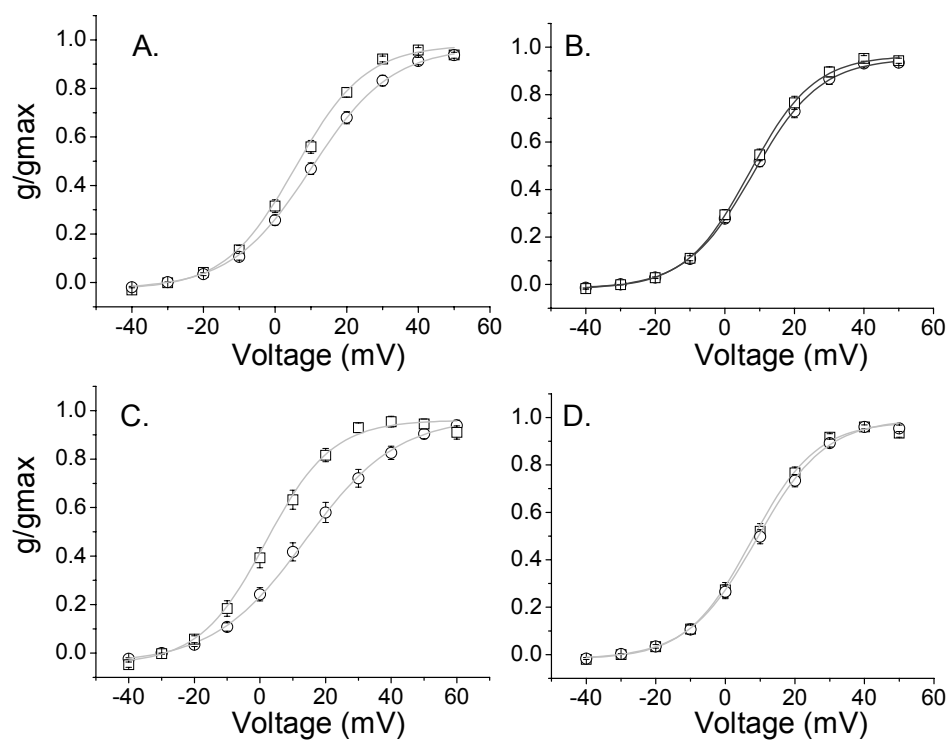
Neuronal N-glycosylation processing regulates the voltage dependence of channel activation and inactivation

Voltage dependence of channel activation was analyzed using peak current amplitudes and current amplitudes at the end of the 200 ms pulse (Figure 25A). The membrane conductance determined from the peak current amplitude vs. applied test potential indicated that more depolarization was required for 50% of wild type Kv3.1 channels to reach activation ($V_{0.5}$ [test potential at which $g/g_{max} = 0.5$] is 10.1 ± 0.8 mV, $n=37$) than when the membrane conductance was determined from the current amplitude at the end of the 100 ms pulse ($V_{0.5}$ is 5.7 ± 0.7 mV, $n=37$). It was also observed that fewer channels were activated as the applied voltage was increased when using peak

Figure 25. Activation (G-V) curves of wild type Kv3.1 and N220Q/N229Q channels

Channel activation versus voltage curves analyzed by using the current amplitude at the peak (\circ) and the last 10 ms of the 100 ms sweep at the applied voltage (\square) for the inactivating current type of wild type Kv3.1 (A, $n = 37$), and N220Q/N229Q (B, $n = 26$), along with the fast (C, $n = 13$), and slow (D, $n = 24$) forms of the inactivating current type for wild type Kv3.1. Each set of data points were fitted with a Boltzmann function of the form: $G = G_{\max}/[1 + \exp(V_{1/2} - V_m)/q]$ where q represents the slope factor, V_m stands for the test potential, $V_{1/2}$ is the potential at which the conductance was half maximal, G is the conductance and G_{\max} is the maximal conductance. The Boltzmann parameter values are reported in both Tables I and II.

Figure 25
Cartwright and Schwalbe, 2008



current amplitudes to determine the slope of normalized membrane conductance voltage relationship (dV [slope of normalized membrane conductance voltage relationship] is 11.2 ± 0.5 mV, $n=37$) than when the membrane conductance was determined from the current amplitude at the end of the sweep (dV is 9.8 ± 0.5 mV, $n=37$). Similar voltage-conductance plots were constructed for the N220Q/N229Q channel. The voltage dependence of activation parameters from either peak current amplitudes or current amplitudes at the end of the pulses for the N220Q/N229Q channel were significantly different ($V_{0.5(\text{peak})}$ is 8.1 ± 0.6 mV; $V_{0.5(\text{ss})}$ is 7.1 ± 0.6 mV, $dV_{(\text{peak})}$ is 9.6 ± 0.3 mV, and $dV_{(\text{ss})}$ is 9.2 ± 0.4 mV, $n=26$). However, the differences between the parameters were not as large as those for the wild type Kv3.1 channel. These results showed that wild type Kv3.1 currents inactivate more readily with time than those of N220Q/N229Q, suggesting a subpopulation of the wild type Kv3.1 channels have faster inactivation rates.

When comparing the voltage dependence of activation parameters determined from current amplitudes at the end of the sweep for wild type Kv3.1 and N220Q/N229Q channels, more depolarization was required to activate 50% of the N220Q/N229Q channels than wild type Kv3.1 channels. In contrast, when peak current amplitudes were utilized to construct the Boltzmann plots, less depolarization was required for 50% of the N220Q/N229Q channels to reach activation than the wild type Kv3.1 channels. Additionally, the percent of wild type Kv3.1 channels activated as a function of applied voltage was less than those for the N220Q/N229Q channel whether determined from peak current amplitudes or current amplitudes at the end of the applied pulses. These results indicated that neuronal N-glycosylation processing of the wild type Kv3.1 protein

generates a subpopulation of glycosylated Kv3.1 channels which requires more depolarization to be activated, and are more readily inactivated than the unglycosylated Kv3.1 channel.

The voltage dependence of channel activation analysis was also conducted for wild type Kv3.1 transfected B35 cells which expressed the fast (Figure 25C) and slow (Figure 25D) forms. Conductance-voltage curves constructed from peak current amplitudes showed more depolarization was required for 50% of the fast form to reach activation than that of the slow form ($V_{0.5 \text{ (peak)}}$: fast form, $13.8 \pm 1.5 \text{ mV}$, $n=13$; slow form, $9.0 \pm 0.8 \text{ mV}$, $n=24$). On the contrary, when determining this same parameter from the current amplitudes at the end of the pulses, then less depolarization was required for 50% of the fast form to reach activation than that of the slow form ($V_{0.5 \text{ (ss)}}$: fast form, $1.8 \pm 1.0 \text{ mV}$, $n=13$; slow form, $7.6 \pm 0.8 \text{ mV}$, $n=24$). Additionally, it was observed that fewer channels were activated as the applied voltage was increased for the fast form (dV is 14.0 ± 1.0 , $n=13$) than for the slow form (dV is 9.9 ± 0.5 , $n=24$) when using peak current amplitudes to determine parameters. However, when using current amplitude at the end of the pulse for the two groups, their parameters were not significantly different. These results indicate that neuronal N-glycosylation processing of the wild type Kv3.1 protein can generate at least two distinct subpopulations of glycosylated Kv3.1 channels which activate and inactivate over a different voltage range. In comparing the slow form of the wild type Kv3.1 channel to the N220Q/N229Q channel, slightly more depolarization was required to activate 50% of the slow form channels and fewer of these channels were activated as the applied voltage increased (Table 1 and 2). Therefore, these

results support that the voltage dependence of Kv3.1 channel activation and inactivation are modulated by neuronal N-glycosylation processing.

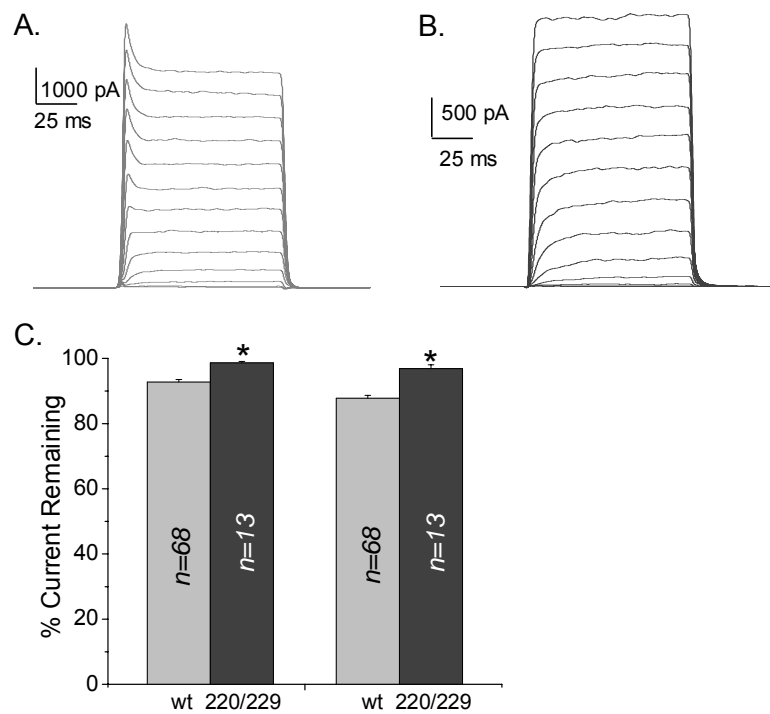
Noninactivating current behavior was more common for the glycosylated Kv3.1 channel

Previously, whole cell recordings of wild type Kv3.1 expressed in mammalian cells (24,26,29) and infected Sf9 cells (35) were shown to have little saturation in current amplitude in response to large depolarization steps. For clarity, this type of whole cell current pattern will be defined as the noninactivating current type. The wild type Kv3.1 (Figure 26A) and N220Q/N229Q (Figure 26B) channels expressed in B35 cells also displayed noninactivating current behavior. The noninactivating currents were the predominant current type expressed by the wild type Kv3.1 channel while inactivating currents were the predominant type for the N220Q/N229Q channel (Table 1). It was also observed that the noninactivating currents of wild type Kv3.1 channels usually had a transient current peak at the initial phase of the sweep (Figure 26A) while the N220Q/N229Q channel usually lacked the transient peak (Figure 26B) (Table 1). Based on the presence and absence of the transient peak at +40 mV, the noninactivating current type was further divided into two groups. One group was referred to as the noninactivating currents with transient peaks, while the other group was referred to as the noninactivating currents without transient peaks. The percent of current remaining at the end of the sweep at +40 mV and +60 mV were determined for both types of noninactivating currents of wild type Kv3.1 and N220Q/N229Q (Figure 26C). The wild

Figure 26. Comparison of the noninactivating current patterns from wild type Kv3.1 and N220Q/N229Q channels

Representative whole cell currents are displayed from B35 cells transfected with wild type Kv3.1 (A) and N220Q/N229Q (B). (C) Percentage of current remaining at +40 mV (left) and +60 mV (right) of the noninactivating current type for wild type Kv3.1 (light gray, 92.8 ± 0.8 at +40 mV; 87.8 ± 0.9 at +60 mV) and N220Q/N229Q (dark gray, 98.6 ± 0.5 at +40 mV, 96.9 ± 1.2 at +60 mV). Asterisks show significant differences ($P < 0.05$) versus wild type Kv3.1. Data are expressed as mean \pm S.E. n corresponds to the number of cells tested.

Figure 26
Cartwright and Schwalbe, 2008



type Kv3.1 channel had a faster inactivation rate at the more depolarized potential while those for the N220Q/N229Q channel were quite similar. Additionally, the inactivation rates were faster for wild type Kv3.1 than N220Q/N229Q at the various potentials (Table 1). The two different types of noninactivating currents for the glycosylated Kv3.1 channel were also reported to inactivate at a faster rate than those of the unglycosylated Kv3.1 channel (Table 1). Moreover, when comparing the two different noninactivating current types displayed by either form of the Kv3.1 channel expressed in B35 cells, the noninactivating current with transient peaks showed a greater inactivation rate than those without transient peaks (Table 1). These results corroborated the inactivation kinetics of the inactivating current type in that the glycosylated Kv3.1 channel inactivates at a faster rate than its unglycosylated counterpart. The results also suggested that the noninactivating current types with transient peaks express a subpopulation of Kv3.1 channels which have faster inactivation kinetic properties, similar to the inactivating current type.

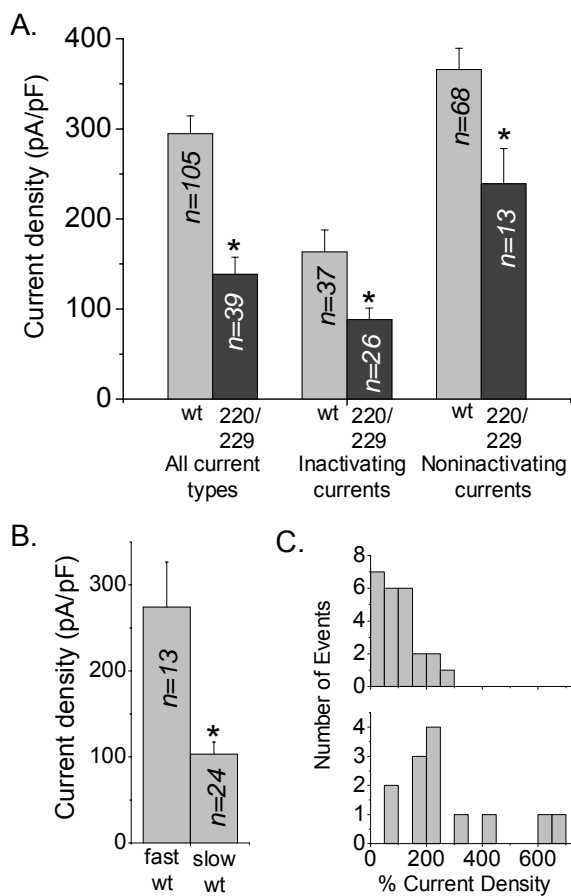
N-Glycosylation of the Kv3.1 channel increased current density

Channel density at the cell surface was determined for all types of current of the wild type Kv3.1 (I_{\max}/cap is 295 ± 20 pA/pF, $n=105$) and N220Q/N229Q (I_{\max}/cap is 138 ± 19 pA/pF, $n=39$) channels (Figure 27A). This larger current density of the wild type Kv3.1 channel correlated with its more prevalent noninactivating current behavior. However, both inactivating and noninactivating currents expressed larger channel densities at the cell surface for wild type Kv3.1 (I_{\max}/cap : 163 ± 24 pA/pF, $n=37$,

Figure 27. Differences in the current density are expressed by the various whole cell current types of the wild type Kv3.1 and N220Q/N229Q channels

(A) Bar graph representing the current densities of all current types, inactivating current type, and noninactivating current type from B35 cells transfected with wild type Kv3.1 (light gray, inactivating current type is 163 ± 24 ; noninactivating current type is 366 ± 24 ; and all types of current is 295 ± 20 pA/pF) and N220Q/N229Q (dark gray, inactivating current type is 88 ± 13 ; noninactivating current type is 239 ± 39 ; and all types of current is 138 ± 19 , pA/pF). (B) Bar graph representing the current densities of the fast (274 ± 53 pA/pF) and slow (103 ± 14 pA/pF) forms of the inactivating current type of the wild type Kv3.1 channel. (C) The plot displays the frequency distribution of current density for the fast (lower panel, $n=13$) and slow (upper panel, $n=24$) forms. Asterisks indicate the level of significance against either wild type Kv3.1 ($P < 0.05$) or fast inactivating currents ($P < 0.01$).

Figure 27
Cartwright and Schwalbe, 2008



inactivating currents; and 366 ± 24 pA/pF, $n=68$, noninactivating currents) than for N220Q/N229Q (I_{\max}/cap : 88 ± 13 pA/pF, $n=26$, inactivating currents; and 239 ± 39 pA/pF, $n=13$, noninactivating currents) (Table 1). These results demonstrated that N-glycosylation of the Kv3.1 channel regulates the current density at the cell surface.

It was determined that the current density for the fast form (I_{\max}/cap is 274 ± 53 pA/pF, $n=13$) of the wild type Kv3.1 channel was at least 2.5 times larger than the slow form (I_{\max}/cap is 103 ± 14 pA/pF, $n=24$). The frequency distribution of the current densities for the slow form was quite narrow while the fast form covered a broad range. In fact, close to 80% of the slow form expressed current densities of less than 150 pA/pF while only approximately 15% of the fast form expressed these small current densities. The large current densities for the fast form support that the fast inactivation of the wild type Kv3.1 channel was due to N-glycosylation processing and not to endogenous protein.

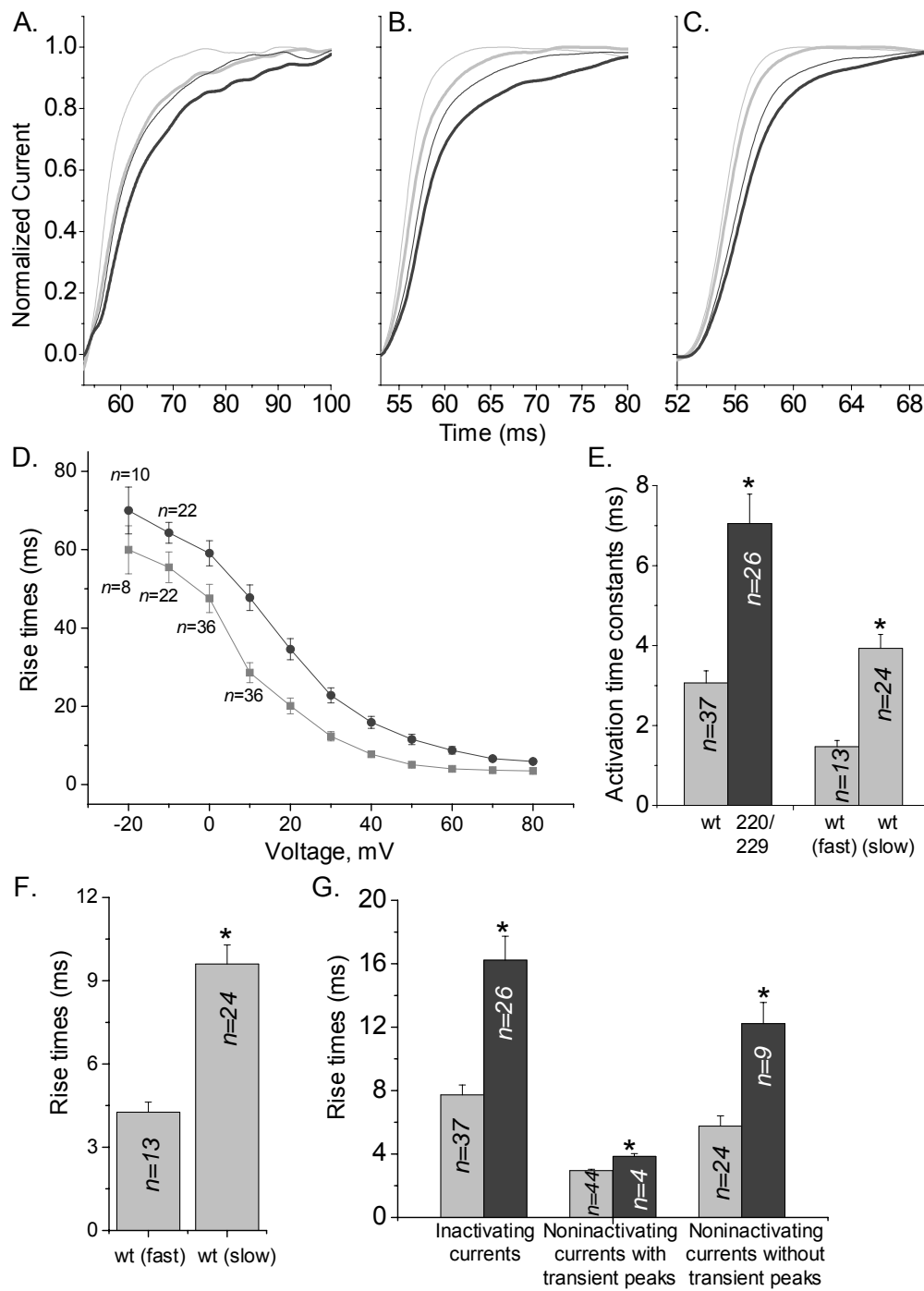
Glycosylated Kv3.1 channels have faster activation rates than their unglycosylated counterpart

To compare activation kinetics of the inactivating currents, the whole cell current recordings of wild type Kv3.1 and N220Q/N229Q were normalized at +20 mV and +30 mV (Figure 28A), +40 mV and +50 mV (Figure 28B) and +60 and +70 mV (Figure 28C) and overlaid in pairs for clarity. The activation rates were slowest at the lowest applied test potential and fastest at the highest potential for both forms of Kv3.1 which indicates voltage dependence of channel activation. Additionally, the rise times were faster for the

Figure 28. Variations in the activation rates of the various whole cell current types for wild type Kv3.1 and N220Q/N229Q channels

Time course of normalized currents from wild type Kv3.1 (light grey curves) and N220Q/N229Q (dark gray curves) at +20 mV (thick lines) and +30 mV (thin lines) (A), +40 mV (thick lines) and +50 mV (thin lines) (B), and +60 mV (thick lines) and +70 mV (thin lines) (C). (D) Plot of activation rise time as a function of applied voltage for wild type Kv3.1 (■, $n=37$ unless indicated) and N220Q/N229Q (●, $n=26$ unless indicated) transfected B35 cells. (E) Bar graph representation of activation time constants (τ_{act}) at +40 mV for wild type Kv3.1 (3.1 ± 0.3 ms), including the fast (1.5 ± 0.2 ms) and slow (3.9 ± 0.4 ms) forms, and N220Q/N229Q (7.1 ± 0.7 ms). (F) Rise time at +40 mV for the fast (light gray, 4.3 ± 0.4 ms) and slow (light gray, 9.6 ± 0.7 ms) forms of wild type Kv3.1. (G) Bar graph characterizing the rise times at +40 mV for wild type Kv3.1 (light gray) and N220Q/N229Q (dark gray) transfected B35 cells for inactivating current type (wild type Kv3.1, 7.7 ± 0.6 ; N220Q/N229Q, 16.2 ± 1.5 ms) and noninactivating current types with (wild type Kv3.1, 3.0 ± 0.1 ; N220Q/N229Q, 3.9 ± 0.2 ms) and without (wild type Kv3.1, 5.8 ± 0.7 ; N220Q/N229Q, 12.2 ± 1.3 ms) transient peaks. Asterisks represent statistical significance compared with either the fast inactivating ($P < 0.01$) or wild type Kv3.1 currents ($P < 0.05$). Data are expressed as mean \pm S.E. n corresponds to the number of cells tested.

Figure 28
Cartwright and Schwalbe, 2008



wild type Kv3.1 channel than the N220Q/N229Q channel at and beyond -20 mV (Figure 28D). The activation time constant at +40 mV for the wild type Kv3.1 channel was more than twice as fast as the N220Q/N229Q channel (Figure 28E). Interestingly, activation time constants (Figure 28E) and rise times (Figure 28F) at +40 mV were at least twice as fast for the fast form of the wild type Kv3.1 channel compared to the slow form. Moreover, the activation rates of the slow form were at least 1.7 times faster than those of the N220Q/N229Q channel. When comparing the rise times of all three types of current for the wild type Kv3.1 channel, the noninactivating current with transient peaks was faster than those without transient peaks while the inactivating current was the slowest (Figure 28G). All three current types for the N220Q/N229Q channel had a similar ranking. In all cases, the rise times of each current type were faster for the wild type Kv3.1 channel compared to those of the N220Q/N229Q channel (Figure 28G). These results demonstrated that N-glycosylation enhances the activation rates of the Kv3.1 channel.

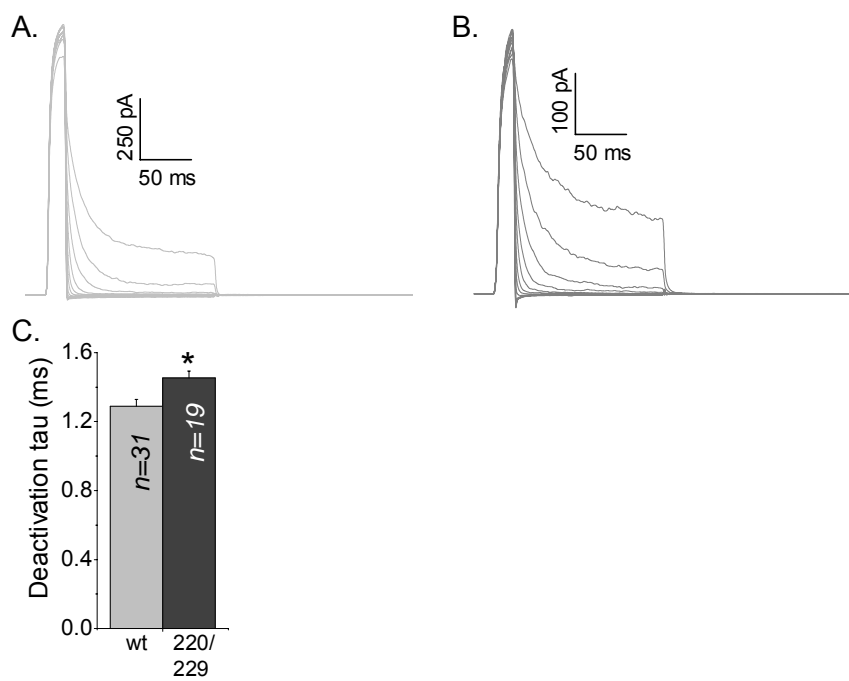
N-Glycosylation of the Kv3.1 channel increases the deactivation rate

The deactivation rates of Kv3 channel are rapid (14). To examine the deactivation kinetics, transfected B35 cells were briefly clamped at +40 mV to activate the wild type Kv3.1 (Figure 29A) and N220Q/N229Q (Figure 29B) channels, and subsequently the channels were deactivated by clamping the cells to less depolarized potentials. Both glycosylated and unglycosylated forms of the Kv3.1 channel displayed rapid deactivation rates (Figure 29C). However, the deactivation rate of the wild type Kv3.1 (τ_{deact} at -60

Figure 29. Deactivation rates of wild type Kv3.1 and N220Q/N229Q channels

Representative deactivation current traces from B35 cells expressing wild type Kv3.1 (A) and N220Q/N229Q (B). Cells were held at -50 mV and depolarized to +40 mV for 25 ms followed by repolarization from -110 mV to 0 mV for 200 ms. (C) Summary of deactivation time constants (τ_{deact}) obtained at -60 mV from B35 cells expressing wild type Kv3.1 (light gray bars, 1.29 ± 0.04 ms) and N220Q/N229Q (dark gray bars, 1.45 ± 0.04 ms). Asterisks denote statistical significance ($P < 0.05$) when compared to wt Kv3.1. Data are expressed as mean \pm S.E. n corresponds to the number of cells tested.

Figure 29
Cartwright and Schwalbe, 2008



mV was 1.29 ± 0.04 ms, $n=31$) channel was significantly faster than that of the N220Q/N229Q (τ_{deact} at -60 mV was 1.45 ± 0.04 ms, $n=19$) channel. These results showed that N-glycosylation of the Kv3.1 channel slightly enhances the deactivation rates of the channel.

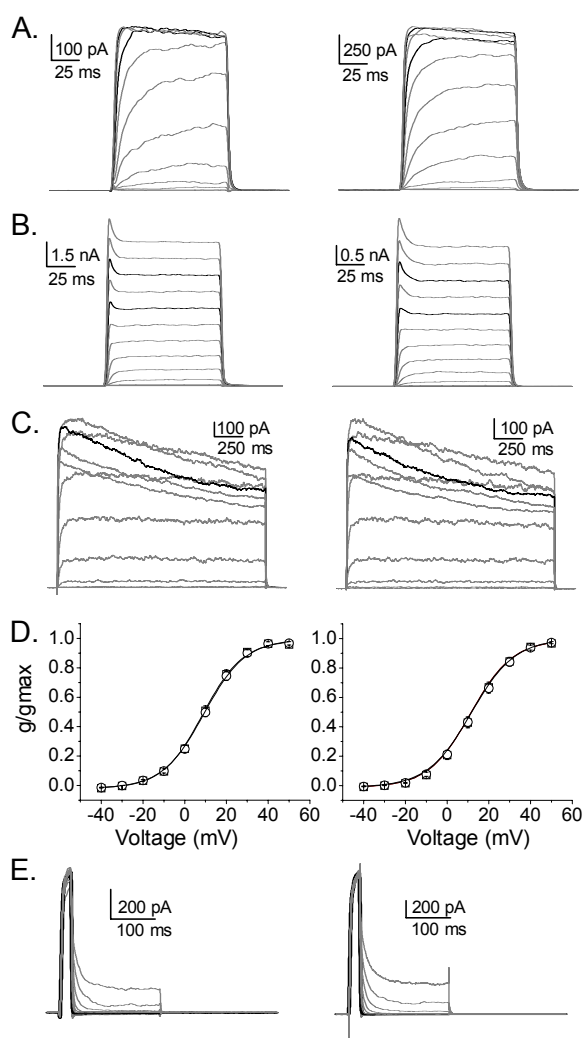
Analysis of the partially glycosylated Kv3.1 channels

After detecting differences in the channel activities of the Kv3.1 protein with both N-glycosylation sites occupied (glycosylated form) and unoccupied (unglycosylated form), we evaluated the channel properties of the Kv3.1 proteins with either 1 of the 2 sites occupied (partially glycosylated forms). Similar whole cell voltage protocols were utilized for the partially glycosylated Kv3.1 forms (N220Q and N229Q) as those for the glycosylated and unglycosylated Kv3.1 channels. Both N220Q (Figure 30A, left panel) and N229Q (Figure 30A, right panel) channels were shown to produce currents when transfected B35 cells were clamped to test potentials >-30 mV and ≥ -20 mV, respectively, for a duration of 200 ms. Similar to the glycosylated and unglycosylated Kv3.1 channels, the partially unglycosylated Kv3.1 channels expressed all three types of current. Inactivating currents were more prevalent than noninactivating currents for the N220Q channel, like the unglycosylated channel. On the other hand, the major current type expressed by the N229Q channel was the noninactivating current, similar to the glycosylated Kv3.1 channel. For both partially glycosylated Kv3.1 forms most of the noninactivating currents had transient peaks, like the glycosylated Kv3.1 channel. The current density, including all current types, of the N220Q channel was significantly

Figure 30. Functional characterization of B35 cells expressing the single N-glycosylation mutants, N220Q and N229Q

Representative whole cell traces of N220Q (left panels) and N229Q (right panels) inactivating current type (A and C) and noninactivating current type (B). The duration of the voltage steps were 100 ms (top and upper middle traces) and 2 sec (lower middle traces). (D) Deactivation current traces from B35 cells expressing the single mutant Kv3.1 channels.

Figure 30
Cartwright and Schwalbe, 2008



smaller than that of the N229Q channel (Table 1). The difference in the overall current density was due to the inactivating currents being the predominant current type of the N220Q channel.

Inactivation kinetics of the N220Q and N229Q were examined using the voltage protocols with both 100 ms (Figure 22A and B) and 2 s (Figure 22C) voltage step durations. Both of the partially glycosylated Kv3.1 channels displayed significantly slower decreases in current with time compared to the glycosylated Kv3.1 channel for the inactivating current type, similar to the unglycosylated Kv3.1 channel (Table 1). In contrast, the current inactivation rates of the noninactivating currents for the N220Q and N229Q channels were significantly faster than the N220Q/N229Q channel, like the wild type Kv3.1 channel (Table 1). The membrane conductance vs. applied voltage curves were quite similar whether determined from peak current amplitudes or current amplitudes at the end of the pulses for the partially glycosylated Kv3.1 channels, similar to that of the unglycosylated Kv3.1 channel (Figure 30D). This result indicates that the partially unglycosylated channels expressed in transfected B35 cells express slow inactivating kinetics. Somewhat similar amounts of partially glycosylated Kv3.1 channels were activated as the applied voltage was increased, like the unglycosylated Kv3.1 channel. The amount of applied voltage required to activate 50% of the N220Q channel was less depolarized than the N229Q channel and more depolarized than the unglycosylated Kv3.1 channel. The inactivating currents of the partially glycosylated Kv3.1 channels had differences in their activation rates while their noninactivating currents were similar. For instance, the activation rate of the inactivating currents of

N229Q channels was at least 1.7 times slower than the wild type Kv3.1 channel while that of the N220Q channel was at least 0.6 times faster than the N220Q/N229Q channel (Table 1). The deactivation rates of the partially glycosylated Kv3.1 channels were not significantly different (Figure 30E). These results demonstrated that the partially glycosylated Kv3.1 channels share some biophysical properties with the glycosylated Kv3.1 channel and others with the unglycosylated Kv3.1 channel.

DISCUSSION

Heterologous expression of wild type and mutant forms of the Kv3.1 channel in B35 cells were utilized to generate various glycoforms, as well as the aglycoform. Earlier studies have shown that the N-glycan associated with the Kv3.1 protein has α 2,8-linked sialyl residues and that both sites were fully occupied by N-glycans in transfected B35 cells (152) and adult rat brain (35,116,152) (Figure 22A). This atypical linkage leads to the formation of di-, oligo-, or poly-sialyl units (69,70,96,97) and to date a limited number of proteins have been identified to carry these modifications (70,88,90,97,98,100-102,140). Here both sites were shown to be occupied by sialylated N-glycans, and furthermore each was fully occupied when one site was abolished. These results were surprising based on the N-glycosylation survey of membrane glycoproteins which predicts that usually the site after the one closest to the amino-terminus is inefficiently utilized (154). Secondly, the attachment of N-glycans to either both sites or to each site, independently, was inefficient when the Kv3.1 protein was heterologously expressed in infected Sf9 cells (35). Based on previous studies, occupancy of an N-glycosylation site can be regulated by the primary sequence, protein folding and assembly, orientation of the protein to the membrane, and the distance of site to the endoplasmic reticulum membrane (66,79,154). Our present and past (35) studies which utilized two independent heterologous expression systems revealed that occupancy of the N-glycosylation sites of the Kv3.1 protein can also be regulated by cell type. Additionally, the results showed that the efficiency of N-glycan attachment to these sites was independently regulated.

To date, atypical N-glycosylation of endogenously and heterologously expressed Kv glycoproteins has not been established when characterizing channel function. Here we have shown that the processing of the N-glycans to atypical sialoglycoconjugates of the wild type Kv3.1 protein can generate a subpopulation of wild type Kv3.1 channels with enhanced inactivation and activation kinetics. As mentioned, the wild type Kv3.1 protein expressed in B35 cells produced an inactivating current type and a noninactivating current type. These current types were based on current saturation at more depolarized potentials and those that lacked current saturation, respectively. Moreover, the inactivating current type of wild type Kv3.1 channel was further divided into the fast form and the slow form which was based on current decay as a function of time. Detection of the fast form was unexpected since the inactivation rate of the wild type Kv3.1 channel has been described to be quite slow in oocytes (20-22) CHO cells (28) native tissue (13,28,29,40) and Sf9 cells (35). However, it appears that when the wild type Kv3.1 channel was expressed in L929 cells the inactivation rates were faster than in the former mentioned expression systems (153), and perhaps more comparable to those expressed in B35 cells. The fast rate of inactivation for the wild type Kv3.1 channel was also supported by the conductance-voltage relationships. The conductance-voltage curve determined from peak current amplitudes showed a rightward shift compared to that determined from current amplitudes near the end of pulses (Figure 25A and 25C). This rightward shift was due to a shallower slope for the conductance-voltage curve determined from peak current amplitudes. These results support increased instability of the open state near the resting potential for the fast form of the wild type Kv3.1 channel

compared to the slow form. The activation rate at +40 mV of the slow form of the wild type Kv3.1 channel was at least 2.2-fold slower than that of the fast form (Table 2). Taken together, these results revealed that a subpopulation of the wild type Kv3.1 channels with faster inactivation and activation kinetics, along with a less stable opening state near the resting potential, exists in the B35 neuroblastoma cellular model.

A subpopulation of wild type Kv3.1 channels with faster inactivation and activation kinetics could also be shown for the noninactivating current type. This type of current was first described when Kv3.1 was expressed in HEK cells, and the transient peak was suggested to be due to the accumulation of external potassium ions (24). In comparing the inactivating and noninactivating current types, we refer to the transient peaks of the noninactivating currents as the subpopulation of wild type Kv3.1 channels with fast inactivation rates while the currents thereafter represent the subpopulation of the wild type Kv3.1 channels with slow inactivation rates. It was determined that the rise times at +40 mV of the noninactivating currents without transient peaks was about 2-fold slower than those of the noninactivating current with transient peaks (Table 1). Additionally, the rise times of the noninactivating currents without transient peaks had slower rise times than the fast form of wild type Kv3.1 but faster than the slow form. This result suggests a third subpopulation of wild type Kv3.1 channels may exist which has the fast activation rates but slow inactivation rates. This third subpopulation of the wild type Kv3.1 channel is also supported when comparing the ratio of the rise times at +40 mV for the slow form to fast form (2.2), and the noninactivating current type without transient peaks to those with transient peaks (1.9). Therefore, two subpopulations of the

wild type Kv3.1 channel with fast activation rates and either fast or slow inactivation rates can be identified for the noninactivating current type.

An explanation of the fast inactivation kinetics displayed by the wild type Kv3.1 channel expressed in B35 cells could be the result of the Kv3.1 protein interacting with the Kv3.4 protein to form a heteromultimer Kv3 channel. For instance, it has been shown that the Kv3.1 channel could contain a fast inactivating component if it forms a heteromultimeric channel with the Kv3.4 protein (14,22). Based on several results, the present study does not support that the Kv3.1 protein interacted with endogenous Kv3.4 protein to form heteromultimeric Kv3 channels. The Kv3.4 protein was not detected as an endogenous protein in B35 cells. Additionally, the current density of the fast form was about 2.7 times greater than the slow form (Figure 27B), and it was also approximately 72 times greater than that of nontransfected B35 cells. Therefore, these results argue against the Kv3.1 protein forming a heteromultimeric Kv3 channel with the Kv3.4 protein in the B35 neuroblastoma cellular model.

Here the results favor that the fast inactivation and activation kinetics of the wild type Kv3.1 channel are due to the occupancy of both sites by sialylated N-glycans. The fast inactivating kinetics of the inactivating current type displayed by transfected B35 cells expressing the wild type Kv3.1 channel were undetected in 55 out of 55 of the transfected B35 cells expressing either the unglycosylated or partially glycosylated forms of the Kv3.1 channel. Moreover, the rise times at +40 mV of the unglycosylated Kv3.1 channel was 2.1-fold slower than the glycosylated wild type Kv3.1 channel. Those of the partially glycosylated Kv3.1 channels were also slower compared to the glycosylated

wild type Kv3.1 channel. The peak current amplitude conductance-voltage curve of the aglycoform was also shifted to the left relative to that of the glycosylated Kv3.1 channel. Additionally, the aglycoform expressed the noninactivating current with transient peaks only 10% of the time, unlike the wild type Kv3.1 channel. The rise times at +40 mV of the noninactivating current type of the aglycoform Kv3.1 channel was 2.5-fold slower than those of the glycosylated Kv3.1 channel. Thus, these results argue that occupancy of the two N-glycosylation sites of the Kv3.1 protein by sialoglycoconjugates are required to generate the subpopulation of Kv3.1 channels with enhanced inactivation and activation rates, and instability of the open state near the resting potential.

The partially glycosylated Kv3.1 channels could produce the subpopulation of Kv3.1 channels with fast inactivation and activation kinetics. However, it depended on the current type and a much higher current density than that of the glycosylated Kv3.1 channel. This result was contradictory to an earlier study which proposed that the fast inactivating component was the result of lower current amplitudes expressed by the wild type Kv3.1 channel in *Xenopus* oocytes (23). Here when the current density of the partially glycosylated channels were high they commonly expressed the noninactivating current type. Moreover, these currents had transient peaks the majority (>75%) of the time, similar to the wild type Kv3.1 channel. The activation rates of the noninactivating current types of the partially glycosylated Kv3.1 channels were also found to be relatively fast, like the glycosylated Kv3.1 channel. Interestingly, it was also discovered that sole occupancy of the Asn at position 220 by a sialoglycoconjugate could generate the subpopulation more than 53% of the time while the sole attachment of the

sialoglycoconjugate at position 229 was only 30% of the time. Therefore, N-glycosylation of the first site could more readily generate the Kv3.1 channels with fast inactivation and activation kinetics than that of the second site due to a greater ability to express noninactivating currents with large current density in B35 cells.

Based on the analysis of the inactivating currents of the various forms of the Kv3.1 channel, vacancy of the N-glycosylation sites, independently or together, had major changes on the voltage dependence of channel activation. The conductance-voltage curve generated by the N220Q channel was almost identical to the slow form of the wild type Kv3.1 channel. Additionally, the activation rate of the N220Q channel was quite comparable to the slow form of the wild type Kv3.1 channel. These results indicated that the sole vacancy of position 220 by an N-glycan could disrupt the production of the fast form of the wild type Kv3.1 channel. When only the second N-glycosylation site was vacant, the threshold potential of Kv3.1 channel activation was more positive (5-10 mV) than the other three forms of the Kv3.1 channel. This slightly greater depolarization potential produced a conductance-voltage curve with a similar shape to the unglycosylated Kv3.1 channel, except that it was shifted to the right. Taken together, these results supported that the vacancy of either one of the N-glycosylation sites will disrupt the production of the fast form, and that the vacancy of position 229 will increase the threshold potential for channel activation. Moreover, it is critical that both sites be occupied simultaneously to confer the unique properties of the Kv3 channel, such as the destabilization of the open state near the resting potential and the fast activation kinetics.

Cell-specific glycoconjugates presented at the cell surface influence the voltage sensor of the wild type Kv3.1 channel. More depolarization (about 6 mV) was required to activate 50% of the Kv3.1 channels expressed in Sf9 cells (35) compared to those expressed in B35 cells. A possible reason for this difference could be explained by the surface potential theory (5) due to sialylated N-glycans of B35 cells (69,138,152) and the lack of these N-glycans for Sf9 cells (35,155). Previously, this theory was applied to explain the removal of sialic acid from N-glycans for the Kv1.1 (58,83) and Kv1.2 (84) channels. However, this does not appear to be a plausible explanation for the Kv 3.1 channel since the slopes of the G-V curves were different in both the Sf9 (35) and B35 cells. Secondly, the voltage sensor of the Kv3.1 channel appeared unaware of the attachment of the atypical sialylated N-glycans since the amount of depolarization to activate similar amounts of the unglycosylated Kv3.1 channel expressed in B35 cells was less. Of interest, the half-maximal conductance of the unglycosylated Kv3.1 channel expressed in Sf9 cells (35) was greater (about 12 mV) than that expressed in B35 cells and the slopes of the G-V curves were quite similar. Taken together, the attachment of sialoglycoconjugates to the cell surface appears to contribute to the uniform transmembrane electrical field detected by the voltage sensor of the Kv3.1 channel. However, attachment of both sialylated N-glycans lacks detection by the voltage sensor when the Kv3.1 channel resides in the matrix of B35 cells.

Mechanisms involved in gating of the Kv3.1 channel are regulated by N-glycosylation. More depolarization was required to activate 50% of the N229Q channel than the wild type Kv3.1 channel. This result suggests that the sialylated N-glycan

attached to position 229 was detected by the voltage sensor. However, the slopes of the G-V curves were different between the N229Q and wild type Kv3.1 channels, and furthermore less depolarization was required to activate the aglycoform than the N229Q channel. These results argue against the voltage sensor detecting the sialylated N-glycan at position 229 of the wild type Kv3.1 channel. Perhaps the voltage dependence of the N229Q channel activation can be more easily explained by the gating stabilizing theory (5), similar to the N220Q and N220Q/N229Q channels. When the attachment of the N-glycan at position 229 was prevented, the open state of the Kv3.1 channel was more destabilized near the resting membrane potential, like the unglycosylated Kv1.1 (58,83) and Kv1.2 (84) channels. An earlier study of the Kir1.1 channel also showed that the open state was destabilized by the absence of N-glycosylation (119). On the other hand, the absence of an N-glycan at position 220 caused more stabilization of the open state near the resting potential, and furthermore when both N-glycans were absent the open state was even more stabilized. Therefore, the results indicated that attachment of both N-glycans cooperate together to destabilize the open state of the Kv3.1 channel near the resting membrane potential. For instance, it may be that attachment of sialylated N-glycans to both positions 220 and 229 are required for the correct placement and orientation of the first extracellular loop in the plasma membrane to favor the various conformational states of the glycosylated Kv3.1 channel.

To date, studies relating the activation kinetics of the Kv3.1 channel to cell-specific N-glycosylation processing are absent. The wild type Kv3.1 protein is associated with simple type N- glycans when heterologously expressed in Sf9 cells (35) while it is

associated with atypical sialylated N-glycans when heterologously expressed in B35 cells (152). The activation rates for both inactivating current and noninactivating current types of the wild type Kv3.1 channel in infected Sf9 cells (35) were much slower than those of the wild type Kv3.1 channel in B35 cells. Additionally, when comparing the ratio of the rise times at +40 mV of the unglycosylated Kv3.1 channel to that of the glycosylated Kv3.1 channel expressed in B35 cells (2.1 for inactivating current type and 2.5 for noninactivating current type) and those in Sf9 cells (1.5 for inactivating current type and 1.4 for noninactivating current type) the ratios were higher for those of B35 cells. These results, along with the slightly faster rise time of the Kv3.1 aglycoform expressed in B35 cells compared to the glycosylated Kv3.1 expressed in Sf9 cells, indicate that the sialylated N-glycans attached to the Kv3.1 channel are enhancing the activation rates to a greater degree than the simple N-glycans attached to the Kv3.1 channel. Utilization of the ratios also eliminates changes of the activation kinetics due to the conserved mutations. Next, when comparing the ratio of the rise times at +40 mV for the glycosylated Kv3.1 channel in Sf9 cells to those in B35 cells (2.5 for inactivating current type and 2.6 for noninactivating current type) and the ratio of the unglycosylated Kv3.1 channel in Sf9 cells to that in B35 cells (1.8 for inactivating current type and 1.5 for noninactivating current type) the ratios were higher for the glycosylated Kv3.1 channel than the aglycoform. Taken together, these results indicate that the sialoglycoconjugates attached to the cell surface have remarkably similar effects on both the wild type Kv3.1 and N220Q/N229Q channels, and furthermore support that the type of N-glycan attached to the Kv3.1 channel regulates the activation rates.

Both the type of N-glycan and current density are critical factors in the production of the subpopulation of Kv3.1 channels with fast activation and inactivation kinetics. When the N-glycans of Kv3.1 were of simple type as found in Sf9 cells the current density was smaller (35) than when atypical sialylated N-glycans were attached to the Kv3.1 channel. Additionally, the number of wild type Kv3.1 transfected B35 cells that expressed the noninactivating current type was about 1.4-fold greater than that from wild type Kv3.1 infected Sf9 cells (35). Another notable difference was the noninactivating currents with transient peaks at +40 mV of the wild type Kv3.1 transfected B35 cells were absent in infected Sf9 cells expressing the wild type Kv3.1 channel (35). These results indicate that current density and current type of the Kv3.1 channel depends on the type of N-glycan carried by the Kv3.1 channel. The production of the subpopulation of Kv3.1 channels with fast activation and inactivation kinetics was undetected in infected Sf9 cells and was only observed in transfected B35 cells when the current density was quite large. For instance, the current density of the fast form of the wild type Kv3.1 channel was about 2.7-fold greater than that of the slow form. Additionally, the noninactivating current type which has the larger current density was needed to generate the fast activation and inactivation kinetics of the Kv3.1 channel for partially glycosylated Kv3.1 channels. Taken together, these results indicated that neuronal N-glycosylation processing is essential in generating the Kv3.1 channel with fast activation and inactivation rates.

Here several subpopulations of the wild Kv3.1 channels expressed in transfected B35 cells have been identified. The glycosylated Kv3.1 channel could produce a

predominant subpopulation with fast activation and inactivation rates for 35% of the cells expressing the inactivating current type. This subpopulation was undetected for the inactivating currents of the aglycoform and partially glycosylated Kv3.1 channels in B35 cells, as well as wild type and glycosylation mutant Kv3.1 channels in Sf9 cells (35). The noninactivating current type of the glycosylated and partially glycosylated Kv3.1 channels revealed a subpopulation with fast activation and slow inactivation. Of note, the subpopulation with fast activation and inactivation kinetics were unobserved for the inactivating current type produced by Kv3.1 channels with simple type N- glycans (35). However, a subpopulation with faster activation rates was suggested by the noninactivating current type. Taken together, the results indicate that the attachment of atypical sialylated N-glycans to the Kv3.1 protein changes the equilibrium of the various subpopulations of Kv3.1 channels in B35 cells, and consequently increases the subpopulations of Kv3.1 channels with fast activation rates.

In conclusion, this study indicates that the attachment of atypical sialylated N-glycans to positions: 220 and 229 of the Kv3.1 channel is essential for stabilizing the open state distal from the resting membrane potential. The atypical sialylated N-glycans were shown to be critical structural determinants in modulating the activation and inactivation rates of the Kv3.1 channel, and therefore the N-glycans were assigned a novel functional role in regulating the transitions of the channel. As mentioned, our results support that the production of the subpopulations of Kv3.1 channels were dependent on both N-glycan type and high current density. Additionally, earlier studies have indicated that sequestration of Kv channels in high density clusters at synapses is

responsible for effective synaptic signaling (30). We propose that neuronal *N*-glycosylation processing of the Kv3.1 channel, as well as other glycosylated ion channels, provides a novel and vital cellular mechanism for sequestering ion channels in high density clusters, and thus in regulating the independent structural and functional plasticity of individual synapses.

CHAPTER 8 - SUMMARY

The primary research goal of this dissertation was to characterize the N-glycan structures of Kv3 and Kv1 glycoproteins in rat brain, as well as to determine how neuronal N-glycosylation processing regulates Kv3.1 voltage-gated K⁺ channel function. In the pursuit of this research goal, the following four specific aims were devised for this investigation: 1) to demonstrate that both absolutely conserved N-glycosylation sites of Kv3.1, Kv3.3, and Kv3.4 channels are occupied by complex oligosaccharides in rat brain, 2) to demonstrate that sialylated N-glycan structures attached to Kv3.1, Kv3.3, and Kv3.4 channels are different throughout the central nervous system of the adult rat, 3) to determine the different linkages of sialyl residues associated with N-glycans attached to Kv3.1, 3.3, 3.4, 1.1, 1.2, and 1.4 channels in rat brain, as well as a rat neuroblastoma cell line and 4) to determine whether atypical sialylated N-glycans associated with the Kv3.1 protein modulate channel activity. Collectively these specific aims are critical to understanding how N-glycan processing of K⁺ channels influences the firing patterns and the duration of action potentials in neurons, as well as regulates cell volume, lymphocyte differentiation and cell proliferation.

The impetus for the present investigation was an observation which was made during a previous study in our laboratory upon treatment of rat brain membranes with PNGase F (35). In this study, it was shown that the Kv3.1 channel protein was N-glycosylated in rat brain, and the N-linked oligosaccharides were of either hybrid or complex type in composition, unlike the simple type detected for Kv3.1 in Sf9 cells (35). Additionally, it was demonstrated that the Kv3.1 protein heterologously expressed in Sf9

cells had both absolutely conserved sites of N-glycosylation utilized. Based on these earlier observations, Specific Aim 1 of this present investigation was designed to ascertain whether the Kv3.3 and Kv3.4 channel proteins derived from rat brain were N-glycosylated, like the Kv3.1 channel protein. Furthermore, occupancy of both absolutely conserved N-glycosylation sites of the Kv3.1, Kv3.3, and Kv3.4 channel proteins, as well as the type of attached N-glycans, were also examined in the adult rat brain.

The results in Specific Aim 1 (chapter 4) demonstrated that the Kv3.1, Kv3.3, and Kv3.4 channel proteins were N-glycosylated in the adult rat brain, and that both absolutely conserved glycosylation sites were completely utilized. The results also demonstrated that at least one N-linked oligosaccharide was of complex type for Kv3.1, Kv3.3, and Kv3.4. In these studies, the demonstration that both absolutely conserved N-glycosylation sites were fully occupied and processed for Kv3.1, Kv3.3, and Kv3.4 proteins provided strong evidence that the S1-S2 linker of these Kv3 channel proteins was topologically extracellular. Furthermore, this finding was also in agreement with utilization of the native N-glycosylation site in the S1-S2 linker of other Kv channels such as Kv1.1 (129), Kv1.2 (123), Kv1.4 (86) and Kv1.5 (130). However, it was in disagreement with the x-ray crystal structure of the bacterial potassium channel KvAP which placed the S1-S2 linker for all Kv channels in the plasma membrane (131). As previously mentioned (Chapter 4, Discussion), this structural difference could be due to differences between bacterial Kv channels and eukaryotic Kv channels. Occupancy of both absolutely conserved N-glycosylation sites of the Kv 3.1, Kv3.3 and Kv3.4 channels

in the rat brain also allows us to speculate that occupancy of these channels would be lower in CDG I patients than normal individuals.

Given the above observation that both absolutely conserved N-glycosylation sites within the S1-S2 extracytoplasmic loop of Kv3.1, Kv3.3, and Kv3.4 channels were occupied in rat brain and that at least one oligosaccharide was of complex type, additional studies were needed to determine whether the N-glycans of these channels were composed of sialyl residues. Further studies were also needed to establish whether the structural composition of the N-glycans attached to the Kv3.1, Kv3.3, and Kv3.4 glycoproteins were distinct in the various regions of the adult rat brain. As demonstrated in Specific Aim 2 (chapter 5) the Kv3.1, Kv3.3, and Kv3.4 glycoproteins expressed in brain were of different sizes and their N-glycans were terminated with at least several sialyl residues. It was also demonstrated that the Kv3.1, Kv3.3, and Kv3.4 glycoproteins were expressed in the hypothalamus, thalamus, cerebellum, cerebral cortex, hippocampus and spinal cord of the adult rat. Our studies also provided the first evidence that each of the Kv3.1, Kv3.3, and Kv3.4 glycoproteins were expressed as different glycoforms in the central nervous system of the adult rat. Additionally, we observed that the N-glycans of the differentially expressed Kv3 glycoforms were sialylated in all six regions of the central nervous system. Taken together, these studies demonstrated that cell specific N-glycosylation of Kv3 channels occurs throughout the central nervous system, and therefore is essential for carrying out physiological responses.

Additionally, it was observed that protein expression levels for Kv3.1 and Kv3.3 were similar with the highest levels observed in the cerebellum, while the lowest levels

were observed in the thalamus and hypothalamus. However, Kv3.3 protein levels were higher in the spinal cord than both the cerebral cortex and hippocampus, while those for Kv3.1 were quite similar to each other. The Kv3.4 protein levels in both the cerebellum and hippocampus were the highest, while the cerebral cortex, thalamus, hypothalamus and spinal cord expressed lower levels. These results differed from those previously reported for the Kv3.1 protein expression levels (38,39), as well as the Kv3.1 (22,32,36), Kv3.3 (38) and Kv3.4 (22) transcript levels.

In Specific Aim 2, we demonstrated that the N-glycan structures attached to brain Kv3 glycoproteins were heavily sialylated. Our laboratory expanded upon these findings in Specific Aim 3 (chapter 5) by further evaluating the sialic acid linkages of the Kv3 glycoproteins in rat brain, as well as in transfected B35 neuroblastoma cells. Previous studies have demonstrated that brain Kv1.1, Kv1.2, and Kv1.4 glycoproteins (16,58-60) contain sialylated N-glycan structures. Therefore, it was of further interest to our laboratory to characterize the sialyl linkages of these carbohydrate chains in Specific Aim 3 as well.

Examination of these sialylated N-glycan structures revealed that the N-glycan chains of brain Kv3.1, Kv3.3, Kv3.4, Kv1.1, Kv1.2 and Kv1.4 glycoproteins were terminated with atypical disialyl units. As stated previously less than 10% of sialylated glycoproteins in the adult rat brain contain disialyl units (70). These same studies also demonstrated that brain Kv3.1, Kv3.3, and Kv3.4 glycoproteins, like Kv3.1 heterologously expressed in B35 cells, have at least one of their carbohydrate chains terminated with an oligo/polysialyl unit. Notably, this is the first time that di/oligosialyl

units have been shown to be associated with voltage-gated K⁺ channels. The biological importance of atypical di/oligosialyl units of glycoproteins is unknown. However, the identification of two classes of voltage gated potassium channels with di/oligosialyl units is the initial step in determining the biological roles of these atypical types of N-glycans. We speculate that perhaps di/oligosialyl units are involved in cell adhesion, differentiation and signal transduction, similar to gangliosides (88).

Additionally, sialyl residues were shown to be linked to internal residues of the carbohydrate chains of the Kv1.1, Kv1.2, and Kv1.4 N-glycans. This unique N-glycan modification of branched sialyl residues was also identified for the Kv3.1, Kv3.3, Kv3.4, and N-CAM glycoproteins. Prior to this investigation, this unusual glycosidic bond for sialyl residues had only been identified in gangliosides (103,104) and not carbohydrate chains of N-glycans. Overall, we conclude that all six Kv channels contribute to the sialylated N-glycan pool in mammalian brain. We speculate that these novel sialylated N-glycans of the Kv3 and Kv1 channels are important modifications in regulating channel function and are responsible for fine tuning the excitable properties of neurons in the nervous system. Additionally, the sialylated N-glycans of the Kv3 and Kv1 proteins may also play an important role in channel expression at the cell surface of either axonal or somatodendritic compartments of neurons.

As described in the text above Specific Aim 3 demonstrated that the Kv3.1 channel heterologously expressed in B35 cells generated a Kv3.1 glycoprotein with atypical sialylated N-glycan structures. To our knowledge the effect of neuronal N-glycosylation processing on Kv3.1 channel activity had not been evaluated in this same

expression system and therefore, laid the scientific ground work for Specific Aim 4 (chapter 7). In this Specific Aim immunoblots of B35 cells heterologously expressing glycosylated (wild type), unglycosylated (N220Q/N229Q) and partially glycosylated (N220Q and N229Q) Kv3.1 channels were utilized to examine site occupancy. These western blotting studies of the various Kv3.1 proteins in B35 cells demonstrated that occupancy of each of the N-glycosylation sites was independent of one another. Moreover, these studies demonstrated that the removal of one or both N-glycosylation sites did not greatly influence Kv3.1 protein expression in B35 cells indicating that Kv3.1 protein can properly fold without the attachment of N-glycans. Immunoband shift assays of partially glycosylated Kv3.1 proteins digested with neuraminidase also indicated that both N-glycosylation sites were occupied by sialylated N-glycans. Finally, immunoblots confirmed that endogenous Kv3.1, Kv3.3, and Kv3.4 glycoprotein expression was below detection limits in nontransfected B35 cells, nor were endogenous Kv3.3 and Kv3.4 glycoproteins found to form heteromultimers with the heterologously expressed Kv3.1 glycoprotein.

In order to examine whether the attachment of uncommon sialylated N-glycan structures affected Kv3.1 channel activity, whole cell current measurements were performed in the whole cell mode of the patch clamp technique. An analysis of whole cell currents identified at least three subpopulations of Kv3.1 channels expressed in B35 which were dependent on N-glycosylation processing. The wild type Kv3.1 channels associated with atypical sialylated N-glycans favored the subpopulation which exhibited fast activation and inactivation rates with much greater frequency than those Kv3.1

channels which lacked N-glycans. The partially glycosylated Kv3.1 channels, like the aglycoform, also lacked the subpopulation with fast activation and inactivation rates for the inactivating current type. However, this subpopulation could be favored by the partially glycosylated Kv3.1 channels, like the glycosylated Kv3.1 channel, when the current density was large, and the current type was noninactivating. It was also observed that the predominant current type for the wild type Kv3.1 and N229Q channels were noninactivating currents while inactivating currents were the predominant type for the unglycosylated and N220Q channels. Additionally, the noninactivating currents of the wild type and the partially glycosylated Kv3.1 channels customarily displayed transient peaks at the initial phase of the sweep while the unglycosylated Kv3.1 channels were generally deficient. These results suggest that the noninactivating current types with transient peaks express a subpopulation of glycosylated or partially glycosylated Kv3.1 channels which have faster or fast inactivation kinetic properties respectively.

In order to analyze the voltage dependence of wild type Kv3.1 and N220Q/N229Q channel activation membrane conductance vs. voltage curves were constructed. These curves showed that more depolarization was required for 50% of the wild type channels to reach activation than that of the aglycoform channels. Therefore, these results argue against the voltage sensor detecting the sialylated N-glycans of the wild type Kv3.1 channels. Moreover, less depolarization was required for 50% of the N220Q channels to reach activation than that of the N229Q channels. These studies also demonstrated that channel density at the B35 cell surface for the unglycosylated channel was greatly reduced compared to the wild type Kv3.1 channel for both inactivating and

noninactivating currents. The current densities, for all current types of the N220Q channel were also significantly smaller than that of the N229Q channel. Furthermore, the activation rates for the wild type Kv3.1 channels were faster compared to the unglycosylated channels. An analysis of the deactivation kinetics showed that the magnitude of the deactivation constant was greater for the wild type Kv3.1 channel than the N220Q/N229Q channel, while the deactivation time constants for the N220Q channel and the N229Q channel were not significantly different. Taken together, these studies support that neuronal N-glycosylation processing of the Kv3.1 protein is critical in regulating the equilibrium of the various subpopulations of Kv3.1 channels. And in particular can favor the subpopulation of Kv3.1 channels with fast activation and inactivation kinetics. We propose that cell-specific N-glycosylation processing of glycosylated channels provides a universal cellular mechanism for regulating ion channel function.

Conclusion

The novel findings of the above studies have provided substantial insight regarding the structures of the N-glycans attached to rat brain Kv3 and Kv1 glycoproteins. Based on these findings we have proposed the following topological model for the Kv3 and Kv1 monomeric α -subunits within the lipid bilayer. As illustrated in Figure 14, Kv3 (A) and Kv1 (B) α -subunits consist of six transmembrane segments (S1-S6) with both N and C termini localized in the cytoplasm. One or two utilized N-glycosylation sites lie within the S1-S2 extracytoplasmic loop of the Kv1 and Kv3

glycoproteins, respectively. The occupied N-glycans (branched structures) of the Kv3 brain glycoproteins were capped with monosialyl residues (single dark gray circles) and disialyl units (rows with one dark gray and one light gray circle). Moreover, at least one antenna was terminated with an oligo/polysialyl unit (row of light gray circles). In contrast, brain Kv1 glycoproteins were capped with disialyl units (rows with one dark gray and one light gray circle). Both brain Kv1 and Kv3 glycoproteins also contained sialyl residues linked to internal residues of the carbohydrate chains (white filled circles).

This investigation has provided the first evidence in the scientific literature that two distinct voltage-gated potassium channel families, Kv3 and Kv1, which are highly expressed in mammalian brain, contain atypical sialylated N-glycan structures. Additionally, these same studies have also demonstrated that the attachment of unique sialylated N-glycans structures to the Kv3.1 glycoprotein are crucial components in regulating channel activation and inactivation rates. To date, only a small number of glycoproteins are known to be carriers of oligo/polysialic acid chains in the adult mammalian brain (70,88,98). Furthermore, information on the cellular roles of these uncommon sialoglycoconjugates is sparse. The identification of six Kv brain glycoproteins with di/oligosialyl units in this dissertation is the initial step in elucidating the roles of these uncommon sialoglycoconjugates. Based on the data presented in this dissertation, we propose that occupancy of Kv3 channel N-glycosylation sites by these uncommon sialoglycoconjugates assists in regulating action potential waveforms by influencing the rates of repolarization. An understanding of the physiological roles of these atypical sialylated N-glycans on channel activities of the Kv3 glycoproteins is

essential for unraveling the complex electrical properties of neurons in maintaining the central nervous system. Furthermore, these studies may be essential in laying the foundation for utilizing occupancy of N-glycosylation sites by atypical sialoglycoconjugates for designing effective therapeutic agents, as well as providing a diagnostic marker for neurodegenerative diseases.

REFERENCES

1. Gutman, G. A., Chandy, K. G., Grissmer, S., Lazdunski, M., McKinnon, D., Pardo, L. A., Robertson, G. A., Rudy, B., Sanguinetti, M. C., Stuhmer, W., and Wang, X. (2005) *Pharmacol Rev* **57**(4), 473-508
2. Sansom, M. S., Shrivastava, I. H., Bright, J. N., Tate, J., Capener, C. E., and Biggin, P. C. (2002) *Biochim Biophys Acta* **1565**(2), 294-307
3. Choe, S. (2002) *Nat Rev Neurosci* **3**(2), 115-121
4. Verma-Kurvari, S., Border, B., and Joho, R. H. (1997) *Brain Res Mol Brain Res* **46**(1-2), 54-62
5. Hille, B. (2001) *Ionic Channels of Excitable Membranes*, 3rd Ed., Sinauer, Sunderland, MA
6. Lujan, R., de Cabo de la Vega, C., Dominguez del Toro, E., Ballesta, J. J., Criado, M., and Juiz, J. M. (2003) *J Chem Neuroanat* **26**(3), 209-224
7. McCormik, D. A. (1998) *The Synaptic Organization of the Brain*, Oxford University Press, New York, NY
8. Jan, L. Y., and Jan, Y. N. (1992) *Annu Rev Physiol* **54**, 537-555
9. Jan, L. Y., and Jan, Y. N. (1997) *Annu Rev Neurosci* **20**, 91-123
10. Pongs, O. (1992) *Physiol Rev* **72**(4 Suppl), S69-88
11. Salkoff, L., Baker, K., Butler, A., Covarrubias, M., Pak, M. D., and Wei, A. (1992) *Trends Neurosci* **15**(5), 161-166
12. Dubois, J. M., and Rouzaille-Dubois, B. (1993) *Prog Biophys Mol Biol* **59**(1), 1-21
13. Coetzee, W. A., Amarillo, Y., Chiu, J., Chow, A., Lau, D., McCormack, T., Moreno, H., Nadal, M. S., Ozaita, A., Pountney, D., Saganich, M., Vega-Saenz de Miera, E., and Rudy, B. (1999) *Ann N Y Acad Sci* **868**, 233-285
14. Rudy, B., and McBain, C. J. (2001) *Trends Neurosci* **24**(9), 517-526
15. Rudy, B., Chow, A., Lau, D., Amarillo, Y., Ozaita, A., Saganich, M., Moreno, H., Nadal, M. S., Hernandez-Pineda, R., Hernandez-Cruz, A., Erisir, A., Leonard, C., and Vega-Saenz de Miera, E. (1999) *Ann N Y Acad Sci* **868**, 304-343
16. Misonou, H., and Trimmer, J. S. (2004) *Crit Rev Biochem Mol Biol* **39**(3), 125-145
17. Hodgkin, A. L., and Huxley, A. F. (1952) *J Physiol* **116**(4), 449-472
18. Luneau, C. J., Williams, J. B., Marshall, J., Levitan, E. S., Oliva, C., Smith, J. S., Antanavage, J., Folander, K., Stein, R. B., Swanson, R., and et al. (1991) *Proc Natl Acad Sci U S A* **88**(9), 3932-3936
19. Yokoyama, S., Imoto, K., Kawamura, T., Higashida, H., Iwabe, N., Miyata, T., and Numa, S. (1989) *FEBS Lett* **259**(1), 37-42
20. McCormack, T., Vega-Saenz de Miera, E. C., and Rudy, B. (1990) *Proc Natl Acad Sci U S A* **87**(13), 5227-5231
21. Tagliatalata, M., Vandongen, A. M., Drewe, J. A., Joho, R. H., Brown, A. M., and Kirsch, G. E. (1991) *Mol Pharmacol* **40**(2), 299-307
22. Weiser, M., Vega-Saenz de Miera, E., Kentros, C., Moreno, H., Franzen, L., Hillman, D., Baker, H., and Rudy, B. (1994) *J Neurosci* **14**(3 Pt 1), 949-972

23. Ito, Y., Yokoyama, S., and Higashida, H. (1992) *Proc Biol Sci* **248**(1322), 95-101
24. Critz, S. D., Wible, B. A., Lopez, H. S., and Brown, A. M. (1993) *J Neurochem* **60**(3), 1175-1178
25. Grissmer, S., Nguyen, A. N., Aiyar, J., Hanson, D. C., Mather, R. J., Gutman, G. A., Karmilowicz, M. J., Auperin, D. D., and Chandy, K. G. (1994) *Mol Pharmacol* **45**(6), 1227-1234
26. Kanemasa, T., Gan, L., Perney, T. M., Wang, L. Y., and Kaczmarek, L. K. (1995) *J Neurophysiol* **74**(1), 207-217
27. Wang, L. Y., Gan, L., Perney, T. M., Schwartz, I., and Kaczmarek, L. K. (1998) *Proc Natl Acad Sci U S A* **95**(4), 1882-1887
28. Hernandez-Pineda, R., Chow, A., Amarillo, Y., Moreno, H., Saganich, M., Vega-Saenz de Miera, E. C., Hernandez-Cruz, A., and Rudy, B. (1999) *J Neurophysiol* **82**(3), 1512-1528
29. Macica, C. M., von Hehn, C. A., Wang, L. Y., Ho, C. S., Yokoyama, S., Joho, R. H., and Kaczmarek, L. K. (2003) *J Neurosci* **23**(4), 1133-1141
30. Trimmer, J. S., and Rhodes, K. J. (2004) *Annu Rev Physiol* **66**, 477-519
31. Luneau, C., Wiedmann, R., Smith, J. S., and Williams, J. B. (1991) *FEBS Lett* **288**(1-2), 163-167
32. Rudy, B., Kentros, C., Weiser, M., Fruhling, D., Serodio, P., Vega-Saenz de Miera, E., Ellisman, M. H., Pollock, J. A., and Baker, H. (1992) *Proc Natl Acad Sci U S A* **89**(10), 4603-4607
33. Vega-Saenz de Miera, E., Moreno, H., Fruhling, D., Kentros, C., and Rudy, B. (1992) *Proc Biol Sci* **248**(1321), 9-18
34. Varshney, A., and Mathew, M.K. (2004) *Current Science* **87**, 166-174
35. Brooks, N. L., Corey, M. J., and Schwalbe, R. A. (2006) *Febs J*
36. Perney, T. M., Marshall, J., Martin, K. A., Hockfield, S., and Kaczmarek, L. K. (1992) *J Neurophysiol* **68**(3), 756-766
37. Schwalbe, R. A., Corey, M. J., and Cartwright, T. A. (2008) *Biochem Cell Biol* **86**(1), 21-30
38. Weiser, M., Bueno, E., Sekirnjak, C., Martone, M. E., Baker, H., Hillman, D., Chen, S., Thornhill, W., Ellisman, M., and Rudy, B. (1995) *J Neurosci* **15**(6), 4298-4314
39. Gelband, C. H., Warth, J. D., Mason, H. S., Zhu, M., Moore, J. M., Kenyon, J. L., Horowitz, B., and Sumners, C. (1999) *Circ Res* **84**(3), 352-359
40. Du, J., Zhang, L., Weiser, M., Rudy, B., and McBain, C. J. (1996) *J Neurosci* **16**(2), 506-518
41. Espinosa, F., Marks, G., Heintz, N., and Joho, R. H. (2004) *Genes Brain Behav* **3**(2), 90-100
42. Porcello, D. M., Ho, C. S., Joho, R. H., and Huguenard, J. R. (2002) *J Neurophysiol* **87**(3), 1303-1310
43. Hurlock, E. C., McMahon, A., and Joho, R. H. (2008) *J Neurosci* **28**(18), 4640-4648
44. Espinosa, F., McMahon, A., Chan, E., Wang, S., Ho, C. S., Heintz, N., and Joho, R. H. (2001) *J Neurosci* **21**(17), 6657-6665

45. Gutman, G. A., Chandy, K. G., Adelman, J. P., Aiyar, J., Bayliss, D. A., Clapham, D. E., Covarriubias, M., Desir, G. V., Furuichi, K., Ganetzky, B., Garcia, M. L., Grissmer, S., Jan, L. Y., Karschin, A., Kim, D., Kuperschmidt, S., Kurachi, Y., Lazdunski, M., Lesage, F., Lester, H. A., McKinnon, D., Nichols, C. G., O'Kelly, I., Robbins, J., Robertson, G. A., Rudy, B., Sanguinetti, M., Seino, S., Stuehmer, W., Tamkun, M. M., Vandenberg, C. A., Wei, A., Wulff, H., and Wymore, R. S. (2003) *Pharmacol Rev* **55**(4), 583-586
46. Baumann, A., Grupe, A., Ackermann, A., and Pongs, O. (1988) *Embo J* **7**(8), 2457-2463
47. Chandy, K. G., Williams, C. B., Spencer, R. H., Aguilar, B. A., Ghanshani, S., Tempel, B. L., and Gutman, G. A. (1990) *Science* **247**(4945), 973-975
48. Grupe, A., Schroter, K. H., Ruppertsberg, J. P., Stocker, M., Drewes, T., Beckh, S., and Pongs, O. (1990) *Embo J* **9**(6), 1749-1756
49. Kalman, K., Nguyen, A., Tseng-Crank, J., Dukes, I. D., Chandy, G., Hustad, C. M., Copeland, N. G., Jenkins, N. A., Mohrenweiser, H., Brandriff, B., Cahalan, M., Gutman, G. A., and Chandy, K. G. (1998) *J Biol Chem* **273**(10), 5851-5857
50. Stuhmer, W., Ruppertsberg, J. P., Schroter, K. H., Sakmann, B., Stocker, M., Giese, K. P., Perschke, A., Baumann, A., and Pongs, O. (1989) *Embo J* **8**(11), 3235-3244
51. Tempel, B. L., Jan, Y. N., and Jan, L. Y. (1988) *Nature* **332**(6167), 837-839
52. Grissmer, S., Dethlefs, B., Wasmuth, J. J., Goldin, A. L., Gutman, G. A., Cahalan, M. D., and Chandy, K. G. (1990) *Proc Natl Acad Sci U S A* **87**(23), 9411-9415
53. Adda, S., Fleischmann, B. K., Freedman, B. D., Yu, M., Hay, D. W., and Kotlikoff, M. I. (1996) *J Biol Chem* **271**(22), 13239-13243
54. Mason, D. E., Mitchell, K. E., Li, Y., Finley, M. R., and Freeman, L. C. (2002) *Mol Pharmacol* **61**(1), 201-213
55. Dixon, J. E., and McKinnon, D. (1994) *Circ Res* **75**(2), 252-260
56. Pappone, P. A., and Ortiz-Miranda, S. I. (1993) *Am J Physiol* **264**(4 Pt 1), C1014-1019
57. Ouadid-Ahidouch, H., Van Coppenolle, F., Le Bourhis, X., Belhaj, A., and Prevarskaya, N. (1999) *FEBS Lett* **459**(1), 15-21
58. Thornhill, W. B., Wu, M. B., Jiang, X., Wu, X., Morgan, P. T., and Margiotta, J. F. (1996) *J Biol Chem* **271**(32), 19093-19098
59. Shi, G., and Trimmer, J. S. (1999) *J Membr Biol* **168**(3), 265-273
60. Manganas, L. N., and Trimmer, J. S. (2000) *J Biol Chem* **275**(38), 29685-29693
61. Gahmberg, C. G., and Tolvanen, M. (1996) *Trends Biochem Sci* **21**(8), 308-311
62. Cheung, J. C., and Reithmeier, R. A. (2007) *Methods* **41**(4), 451-459
63. Jaeken, J. (2003) *J Inherit Metab Dis* **26**(2-3), 99-118
64. Freeze, H. H., and Aebi, M. (2005) *Curr Opin Struct Biol* **15**(5), 490-498
65. Keir, G., Winchester, B. G., and Clayton, P. (1999) *Ann Clin Biochem* **36** (Pt 1), 20-36
66. Nilsson, I. M., and von Heijne, G. (1993) *J Biol Chem* **268**(8), 5798-5801
67. Durand, G., and Seta, N. (2000) *Clin Chem* **46**(6 Pt 1), 795-805

68. Roth, J., Taatjes, D. J., Lucocq, J. M., Weinstein, J., and Paulson, J. C. (1985) *Cell* **43**(1), 287-295
69. Zamze, S., Harvey, D. J., Chen, Y. J., Guile, G. R., Dwek, R. A., and Wing, D. R. (1998) *Eur J Biochem* **258**(1), 243-270
70. Finne, J., Krusius, T., and Rauvala, H. (1977) *Biochem Biophys Res Commun* **74**(2), 405-410
71. Rosenberg, I. M. (2004) *Protein analysis and purification: benchtop techniques*, 2 Ed., Birkhauser, Verlag
72. Katayama, T., Imaizumi, K., Manabe, T., Hitomi, J., Kudo, T., and Tohyama, M. (2004) *J Chem Neuroanat* **28**(1-2), 67-78
73. Lindholm, D., Wootz, H., and Korhonen, L. (2006) *Cell Death Differ* **13**(3), 385-392
74. Dempski, R. E., Jr., and Imperiali, B. (2002) *Curr Opin Chem Biol* **6**(6), 844-850
75. Jaeken, J., van Eijk, H. G., van der Heul, C., Corbeel, L., Eeckels, R., and Eggermont, E. (1984) *Clin Chim Acta* **144**(2-3), 245-247
76. Jaeken, J., and Matthijs, G. (2001) *Annu Rev Genomics Hum Genet* **2**, 129-151
77. Fukuda, M. N., Dell, A., and Scartezzini, P. (1987) *J Biol Chem* **262**(15), 7195-7206
78. Fukuda, M. N., Masri, K. A., Dell, A., Luzzatto, L., and Moremen, K. W. (1990) *Proc Natl Acad Sci U S A* **87**(19), 7443-7447
79. Kornfeld, R., and Kornfeld, S. (1985) *Annu Rev Biochem* **54**, 631-664
80. Ioffe, E., and Stanley, P. (1994) *Proc Natl Acad Sci U S A* **91**(2), 728-732
81. Metzler, M., Gertz, A., Sarkar, M., Schachter, H., Schrader, J. W., and Marth, J. D. (1994) *Embo J* **13**(9), 2056-2065
82. Lowe, J. B., and Marth, J. D. (2003) *Annu Rev Biochem* **72**, 643-691
83. Watanabe, I., Wang, H. G., Sutachan, J. J., Zhu, J., Recio-Pinto, E., and Thornhill, W. B. (2003) *J Physiol* **550**(Pt 1), 51-66
84. Watanabe, I., Zhu, J., Sutachan, J. J., Gottschalk, A., Recio-Pinto, E., and Thornhill, W. B. (2007) *Brain Res* **1144**, 1-18
85. Napp, J., Monje, F., Stuhmer, W., and Pardo, L. A. (2005) *J Biol Chem* **280**(33), 29506-29512
86. Watanabe, I., Zhu, J., Recio-Pinto, E., and Thornhill, W. B. (2004) *J Biol Chem* **279**(10), 8879-8885
87. Petrecca, K., Atanasiu, R., Akhavan, A., and Shrier, A. (1999) *J Physiol* **515** (Pt 1), 41-48
88. Sato, C., Fukuoka, H., Ohta, K., Matsuda, T., Koshino, R., Kobayashi, K., Troy, F. A., 2nd, and Kitajima, K. (2000) *J Biol Chem* **275**(20), 15422-15431
89. Oetke, C., Hinderlich, S., Brossmer, R., Reutter, W., Pawlita, M., and Keppler, O. T. (2001) *Eur J Biochem* **268**(16), 4553-4561
90. Yabe, U., Sato, C., Matsuda, T., and Kitajima, K. (2003) *J Biol Chem* **278**(16), 13875-13880
91. Rohrer, J. S., Thayer, J., Weitzhandler, M., and Avdalovic, N. (1998) *Glycobiology* **8**(1), 35-43

92. Schwartz, E. L., Hadfield, A. F., Brown, A. E., and Sartorelli, A. C. (1983) *Biochim Biophys Acta* **762**(4), 489-497
93. Varki, A. (1997) *Faseb J* **11**(4), 248-255
94. Varki, A. (1993) *Glycobiology* **3**(2), 97-130
95. Krusius, T., and Finne, J. (1978) *Eur J Biochem* **84**(2), 395-403
96. Varki, A., Cummings, R., Esko, J., Freeze, H., Hart, G., and Marth, J. (1999) *The Consortium of Glycobiology*, Cold Spring Laboratory Press, Cold Spring Harbor, New York
97. Finne, J. (1982) *J Biol Chem* **257**(20), 11966-11970
98. Zuber, C., Lackie, P. M., Catterall, W. A., and Roth, J. (1992) *J Biol Chem* **267**(14), 9965-9971
99. Troy, F. A., 2nd. (1992) *Glycobiology* **2**(1), 5-23
100. Curreli, S., Arany, Z., Gerardy-Schahn, R., Mann, D., and Stamatou, N. M. (2007) *J Biol Chem* **282**(42), 30346-30356
101. Muhlenhoff, M., Eckhardt, M., Bethe, A., Frosch, M., and Gerardy-Schahn, R. (1996) *Embo J* **15**(24), 6943-6950
102. Close, B. E., Wilkinson, J. M., Bohrer, T. J., Goodwin, C. P., Broom, L. J., and Colley, K. J. (2001) *Glycobiology* **11**(11), 997-1008
103. Taki, T., Hirabayashi, Y., Ishikawa, H., Ando, S., Kon, K., Tanaka, Y., and Matsumoto, M. (1986) *J Biol Chem* **261**(7), 3075-3078
104. Yamamoto, H., Iida-Tanaka, N., Kasama, T., Ishizuka, I., Kushi, Y., and Handa, S. (1999) *J Biochem* **125**(5), 923-930
105. Yan, A., and Lennarz, W. J. (2005) *J Biol Chem* **280**(5), 3121-3124
106. Neher, E., Sakmann, B., and Steinbach, J. H. (1978) *Pflugers Arch* **375**(2), 219-228
107. Peterson, G. L. (1979) *Anal Biochem* **100**(2), 201-220
108. Stummeyer, K., Dickmanns, A., Muhlenhoff, M., Gerardy-Schahn, R., and Ficner, R. (2005) *Nat Struct Mol Biol* **12**(1), 90-96
109. Iwamori, M., Ohta, Y., Uchida, Y., and Tsukada, Y. (1997) *Glycoconj J* **14**(1), 67-73
110. Prime, S., Dearnley, J., Ventom, A. M., Parekh, R. B., and Edge, C. J. (1996) *J Chromatogr A* **720**(1-2), 263-274
111. Uchida, Y., Tsukada, Y., and Sugimori, T. (1979) *J Biochem* **86**(5), 1573-1585
112. Roggentin, P., Kleineidam, R. G., and Schauer, R. (1995) *Biol Chem Hoppe Seyler* **376**(9), 569-575
113. Glasgow, L. R., Paulson, J. C., and Hill, R. L. (1977) *J Biol Chem* **252**(23), 8615-8623
114. Sambrook, J., Fritsch, E., and Maniatis, T. (1992) *Molecular Cloning: A Laboratory Manual*, Coldspring Harbour Laboratory, Coldspring Harbour
115. Varki, A. (1994) *Methods Enzymol* **230**, 16-32
116. Cartwright, T. A., Corey, M. J., and Schwalbe, R. A. (2007) *Biochim Biophys Acta* **1770**(4), 666-671
117. Schachter, H. (2002) *Biochim Biophys Acta* **1573**(3), 292-300

118. Wang, Y., Schachter, H., and Marth, J. D. (2002) *Biochim Biophys Acta* **1573**(3), 301-311
119. Schwalbe, R. A., Wang, Z., Wible, B. A., and Brown, A. M. (1995) *J Biol Chem* **270**(25), 15336-15340
120. Schwalbe, R. A., Wang, Z., Bianchi, L., and Brown, A. M. (1996) *J Biol Chem* **271**(39), 24201-24206
121. Schwalbe, R. A., Bianchi, L., and Brown, A. M. (1997) *J Biol Chem* **272**(40), 25217-25223
122. Schwalbe, R. A., Rudin, A., Xia, S. L., and Wingo, C. S. (2002) *J Biol Chem* **277**(27), 24382-24389
123. Zhu, J., Watanabe, I., Poholek, A., Koss, M., Gomez, B., Yan, C., Recio-Pinto, E., and Thornhill, W. B. (2003) *Biochem J* **375**(Pt 3), 769-775
124. Benoit, A., Vargas, M. A., Desgroseillers, L., and Boileau, G. (2004) *Biochem J* **380**(Pt 3), 881-888
125. Sobko, A., Peretz, A., Shirihai, O., Etkin, S., Cherepanova, V., Dagan, D., and Attali, B. (1998) *J Neurosci* **18**(24), 10398-10408
126. McMahan, A., Fowler, S. C., Perney, T. M., Akemann, W., Knopfel, T., and Joho, R. H. (2004) *Eur J Neurosci* **19**(12), 3317-3327
127. Xu, C., Tang, G., Lu, Y., and Wang, R. (2000) *Life Sci* **66**(21), 2023-2033
128. Santacruz-Toloza, L., Huang, Y., John, S. A., and Papazian, D. M. (1994) *Biochemistry* **33**(18), 5607-5613
129. Deal, K. K., Lovinger, D. M., and Tamkun, M. M. (1994) The brain Kv1.1 potassium channel: in vitro and in vivo studies on subunit assembly and posttranslational processing. In: *J Neurosci*
130. Philipson, L. H., Malayev, A., Kuznetsov, A., Chang, C., and Nelson, D. J. (1993) *Biochim Biophys Acta* **1153**(1), 111-121
131. Jiang, Y., Lee, A., Chen, J., Ruta, V., Cadene, M., Chait, B. T., and MacKinnon, R. (2003) *Nature* **423**(6935), 33-41
132. Jones, J., Krag, S. S., and Betenbaugh, M. J. (2005) *Biochim Biophys Acta* **1726**(2), 121-137
133. Drickamer, K., and Taylor, M. E. (1998) *Trends Biochem Sci* **23**(9), 321-324
134. Freeze, H. H., and Aebi, M. (1999) *Biochim Biophys Acta* **1455**(2-3), 167-178
135. Eckhardt, M., Bukalo, O., Chazal, G., Wang, L., Goridis, C., Schachner, M., Gerardy-Schahn, R., Cremer, H., and Dityatev, A. (2000) *J Neurosci* **20**(14), 5234-5244
136. Angata, K., and Fukuda, M. (2003) *Biochimie* **85**(1-2), 195-206
137. Galuska, S. P., Oltmann-Norden, I., Geyer, H., Weinhold, B., Kuchelmeister, K., Hildebrandt, H., Gerardy-Schahn, R., Geyer, R., and Muhlenhoff, M. (2006) *J Biol Chem* **281**(42), 31605-31615
138. Albach, C., Klein, R. A., and Schmitz, B. (2001) *Biol Chem* **382**(2), 187-194
139. Varki A., Cummings R., Esko J., Freeze H., Hart G., and J., M. (1999) *The Consortium of Glycobiology Editors, La Jolla California, Cold Spring Harbor Laboratory Press, Cold Spring Harbor*
140. Close, B. E., and Colley, K. J. (1998) *J Biol Chem* **273**(51), 34586-34593

141. Finne, J., Krusius, T., Rauvala, H., and Hemminki, K. (1977) *Eur J Biochem* **77**(2), 319-323
142. Acheson, A., Sunshine, J. L., and Rutishauser, U. (1991) *J Cell Biol* **114**(1), 143-153
143. Cunningham, B. A., Hemperly, J. J., Murray, B. A., Prediger, E. A., Brackenbury, R., and Edelman, G. M. (1987) *Science* **236**(4803), 799-806
144. Theodosis, D. T., Rougon, G., and Poulain, D. A. (1991) *Proc Natl Acad Sci U S A* **88**(13), 5494-5498
145. Bouwstra, J. B., Deyl, C. M., and Vliegenthart, J. F. (1987) *Biol Chem Hoppe Seyler* **368**(3), 269-275
146. Finne, J., Finne, U., Deagostini-Bazin, H., and Goridis, C. (1983) *Biochem Biophys Res Commun* **112**(2), 482-487
147. Orlandini, M., Santucci, A., Tramontano, A., Neri, P., and Oliviero, S. (1994) *Protein Sci* **3**(9), 1476-1484
148. Koeppen, A. H., Dickson, A. C., and McEvoy, J. A. (1995) *J Neuropathol Exp Neurol* **54**(3), 395-403
149. Jett, M., Jamieson, G. A., and DeBernardo, S. L. (1971) *J Biol Chem* **246**(11), 3686-3693
150. D'Andrea, G., D'Alessandro, A. M., Salucci, M. L., and Oratore, A. (1994) *J Protein Chem* **13**(1), 31-36
151. Hallenbeck, P. C., Vimr, E. R., Yu, F., Bassler, B., and Troy, F. A. (1987) *J Biol Chem* **262**(8), 3553-3561
152. Cartwright, T. A., and Schwalbe, R. A. (2008) *Biosci Rep*
153. Grissmer, S., Ghanshani, S., Dethlefs, B., McPherson, J. D., Wasmuth, J. J., Gutman, G. A., Cahalan, M. D., and Chandy, K. G. (1992) *J Biol Chem* **267**(29), 20971-20979
154. Landolt-Marticorena, C., and Reithmeier, R. A. (1994) *Biochem J* **302** (Pt 1), 253-260
155. O'Reilly, D. R., Miller, L. K., and Lucklow, V. A. (1994) *Baculovirus Expression Vector: A Lab Manual*, Oxford University Press, New York

APPENDIX A: COPYWRITE PERMISSION

From: Jones, Jennifer (ELS-OXF)
Sent: Fri 8/8/2008 5:29 AM
To: Cartwright, Tara Ann
Subject: RE: manuscript permission

Dear Tara Ann Cartwright

As author of the requested article, you do not need Elsevier's permission to include it in your thesis as it is part of the author's rights you retain as an Elsevier journal author.

For further information on the rights you retain as an Elsevier journal author, please visit our web page at http://www.elsevier.com/wps/find/authorsview_authors/copyright.

Yours sincerely
Jennifer Jones
Rights Assistant
Global Rights Department

Elsevier Ltd
PO Box 800
Oxford OX5 1GB
UK

Elsevier Limited, a company registered in England and Wales with company number 1982084, whose registered office is The Boulevard, Langford Lane, Kidlington, Oxford, OX5 1GB, United Kingdom.

APPENDIX B: COPYWRITE PERMISSION

From: Landriault, Roxanne [mailto:Roxanne.Landriault@nrc-cnrc.gc.ca]
Sent: Thu 8/7/2008 6:58 AM
To: Cartwright, Tara Ann
Subject: FW: Permission to Reproduce Article

Permission is granted for use of the material, as described below, provided that acknowledgement is given to the source.

Sincerely
 Mike Boroczki
 Business Manager
 NRC Research Press
 Tel: 613-993-9108
 Fax: 613-952-7656

-----Original Message-----

From: rp.business@nrc-cnrc.gc.ca [<mailto:rp.business@nrc-cnrc.gc.ca>]
 Sent: Wednesday, August 06, 2008 10:27 PM
 To: CISTI, Research Press Business
 Subject: Permission to Reproduce Article

Below is the result of your feedback form. It was submitted by
 (rp.business@nrc-cnrc.gc.ca) on Wednesday, August 06, 2008 at 22:26:45

 name: Tara A. Cartwright
 address: Department of Biochemistry & Molecular Biology Brody
 School of Medicine at ECU 600 Moye Blvd Greenville, NC 27834
 phone: 347-517-5330
 email: TAC0421@ecu.edu
 fax: 252-744-3383
 publication: Biochemistry and Cell Biology
 Volume: 86
 issue: 1
 pages: entire publication
 Pub Author: Schwalbe RA, Corey MJ, Cartwright TA
 date: 02/2008
 purpose: The requested material will be used in my dissertation

APPENDIX C: COPYWRITE PERMISSION

Ref: BSR080001

Tara A Cartwright and Ruth A Schwalbe
 Biochemistry and Molecular Biology, Brody School of Medicine at East Carolina
 University
 Greenville
 NC 27834
 U.S.A.
 TAC0421@ecu.edu

Portland Press Ltd
 Third Floor, Eagle House
 16 Procter Street
 London WC1V 6NX, UK

Tel: +44(0)20 7280 4110
 Fax: +44(0)20 7280 4169
 editorial@portlandpress.com
 http://www.portlandpress.com

23/12/2008



PORTLAND
 PRESS

Dear Tara Cartwright and Ruth A Schwalbe

Thank you for contacting Portland Press to apply for permission to include the following paper in your thesis:

Tara A Cartwright, Ruth A Schwalbe (2008) Atypical sialylated N-glycan structures are attached to neuronal voltage gated potassium channels, *Bioscience Reports* DOI: 10.1042/BSR20080149

I am happy to grant you permission to reproduce the paper in your thesis provided that it is not used for commercial purposes and subject to the following conditions:

1. If any part of the material to be used is credited to another source, permission must be sought from that source.
2. The following credit line is to be placed on the page where the material appears: Reproduced, with permission, from Author(s), published as an immediate publication (year) – Digital Object Identifier: 10.1042/BJ20051073 © the Biochemical Society
3. This permission is granted for one-time use only and is for non-exclusive world rights in volume form in print and electronic format.

Yours sincerely,

Lucy White
 Pre-Press Specialist
 editorial@portlandpress.com

Registered No. 2453983 <http://www.portlandpress.com> e-mail: editorial@portlandpress.com



THE
 BIOCHEMICAL
 SOCIETY